Spring 2006

Paleocene to early Eocene dinoflagellate cyst biostratigraphy in Southeast Nigeria and the Cote d'Ivoire-Ghana transform margin (ODP site 959)

Hernan Antolinez-Delgado

Department:

PALEOCENE TO EARLY EOCENE DINOFLAGELLATE CYST BIOSTRATIGRAPHY IN SOUTHEAST NIGERIA AND THE CÔTE D'IVOIRE-GHANA TRANSFORM MARGIN (ODP SITE 959)

by

HERNAN ANTOLINEZ-DELGADO

A THESIS

Presented to the Faculty of the Graduate School of the

UNIVERSITY OF MISSOURI-ROLLA

In Partial Fulfillment of the Requirements for the Degree

MASTER OF SCIENCE IN GEOLOGY AND GEOPHYSICS

2006

Approved by

Francisca E. Oboh-Ikuenobe, Advisor

John P. Hogan

Ronald L. Frank

ABSTRACT

This study represents a contribution to Early Paleogene biostratigraphy in the tropics where published studies are sparse in comparison with mid and high latitude regions. Data were derived from a comprehensive analysis of dinoflagellate cysts (dinocysts) in 45 samples from the Early Paleocene to Early Eocene interval at two localities in West Africa, namely Alo-1 well in the Anambra Basin, southeastern Nigeria, and Ocean Drilling Program Hole 959D (ODP Leg 159) in the Côte d'Ivoire-Ghana Transform Margin. Dinocyst recovery varied from very good to poor, and the specimens were commonly well preserved. The dinocyst data were calibrated with existing calcareous nannofossil biozonations for Hole 959D, which allowed for a valid comparison with published dinocyst studies in well-dated rock sections in northwestern Europe, the Mediterranean region, New Zealand, and Tasmania. There is a closer correlation between the tropical and mid latitude assemblages than those of high latitude regions.

Last appearance and/or last abundance events of dinocysts were used to identify five informal zones in Hole 959D, four of which occur in Alo-1 well. Abundant thermophilic taxa that include the *Cordosphaeridium* group dominate the Early Paleocene to early Late Paleocene (Danian to mid Thanetian) interval. The presence of abundant to extremely abundant numbers of *Apectodinium* in the succeeding Late Paleocene (late Thanetian) sediments appears to record an important global warming event. This event is likely related to the episodes of intense climatic warming or "hyperthermals" that characterized the latest Paleocene to earliest Eocene time worldwide.

Twelve potentially new species attributable to *Achomosphaera*, *Apteodinium*, *Areosphaeridium*, *Diphyes*, *Ifecysta*, *Kallosphaeridium*, *Palaeocystodinium*, and *Wilsodinium* were identified in this study. A revision of the generic diagnosis of *Ifecysta* is proposed. In addition, lithostratigraphic and biostratigraphic analyses suggested a late Danian age for the contact between the Imo and Nsukka formations in Alo-1 well, where lower Eocene sediments were probably not recovered. In Hole 959D, the concentration of several dinocyst events in Late Paleocene interval confirms the presence of hiatuses or condensed horizons as suggested by previous studies in the Côte d'Ivoire-Ghana Transform Margin.

ACKNOWLEDGMENTS

I wish to thank Dr. Francisca Oboh-Ikuenobe for her very useful advice on this project. I would like to thank Dr. Robert Fensome and Dr. Graham Williams from the Geological Survey of Canada in Dartmouth, for allowing me to use their extensive literature collection and for enlightening discussions and sharing of ideas about the taxonomy of dinocysts. Thanks go to Dr. John Hogan and Dr. Ronald Frank whose support and service on my advisory committee were valuable to me. Acknowledgement is made to the AAPG Foundation Grants-in-Aid Program and to the University of Missouri-Rolla Department of Geological Sciences and Engineering for providing partial funding for the project.

Special thanks go to my parents and my brother for their continuous and unconditional support through my schooling years.

TABLE OF CONTENTS

Page

ABSTRACT iii
ACKNOWLEDGMENTS iv
LIST OF ILLUSTRATIONS vii
LIST OF TABLES viii
1. INTRODUCTION 1
2. GEOLOGIC SETTING 4
2.1. SOUTHERN NIGERIA 4
2.1.1. Tectonics. 4
2.1.2. Stratigraphy and sedimentology. 6
2.2. CÔTE D'IVOIRE-GHANA TRANSFORM MARGIN 8
2.2.1. Tectonics. 8
2.2.2. Stratigraphy and sedimentology. 11
3. LITERATURE REVIEW 13
3.1. OVERVIEW OF TROPICAL PALEOGENE PALYNOLOGY 13
3.2. EARLY PALEOGENE DINOCYST STUDIES 14
3.3. PREVIOUS BIOSTRATIGRAPHIC RESEARCH IN THE STUDY AREA . 15
3.3.1. Southeastern Nigeria. 15
3.3.2. Cote d'Ivoire Ghana Transform Margin. 17
4. MATERIAL AND METHODS 19
5. RESULTS 23
5.1. INTRODUCTION 23
5.2. SYSTEMATIC PALEONTOLOGY 24
5.3. STRATIGRAPHIC DISTRIBUTION OF DINOCYSTS 38
5.3.1. Alo-1 38
5.3.2. Hole 959D. 39
5.4. QUANTITATIVE CHANGES IN THE DINOCYST DISTRIBUTION 41
5.4.1. Alo-1 42
5.4.2. Hole 959D. 42

6. DISCUSSION 45
6.1. INFERRED LITHOSTRATIGRAPHY OF ALO-1 WELL 45
6.2. COMPARISON OF THE ALO-1 AND HOLE 959D DINOCYST ASSEMBLAGES 46
6.3. BIOSTRATIGRAPHY 47
6.4. COMPARISON WITH PREVIOUS DINOCYST STUDIES 51
6.4.1. Mid- to high-latitudes. 51
6.4.2. Mid latitudes. 53
6.4.3. Significance for Early Paleogene paleoclimatic reconstruction. 54
7. CONCLUSIONS 55
APPENDICES
A. ILLUSTRATIONS OF SELECTED DINOCYSTS IDENTIFIED IN ALO-1 AND HOLE 959D 57
B. QUANTITATIVE DINOCYST DATA FOR HOLE 959D 70
C. QUANTITATIVE DINOCYST DATA FOR ALO-1 WELL 73
D. GLOSSARY OF THE TERMINOLOGY APPLIED TO DINOCYSTS 78
BIBLIOGRAPHY 89
VITA 100

LIST OF ILLUSTRATIONS

Figure Page

Figure 1.1. Maps of Nigeria and the Côte d'Ivoire-Ghana Transform Margin in West Africa. 3

Figure 2.1. Megatectonic frame of Southern Nigeria sedimentary basin. 5

Figure 2.2. Summary of stratigraphic data on the Paleogene succession in southeastern Nigeria. 6

Figure 2.3. Simplified bathymetry and main morphostructural domains of the Côte d'Ivoive-Ghana Transform Margin. 9

Figure 2.4. Interpretative schematic cross sections of the Deep Ivorian Basin and Côte d'Ivore-Ghana Transform Margin. 10

Figure 2.5. Schematic stratigraphic column for ODP site 959. 11

Figure 3.1. Summary of biostratigraphic and lithologic data for Alo-1 well 16

Figure 3.2. Calcareous nannofossil biostratigraphy and lithology in the interval studied in ODP Hole 959D. 18

Figure 4.1. Calcareous nannoplankton bioevents in the Paleocene-Early Eocene interval 22

Figure 5.1. Plot of the percent terrestrial palynomorphs with depth in Alo-1 well and Hole 959D. 23

Figure 5.2. Stratigraphic distribution of selected dinocysts in Alo-1 well. 39

Figure 5.3. Stratigraphic distribution of selected dinocysts in Hole 959D 41

Figure 5.4. Quantitative distribution of dinocyst morphogroups in the Paleocene-Early Eocene interval of Alo-1 well. 43

Figure 5.5. Quantitative distribution of dinocyst morphogroups in the Paleocene-Early Eocene interval of Hole 959D. 44

Figure 6.1. Inferred lithostratigraphy for the interval studied in Alo-1 45

Figure 6.2. Biostratigraphic summary for the Early Paleogene interval of Alo-1 well 50

Figure 6.3. Biostratigraphic summary for the Early Paleogene interval of ODP Hole 959D. 51

LIST OF TABLES

Table Page

Table 2.1. Correlation of subsurface formations in the Niger Delta with surface equivalents in Southeastern Nigeria 8

Table 4.1. List of samples and sample depths for Alo-1 well 20

Table 4.2. List of samples and sample depths for ODP Hole 959D. 20

Table 6.1. List of dinocyst species recorded in only one section. 46

1. INTRODUCTION

The Early Paleogene (~ 65.5 to 48.6 My), represents a highly dynamic period in earth's history. It was associated with major perturbations in the carbon cycle and global climate, high surface temperatures, and significant evolutionary turnovers and extinctions in the marine and terrestrial biota (e.g., Crouch, 2001; Zachos et al., 2001). Latitudinal sea surface temperature gradients were apparently much reduced relative to the present-day, with high latitude values being notably warmer than current values (Zachos et al., 1994). Ice free conditions prevailed and atmospheric CO_2 levels were elevated (Zachos et al., 1994; Royer et al., 2001). Warm-water pelagic marine organisms and thermophilic vertebrates were present in polar latitudes (Stott and Kennett, 1990; Gingerich, 2003), and vegetation and soil types suggest that the high latitudes in both hemispheres were warm (Wing and Greenwood, 1993).

A substantial amount of information about the Early Paleogene is currently available from mid to high latitudes (see Berggren et al., 1998), but very little is known about tropical regions. Recognition of Early Paleogene successions in tropical areas is rather sparse due to the absence of a reasonably good biostratigraphic framework and a relatively recent history of geological research. The few published biostratigraphic studies, such as Germeraad et al. (1968), Muller et al. (1987), Salard-Cheboldaeff (1990), Jaramillo and Dilcher (2001), indicate that pollen and spores are the most reliable biostratigraphic tools in the continental and nearshore deposits that accumulated during this time interval. However, pollen and spores are not used for defining the standard geologic time scale for the Paleogene (Berggren et al., 1995; Gradstein et al., 2004). It is defined by calcareous marine microfossils such as planktonic foraminifera and coccolithophorids, which do not occur in continental deposits and are rare in nearshore sediments. Pollen and spores have also yielded important information in terms of tropical paleogeography, paleoclimatology, and floral evolution (Rull, 1999; Jaramillo, 2002), but integration of these studies with those derived from other parts of the world is rather difficult in the absence of a well-callibrated biostratigraphic timeframe.

This problem can be solved by studying organic-walled dinoflagellate cysts (dinocysts) which are preserved in nearshore sediments. Dinocysts have been

successfully used in detailed Paleogene biostratigraphic and paleoecologic studies of mostly mid and high latitudes (e.g., Crouch, 2001; Sluijs et al., 2005). They have been shown to yield sea-surface temperature, salinity and productivity signals in coastal and neritic settings, making them ideal fossils to unravel the changes occurring throughout the Early Paleogene. Furthermore, since they occur alongside pollen and spores in inner neritic to oceanic settings and are not limited by carbonate sedimentation, they can be used to correlate continental, neritic and more offshore marine sequences (Traverse, 1988).

Previous Paleogene dinocyst research in tropical areas documented well-preserved and diverse dinocysts assemblages, especially in West Africa (Jan du Chêne and Adediran, 1985; Jan du Chêne, 1988; Willumsen et al., 2004). However, these studies dealt mainly with taxonomical aspects and did not provide information about the stratigraphic distribution and/or the paleoenvironmental significance of the associations. Nevertheless, they provided insight into the general composition of tropical dinocyst associations during the Early Paleogene.

The objectives of this study therefore, are: 1) taxonomical identification of dinocysts in Lower Paleogene sediments from the Alo-1 well, in the Anambra basin in Southern Nigeria, and ODP Hole 959D in the Côte d'Ivoire-Ghana Transform Margin (Fig. 1.1); 2) calibration of the dinocyst biostratigraphy with published calcareous microfossil data from ODP Hole 959D (Shafik et al., 1998) and biochronological information from global dinocyst charts (e.g., Stover et al., 1996; Williams et al., 2004); and 3) comparison of the assemblages with those from other parts of the world, such as northwest Europe, the Mediterranean region, and New Zealand, where detailed Paleogene dinocyst studies have been undertaken.

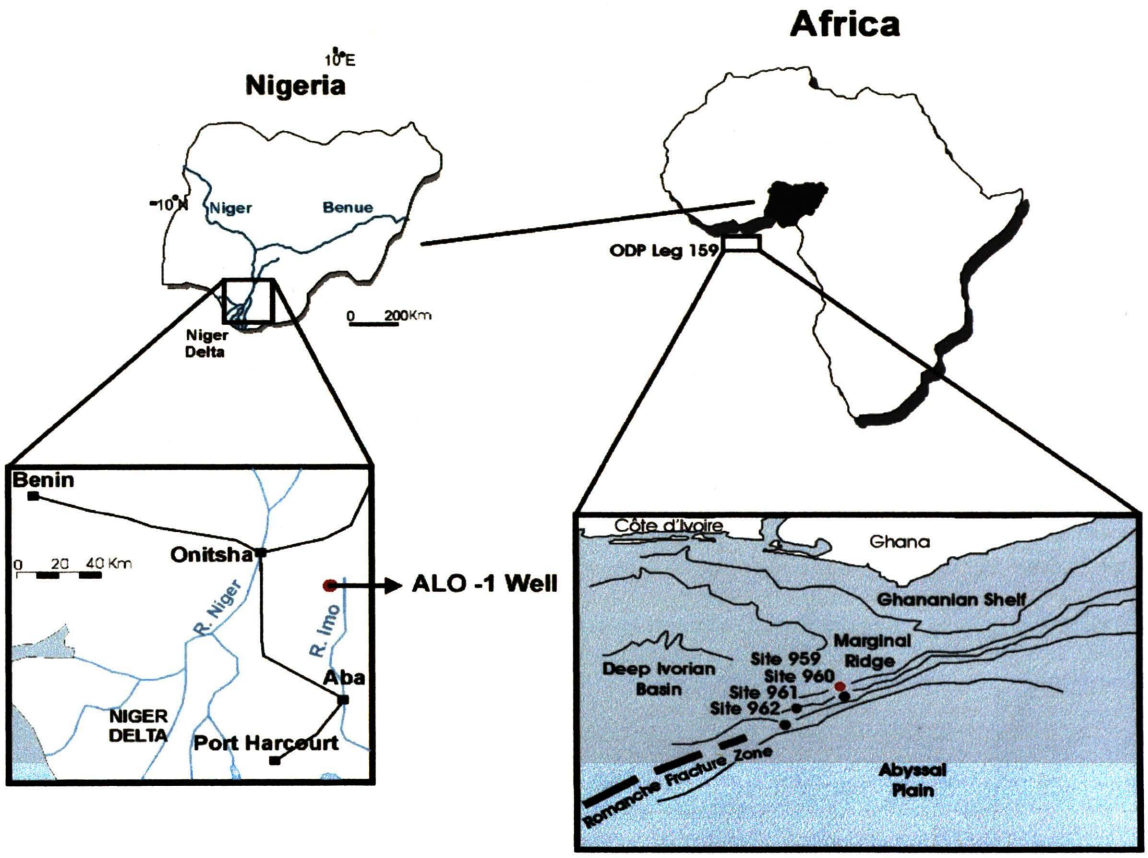

Figure 1.1. Maps of Nigeria and the Côte d'Ivoire-Ghana Transform Margin in West Africa. Insets show the locations of borehole sections used in this study: Alo-1 well in the Anambra Basin, southern Nigeria and ODP Hole 959D in the Côte d'Ivoire-Ghana Transform Margin.

2. GEOLOGIC SETTING

2.1. SOUTHERN NIGERIA

The Southern Nigeria sedimentary basin comprises the Anambra Basin, the southern Benue Trough, the Niger Delta, the Benin Embayment, the Abakaliki Fold Belt, the Afikpo Syncline, and the Calabar Flank (Fig. 2.1). The depositional and tectonic histories of the basin are related to the tectonic stages and epeirogenic movements associated with the separation of Africa and South America during the Early Cretaceous (Burke et al., 1971; Murat, 1972; Burke, 1996).

2.1.1. Tectonics. The tectonic framework of the Anambra sedimentary basin is controlled by a much larger and older tectonic feature, the Benue Trough, which is a NE-SW folded rift basin (Fig. 2.1) representing a failed arm of an aulacogen that runs diagonally across Nigeria. It formed simultaneously with the opening of the Gulf of Guinea and the Equatorial Atlantic in Aptian-Albian times, when the equatorial part of Africa and South America began to separate (Burke et al., 1971). Taphrogenic subsidence along fundamental transform faults which had cut through the lithosphere and are the landward continuations of the Chain and Charcot oceanic fracture zones (Emery et al., 1975), initiated the Benue Trough. It also later controlled the location of the main axis of subsidence of the resultant basins. The Chain Fracture Zone coincides with the Benin Hinge Line of the western Benue Trough, whereas the eastern portion of the trough, referred to as the Calabar Flank (Reyment, 1965), is more complicated, with NW-SE tending structures such as the Ikang Trough, the Ituk High, and the Calabar Hinge Line (Fig. 2.1). Sinistral transcurrent shearing along the fracture zones caused deformation in the Benue Trough and modified the Gulf of Guinea continental margin from the simple pull-apart basement structures with half-grabens that underlie the West African continental margins north and south of the Gulf of Guinea (Reijers et al., 1997).

Murat (1972) advocated three tectonic phases in the stratigraphic history of the region during which the axis of the main basin shifted, giving rise to the following three successive basins. These three phases were: (1) the Abakaliki-Benue phase (Aptian-Santonian), (2) the Anambra-Benin phase (Campanian-Mid Eocene), and (3) the Niger Delta phase (late Eocene-Pliocene).

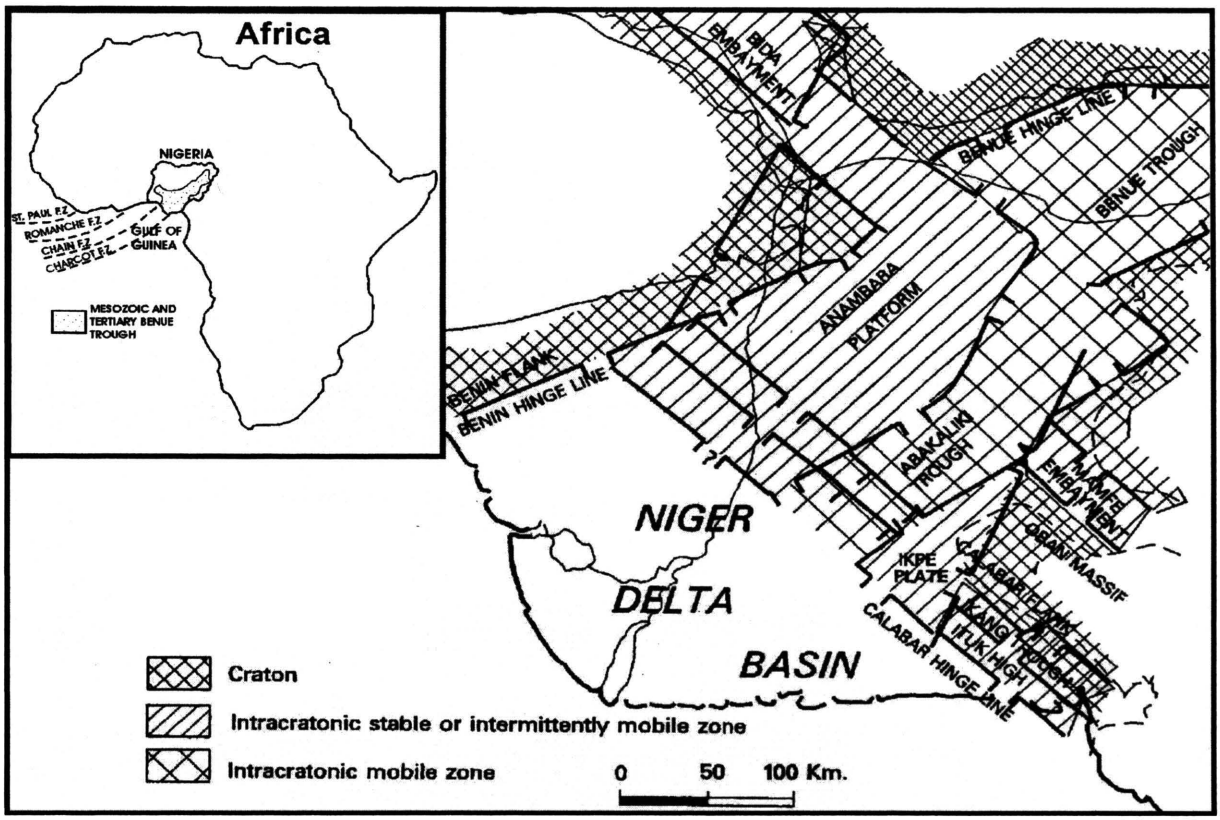

Figure 2.1. Megatectonic frame of Southern Nigeria sedimentary basin (Mid-Albian to Santonian). Inset shows regional setting of the basin (from Reijers et al., 1997).

The Abakaliki-Benue phase commenced during the middle Albian after major northeast-southwest movements caused the faulting that resulted in the rift-like Abakaliki-Benue Trough. Shelf deposits were laid down on the Anambra Platform, between the Calabar and Benin hinge lines and the trough. The Anambra-Benin phase was characterized by compressional movements along the established northeast-southwest trend which resulted in the folding and uplifting of the Abakaliki-Benue Trough during the late Santonian to early Campanian, and in the formation of the Anambra Basin. The adjoining Benin Flank basement underwent a transgression which lasted until the Early Eocene. The Niger Delta phase was initiated by a regression during the Middle and Late Eocene. Vertical movements of blocks bounded by northeast-southwest and northwest-southeast trending faults resulted in the deposition of a large

deltaic complex in the down-dip Anambra Basin. This, however, preceded the subsidence of the Oligocene to Recent Niger Delta basin along the northwest-southeast fault trend.

2.1.2. Stratigraphy and sedimentology. Paleogene time in southeastern Nigeria is represented by a sedimentary succession that is thicker than 3500 m of marine shales (Fig. 2.2), and consists of the Nsukka Formation (~350 m), Imo Formation (~1000 m), Ameki Group (~1900 m), and Ogwashi-Asaba Formation (~250 m) (Oboh-Ikuenobe et al., 2005).

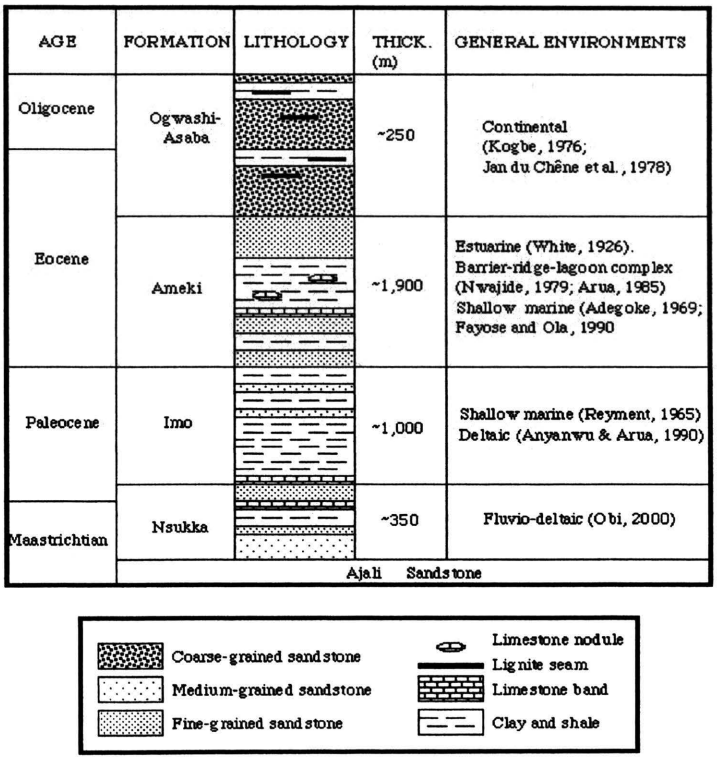

Figure 2.2. Summary of stratigraphic data on the Paleogene succession in southeastern Nigeria (from Oboh-Ikuenobe et al., 2005).

The Nsukka Formation, which overlies the Ajali Sandstone, begins with coarse- to medium-grained sandstones and passes upward into well-bedded blue clays, fine-grained sandstones, and carbonaceous shales with thin bands of limestone (Reyment, 1965; Oboh-Ikuenobe et al., 2005). According to Obi et al. (2001), deposition of the

Nsukka Formation represented a phase of fluvio-deltaic sedimentation that began close to the end of the Maastrichtian and continued during the Paleocene.

The Imo Formation consists of blue-gray clays and shales and black shales with bands of calcareous sandstone, marl and limestone (Reyment, 1965). The sediments reflect shallow-marine shelf conditions in which foreshore and shoreface sands formed occasionally (Reijers et al., 1997). The Imo Formation is considered to be the outcrop lithofacies equivalent of the Akata formation in the subsurface Niger Delta (Avbovbo, 1978; Oboh-Ikuenobe et al., 2005; Table 2.1). The shales contain a significant amount of organic matter and are potential source rocks for hydrocarbons in the eastern part of the Niger Delta and in the Anambra Basin (Reijers et al., 1997).

The Ameki Group consists of the laterally equivalent Nanka Sand, Nsugbe Formation, and Ameki Formation (Nwajide, 1979). It is represented by an alternation of sands, silts, and clays in various proportions and thicknesses. These sediments have been interpreted as continental, prodeltaic, estuarine, lagoonal, and open marine, based on the faunal content (White, 1926; Adegoke, 1969, Nwajide, 1979; Fayose and Ola, 1990; Reijers et al., 1997).

The Ogwashi-Asaba Formation comprises alternating coarse-grained sandstone, lignite seams, and light colored clays of continental origin (Kogbe, 1976). It was deposited in alluvial or upper coastal plains environments following a southward shift of deltaic deposition into a new depocenter (Doust and Omatsola, 1990). The Ameki Group and the Ogwashi-Asaba Formation correlates with the Agbada Formation in the Niger Delta (Table 2.1).

Table 2.1. Correlation of subsurface formations in the Niger Delta with surface equivalents in Southeastern Nigeria (from Oboh-Ikuenobe et al., 2005).

Subsurface			Surface		
Youngest known age	Formation	Oldest known age	Youngest known age	Formation	Oldest known age
Recent	Benin	Oligocene	Plio-Pleistocene	Benin	Oligocene
Recent	Agbada	Eocene	Miocene Eocene	Ogwashi-Asaba Ameki	Eocene Eocene
Recent	Akata	Eocene	Eocene	Imo	Paleocene
Equivalent not known			Paleocene	Nsukka	Maastrichtian

2.2. CÔTE D'IVOIRE-GHANA TRANSFORM MARGIN

The Côte d'Ivoire-Ghana (CIG) Transform Margin was the focus of drilling during ODP Leg 159 in January-February, 1995. The four sites (959 though 962) were drilled on the Côte d'Ivoire-Ghana Marginal Ridge (Fig. 2.3), a prominent marginal ridge that defines the continental margin along a fossil transform boundary (Mascle et al., 1996). This study focuses on the Early Paleogene interval of Site 959, which is situated on the continental slope off the southwest coast of Ghana at a water depth of 2090.7 m (Figs. 1.1 and 2.3).

2.2.1. Tectonics. The Romanche Fracture Zone, which offsets the equatorial Mid-Atlantic Ridge, resulted from major transform displacement between the African and South American plate boundaries during the Early Cretaceous (Benkhelil et al., 1998). The CIG Transform Margin is a product of this motion and it exhibits a characteristically north-south segmented trend off the western shore of Africa. The northern region is composed of the eastern Ivorian continental slope and the southwestern Ghanaian upper slope (known provincially as the Deep Ivorian Basin). It is bordered to the south by the prominent northeast/southwest trending segment defining the continental margin, known as the Côte d'Ivoire-Ghana Marginal Ridge. The CIG Marginal Ridge occurs along the transition between laterally thinned continental crust to the north and adjacent oceanic crust to the south. This geographical setting includes a laterally connecting fossil ridge with the Romanche Fracture Zone (Fig. 2.3).

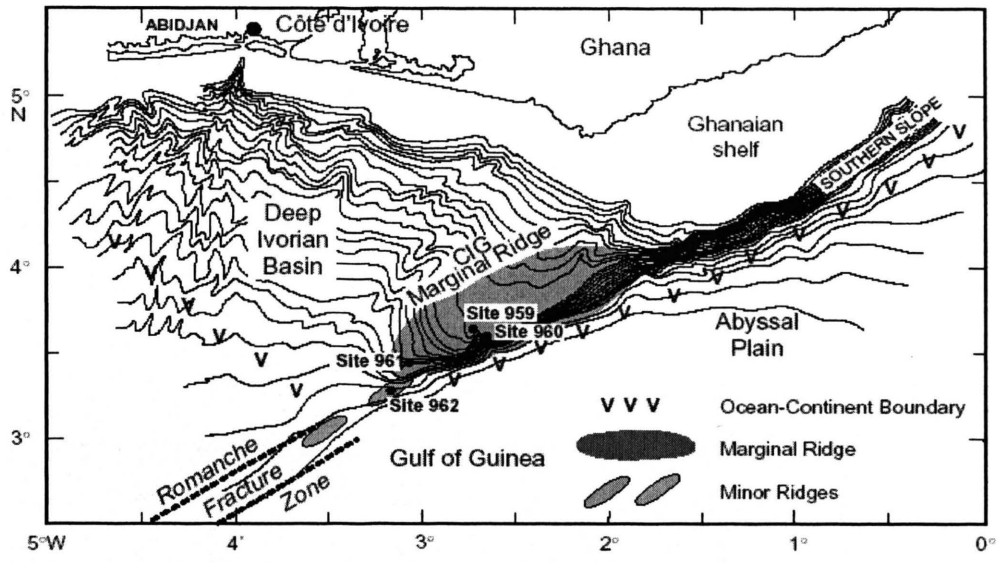

Figure 2.3. Simplified bathymetry and main morphostructural domains of the Côte d'Ivoive-Ghana Transform Margin: solid circles show location of Leg 159 sites, the Vs indicate the probable continent-ocean transition (from Mascle et al., 1996).

The CIG Transform Margin has undergone four major tectonic phases (Mascle et al., 1996; Benkhelil et al., 1998). The Early Cretaceous (Neocomian and Aptian) rift system formed at the emplacement of the Deep Ivorian Basin and the CIG Marginal Ridge with the still-joined West African and South American blocks. Faulted and tilted blocks created a series of sub-basins subjected to continental sedimentation under fluvial, deltaic and lacustrine conditions (Fig. 2.4). The Aptian-Albian marine siliciclastic sediments represent the syntransform stage. During this stage West Africa and South America split apart along the southern edge of the Deep Ivorian Basin, producing a wide zone of wrenching with the formation of pull-apart basins. This was followed by the end of syntransform stage during the Late-Albian (Fig. 2.4). Transcurrent tectonics were active throughout Albian times and were probably responsible for uplift of the CIG Marginal Ridge. The uplift initiated during the previous stage was accentuated, the sediments were deformed, and the marginal ridge top was extensively eroded during part of the Cenomanian as a direct consequence of uplift and subsequent emersion. The commencement of the last stage (passive margin) is marked by a second distinctive unconformity recorded between the uppermost Albian and lower Turonian deposits at all

sites. The West African and South American blocks were separated and the CIG Marginal Ridge bordered on a newly formed oceanic crust.

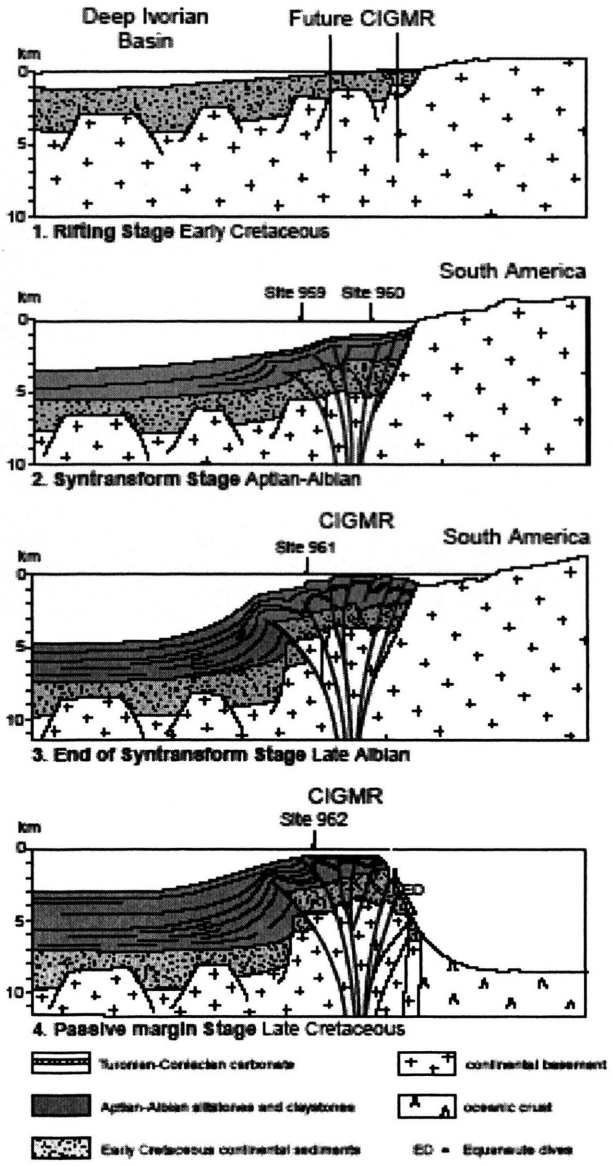

Figure 2.4. Interpretative schematic cross sections of the Deep Ivorian Basin and Côte d'Ivore-Ghana Transform Margin, illustrating evolution from Early Cretaceous to Late Cretaceous times (from Benkhelil et al., 1998).

2.2.2. Stratigraphy and sedimentology. Five lithologic units (I to V) were recognized by the Shipboard Scientific Party (1996), along 1158.9 m of stratigraphic section at site 959 (Fig. 2.5). The following paragraphs are a summary of their findings.

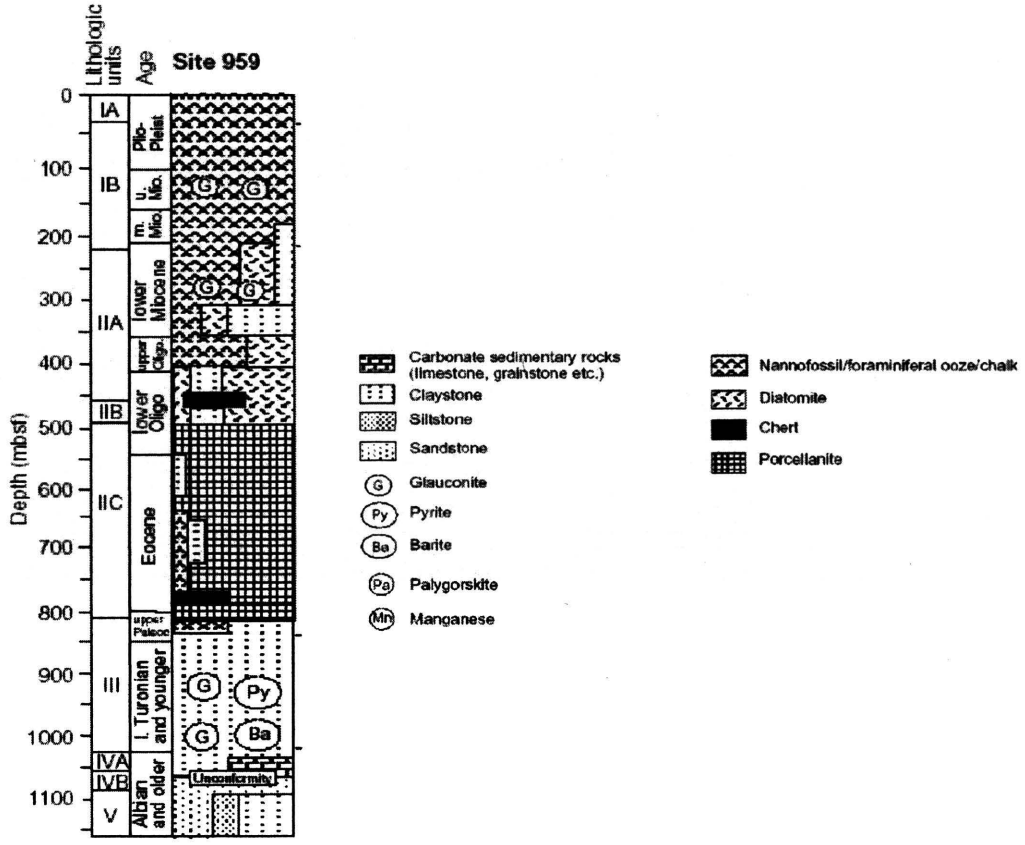

Figure 2.5. Schematic stratigraphic column for ODP site 959. Lithologic units I to V are those determined by the Shipboard Scientific Party (1996) (from Strand, 1998).

Going downsection, lithologic Unit I, Holocene to lower Miocene, comprises 208.0 m of dominantly pelagic, calcareous sediment with two-end member sediment components: nannofossil ooze and chalk, and foraminifer ooze and chalk. This unit was deposited in a basin subjected to cyclic variations in the oxygen content of its bottom waters. It is subdivided into two lithologic subunits because the upper 23 m has a darker color resulting from increased pyrite and organic matter levels.

Unit II comprises 599.3 m of diatomite, chert and porcellanite of Early Miocene to Late Paleocene age. Deposition of this unit indicates general basinal conditions with an increased nutrient supply, which caused siliceous microfossils to dominate the planktonic community. Based upon the preservation of siliceous microfossils, the Shipboard Scientific Party divided this unit into three lithologic subunits IIA to IIC. In general, with increasing depth, siliceous skeletal remains are progressively transformed to opal-CT, an intermediate stage in the recrystallization of biogenic silica to quartz.

Lithologic Unit III ranges in age from Late Paleocene to early Coniacian and comprises 231.0 m of dark gray to black claystone and claystone with microfossils. Based on benthic foraminiferal and trace fossil assemblages, the claystones have been interpreted to represent deposition in a deep-sea environment which underwent pelagic to hemipelagic sedimentation (Shipboard Scientific Party, 1996; Strand, 1998). Lithologic Unit IV comprises 38.4 m of sandy limestone, sandy dolomite, calcareous sandstone, and limestone of early Coniacian to early Turonian and older age. The limestones of lithologic unit IV indicate reef formation processes in a shallow shelf environment but likely represent periplatform deposits transported from shallow shelf settings (Strand, 1998). Lithologic Unit V comprises quartz sandstones embedded with silty claystone of Late Albian age. It represents intracontinental sedimentation under mixed deltaic, fluvial and lacustrine conditions (Strand, 1998).

3. LITERATURE REVIEW

The first part of this section provides an overview of previous palynological studies that focused on pollen, spores and particulate organic matter on Paleogene strata in tropical regions. It is followed by reviews of Early Paleogene dinocyst studies from various parts of the world, and previous biostratigraphic studies from the study area.

3.1. OVERVIEW OF TROPICAL PALEOGENE PALYNOLOGY

Few published studies of the Paleogene palynology of tropical areas exist, and this is due in part to the confidentiality of the petroleum companies working in these regions. The few publications comprise studies in northern South America (van der Hammen and Wijmstra, 1964; Muller et al., 1987; Jaramillo and Dilcher, 2001; Pardo-Trujillo et al., 2003, among others), West Africa (e.g., van Hoeken-Klinkenberg, 1966; Salard-Cheboldaeff, 1978; 1979; 1990), and Asia (e.g., Kar, 1985; Frederiksen, 1994; Mandal et al., 1994). The most reliable and commonly used zonation for the Tertiary of tropical areas was developed by Germeraad et al. (1968). They erected four types of zonations (Pantropical, Atlantic, Caribbean, and Borneo) for the Cretaceous to Pleistocene and based their interpretations on palynological information from outcrop and borehole materials in Venezuela, Nigeria and Borneo. Later publications by Regali et al. (1974), Muller et al. (1987), El Beialy (1998), and Jaramillo and Dilcher (2001), provided improved taxonomic and biostratigraphic resolution for tropical Paleogene palynomorphs.

Majority of the palynologic studies of the Paleogene of West Africa have been carried out in southern Nigeria, but publications from these studies are nevertheless few (e.g., Legoux et al., 1971; Adegoke et al., 1978; Jan du Chêne et al., 1978; Jan du Chêne and Salami, 1978; Legoux, 1978; Salard-Cheboldaeff, 1979; Keiser and Jan du Chêne, 1979; Salami, 1984). These studies focused on pollen and spores from continental and marine sediments. A brief synopsis of Cretaceous and Tertiary paleobotanical (mega- and microfossils) studies in Nigeria was done by Rao and Kumaran (1988). Publications by Salard-Cheboldaeff (1990) and Salard-Cheboldaeff and Dejax (1991) provided overviews of the Cretaceous to Recent paleofloral succession of West Africa; Salard-Cheboldaeff

and Dejax (1991) provided a Neocomian to Pliocene palynostratigraphic scale for marker pollen and spores.

A palynological study of Mid Cretaceous to Pliocene sediments of the Côte d'Ivore-Ghana Transform Margin was undertaken by Oboh-Ikuenobe et al. (1997). They used palynofacies and sporomorph thermal alteration index (TAI) data from all the ODP Leg 159 sites, to interpret thermal maturation, sediment provenance, and paleobathymetry. Oboh-Ikuenobe et al. (1999) studied the palynofacies and dinocysts of the Late Oligocene to Miocene interval in Hole 959D. Other palynological studies have focused on the palynostratigraphy of the Cretaceous and Early Paleocene intervals (Masure et al., 1998, and Oboh-Ikuenobe et al., 1998). De la Rue (2000) and de la Rue and Oboh-Ikuenobe (2003) studied the sporomorph (pollen-spores) composition and distribution of the dispersed organic material in the upper Paleocene-to lower Oligocene sediments at site 959. They interpreted how climate-driven vegetation successions responded to fluctuations in humidity and precipitation. In addition, they used fluctuations in the microplankton (dinocysts and acritarchs) populations to recognize episodic, pronounced intervals of nutrient enrichment in marine surface waters.

3.2. EARLY PALEOGENE DINOCYST STUDIES

Summaries of biostratigraphic and paleoecologic dinocyst studies of Paleogene strata across the world can be found in several papers, including Williams and Bujak (1985), Stover et al. (1996), Williams et al. (2004), and Sluijs et al. (2005). Primarily, detailed records of Early Paleogene dinocysts come from mid- and high latitudes of the northern hemisphere (e.g., Caro, 1973; Costa and Downie, 1976, Chateauneuf and Gruas-Cavagnetto, 1978), where intensive research related mainly to petroleum exploration has resulted in a number of biostratigraphic studies for such areas as the North Sea Basin (Bujak and Mudge, 1994; Mudge and Bujak 1996), Denmark (Heilmann-Clausen, 1985), southeast England (Powell et al., 1996), western North Atlantic (Damassa, et al., 1990), and western Siberia (Iakovleva and Kulkova, 2003). Dinocyst data from the southern hemisphere are confined mainly to such high latitude areas as Southern Chile (Quattrocchio and Sarjeant, 2003), Australia (Deflandre and Cookson, 1955; Cookson and Eisenack, 1965; 1967; Patridge, 1976), New Zealand (Wilson, 1984; 1988; Crouch,

2001), Antarctica (Wrenn and Hart, 1984), and Tasmania (Brinkhuis et al., 2003; Williams et al., 2004).

Some dinocyst research has been carried out in low to mid latitude areas, specifically Tunisia (Crouch et al., 2003; Guasti et al., 2005), Pakistan (Kothe et al., 1988), India (Varma and Dangwal, 1964; Mehrotra and Singh, 2003), the US Gulf Coast (Firth, 1987; Gregory and Hart, 1995), and California (Damassa, 1979a, 1979b). The dinocyst data available for equatorial areas are rather sparse and are derived mainly from West Africa (e.g., Jan du Chêne and Adediran, 1985; Jan du Chêne, 1988) and northern South America (Jaramillo and Dilcher, 2001; Regali et al., 1974), but these studies have yet to be calibrated with other microfossil groups. Tropical dinocyst zonal schemes are currently unavailable for the Early Paleogene.

3.3. PREVIOUS BIOSTRATIGRAPHIC RESEARCH IN THE STUDY AREA

3.3.1. Southeastern Nigeria. The Early Paleogene calcareous microfossil biostratigraphy of Southeastern Nigeria has been studied by Berggren (1960), Reyment, (1965), and Adegoke (1969). Relevant macrofossil (vertebrate and invertebrate) biostratigraphic and paleoenvironmental studies include those by White (1926), Adegoke et al. (1980), and Arua (1980).

In the Alo-1 well, analyses of terrestrial and marine palynomorphs provide the main biostratigraphic control for the section. In a preliminary unpublished biostratigraphic study, Shell Petroleum Development Company of Nigeria identified the tops of two pollen zones, P200 and P100, at 274 m and 622 m respectively (Shell Petroleum, 1976). According to Evamy et al. (1978), zone P200 is Late Paleocene in age, while zone P100 is Early Paleocene. No further palynomorph zones were identified in that study (Fig. 3.1).

Willumsen et al. (2004) identified four informal dinocyst zones A to D in the interval from 878 to 1694 m. Based on the presence of some stratigraphically important taxa, zones A to C were assigned an Upper Maastrichtian age and the uppermost zone D (878 to 1097 m) was assigned a Lower Paleocene (Danian) age. Samples for this study were collected from above the interval studied by Willumsen et al. (Fig. 3.1).

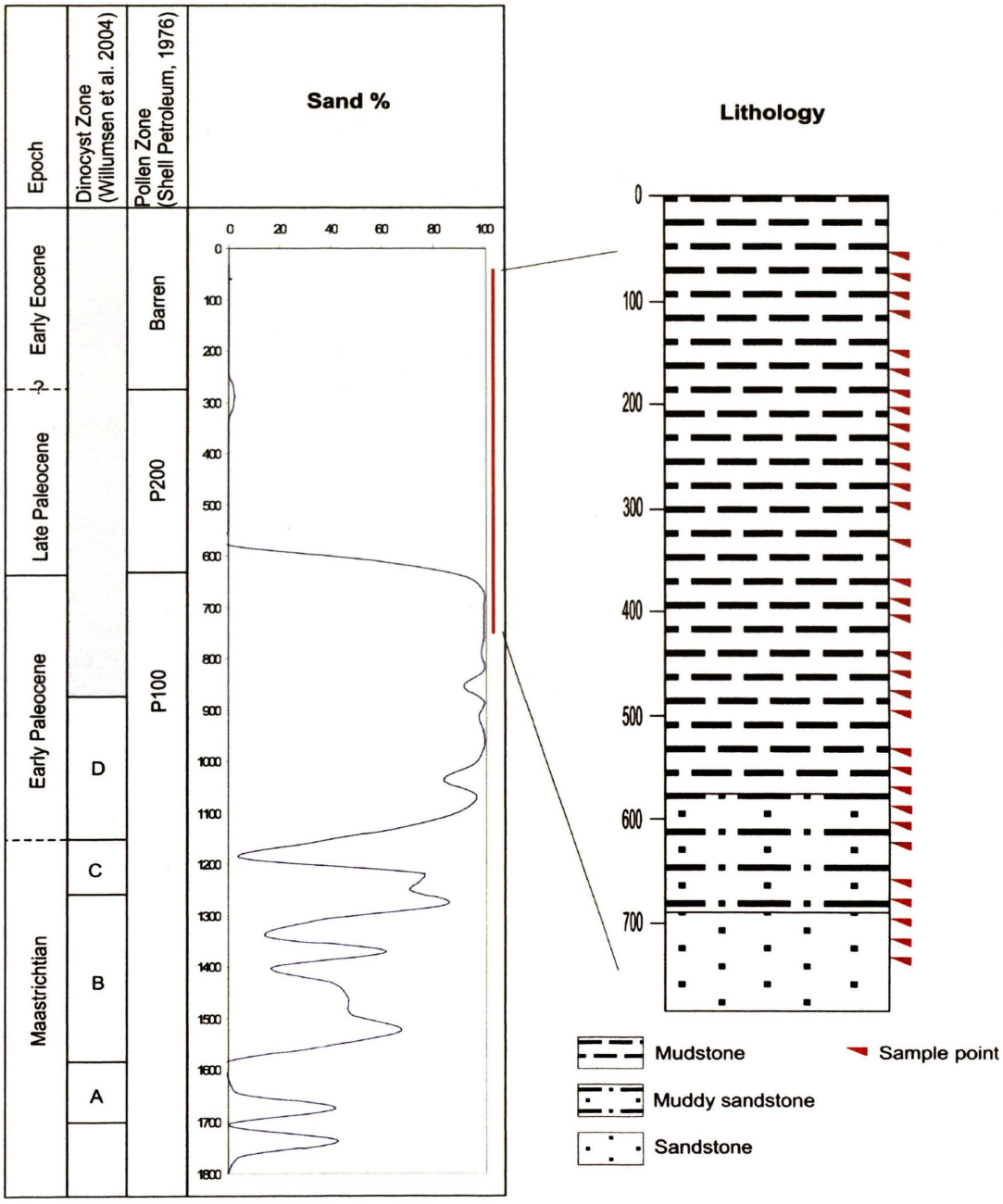

Figure 3.1. Summary of biostratigraphic and lithologic data for Alo-1 well. A lithological column for the interval studied and sample points are shown. Sand percentage profile was constructed from Sand versus Shale data provided by Shell Petroleum (1976).

3.3.2. Cote d'Ivoire Ghana Transform Margin. Several microfossil biostratigraphic studies exist for the Paleogene interval in the Côte d'Ivore-Ghana Transform Margin (Shafik et al., 1998; Kuhnt et al., 1998; Bignot, 1998, Norris, 1998). Of these studies, Shafik et al. (1998) and Kuhnt et al. (1998) are the most relevant to this study because they proposed revised ages for portions of lithologic Unit III, and subunit IIC at site 959.

Kuhnt et al. (1998) studied the deep-water agglutinated foraminiferal biostratigraphy of the Campanian-Paleocene interval in Hole 959D (cores 159-959D-65R to 43R). They assigned an Early Paleocene age to core 159-459D-48R (860.6-870.2 mbsf), which is characterized by an acme of *Spiroplectammina spectabilis.* In addition, based on the first occurrence of *Reticulophragmoides jarvisi,* a Late Paleocene (Selandian/Thanetian) age was assigned to the interval above sample 159-959D-44R, CC (831.2 mbsf). Samples above this depth contain typical Late Paleocene taxa.

Shafik et al. (1998) studied the Late Paleocene-Early Eocene calcareous nannofossil biostratigraphy in Hole 959D, and identified five (sub)zones (CP7-CP9b). They placed the approximate top of the Paleocene at the CP8a-CP8b subzonal boundary (section 159-959D-41R-CC at ~808 mbsf), which was defined using the last occurrence of species of *Fasciculithus.* Erection of zones for the Early Paleocene was precluded because of the absence of calcareous nannoplankton in the black claystones of lithologic Unit III (Fig. 3.2).

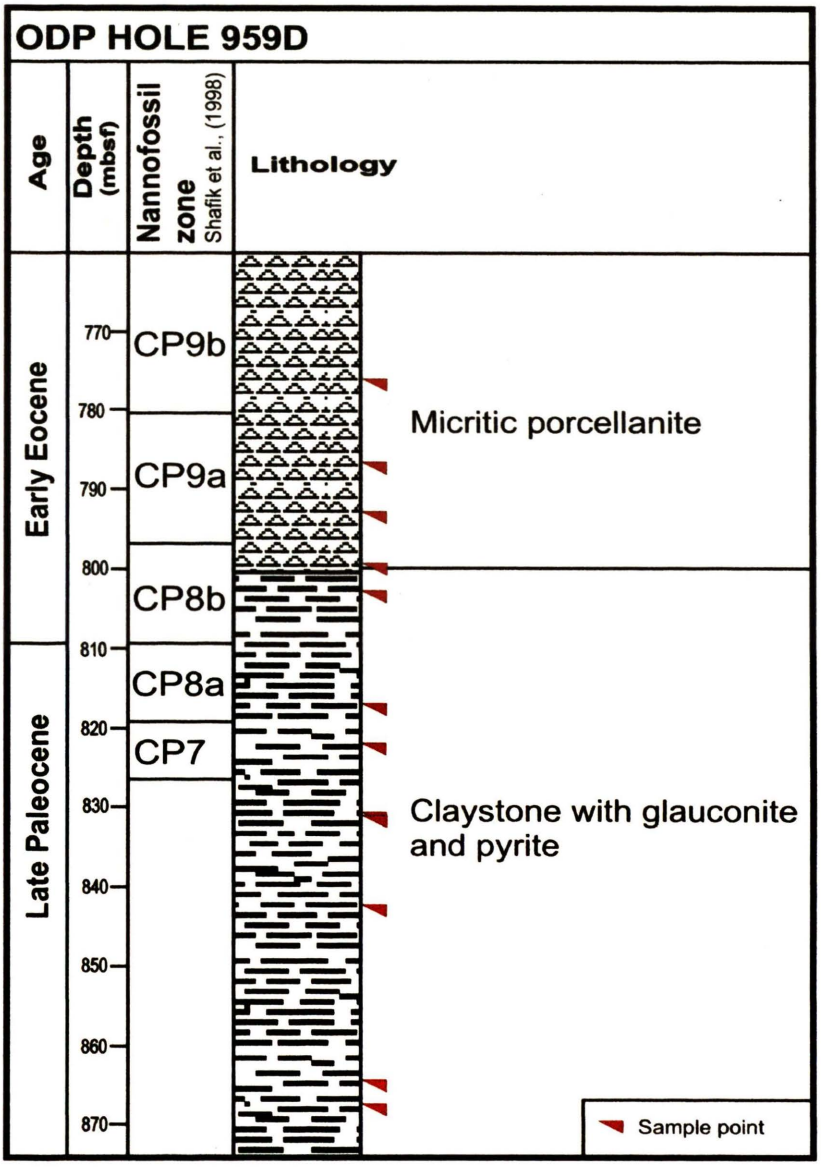

Figure 3.2. Calcareous nannofossil biostratigraphy and lithology in the interval studied in ODP Hole 959D.

4. MATERIAL AND METHODS

Palynological samples for this study come from two sources: 1) Ditch cutting samples from the Alo-1 well, drilled in the Anambra Basin, Southeastern Nigeria by Shell Petroleum Development Company of Nigeria in 1976; and 2) Core samples from ODP Hole 959D, drilled in 1995 on the continental slope off the southwest coast of Ghana (position 3°37.656'N, 2°44.149'W), at a water depth of 2090.7 m (see Fig. 1.1). Thirty-three samples from the Paleocene-Early Eocene interval in Alo-1 and 12 samples from Hole 959D, were analyzed for their dinocyst content. The sample locations in the intervals examined for Alo-1 and Hole 959D are shown in Figures 3.1 and 3.2, respectively. Tables 4.1 and 4.2 list all the samples analyzed in this study.

Standard laboratory techniques of digesting the sediments in hydrochloric and hydrofluoric acids, and centrifuging in heavy liquid ($ZnBr_2$) were used to separate the organic fraction of the samples (Traverse, 1988). Organic residues were then oxidized using Schultze solution ($KClO_3$ plus HNO_3), and screened through 10 μm sieves. Both unoxidized and oxidized palynological residues were used for mounting the palynological slides. Since oxidation, heavy liquid separation, and sieving remove much of the very fine organic matter of the sample, a palynofacies analysis was not conducted. The slides from Hole 959D used for dinocyst analyses were stained red with safranin, while those from Alo-1 were not stained. Slides are currently being stored in the palynological collection of the Paleontology Laboratory at the University of Missouri-Rolla (UMR). They will be permanently curated at a national museum to be chosen later.

For routine identification and description of the dinocysts, a Leica CME transmitted light microscope (#5 in the Paleontology Lab at UMR) was used. Taxonomical assignations were done by comparison with published illustrations and by consulting the original descriptions of taxa in the palynological collection of the Geological Survey of Canada in Dartmouth, Nova Scotia. Taxa of major relevance to this study were photographed using bright field phase contrast on a Zeiss Axioplan 2 microscope and differential interference contrast illumination on Nikon Optiphot2-Pol and Zeiss Axioskop 2 Plus microscopes. Microphotographs were taken using Nikon Coolpix cameras. Corel PHOTO-PAINT was used to enhance brightness and contrast.

Table 4.1. List of samples and sample depths for Alo-1 well. The prefixes R- and B- denote two batches of samples processed at different times.

Sample #	Depth (m)		Sample #	Depth (m)		Sample #	Depth (m)
R-1134-2	54.9		R-1134-7	329.2		B-12275	621.8
B-11286	73		B-11294	365.8		R-1134-13	658.4
B-11287	91.4		R-1134-8	384		B-12276	676.6
R-1134-3	109.7		B-11295	402.3		B-12277	695
B-11288	146.3		R-1134-9	438.9		R-1134-14	713.2
R-1134-4	164.6		B-12270	457.2		B-12278	731.5
B-11289	182.9		B-12271	475.5		R-1134-15	768.1
B-11290	201		R-1134-10	493.7			
R-1134-5	219.4		B-12272	530.3			
B-11291	237.7		R-1134-11	548.6			
B-11292	256		B-12273	566.9			
R-1134-6	274.3		B-12274	585.2			
B-11293	292.6		R-1134-12	603.5			

Table 4.2. List of samples and sample depths for ODP Hole 959D.

Sample, hole-core-section, Interval (cm)	Depth (mbsf)		Sample, hole-core-section, Interval (cm)	Depth (mbsf)
159-959D-39R-2, 51-56	776.32		159-959D-44R-7, 133-136	830.93
159-959D-40R-3, 80-86	787.35		159-959D-45R-1, 0-4	831.64
159-959D-41R-1, 32-37	793.35		159-959D-46R-1, 95-100	842.25
159-959D-41R-5, 85-91	799.88		159-959D-48R-3, 65-68	864.25
159-959D-42R-1, 52-56	803.12		159-959D-48R-5, 96-100	867.6
159-959D-43R-4, 50-53	817.3			
159-959D-44R-2, 4-6	822.14			

A minimum of 300 dinocysts were counted per slide, except for those samples with poor yields, in order to record the relative abundance of each taxon. After counting, the slides were scanned and the presence of species that were not included in the count was recorded. Additionally, a minimum of 200 sporomorphs vs. dinocysts were counted in order to record variations in the proportion of terrestrial and marine components related to changes in the depositional site. The quantitative data were converted to percentages and discussed with reference to the following percentage categories: rare (1-5%), common (6-10%), frequent (11-20%), abundant (21-40%) and superabundant (>40%).

Once the geologic ranges of dinocyst taxa in Alo-1 and Hole 959D were established, the boreholes were correlated using last appearance datum (LAD) or last abundance datum of one or more taxa. The use of first appearance datum (FAD) or first abundance datum was avoided because all the palynological samples from Alo-1 are ditch cuttings that may have been contaminated by caving. Published calcareous nannoplankton data of the Early Paleogene interval of ODP Hole 959D (Shafik et al., 1998) was used to calibrate the dinocyst bioevents with the geologic time scale of Berggren et al. (1995; Fig. 4.1). The chronological terminology for the Paleocene/Eocene boundary adopted in this study was proposed by Aubry et al. (2003), who recommended the reintroduction of the Sparnacian Stage for the interval between the Paleocene/Eocene boundary (placed at the level of the carbon isotope excursion at 55.5 Ma), and the base of the Ypresian stage (Fig. 4.1).

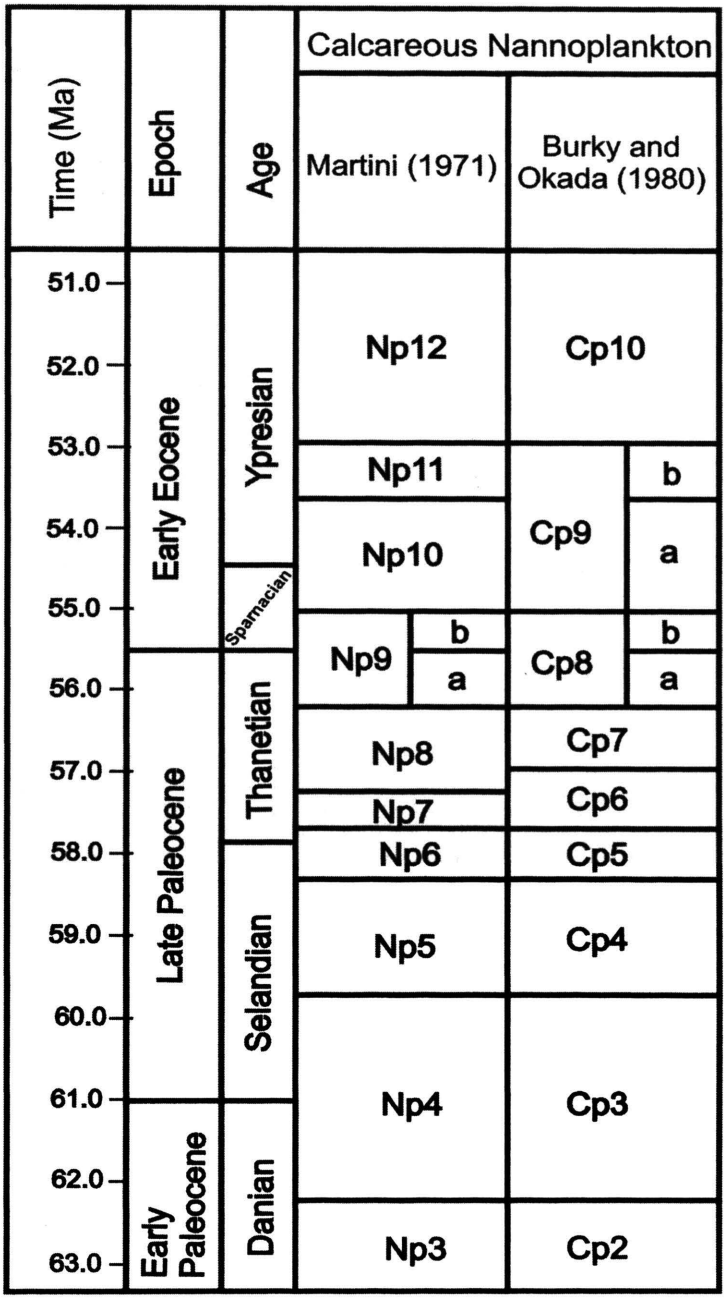

Figure 4.1. Calcareous nannoplankton bioevents in the Paleocene-Early Eocene interval (~63-51 Ma), according to the chronology of Berggren et al. (1995). The terminology for the Paleocene/Eocene boundary was proposed by Aubry et al. (2003). NP (nannofossils-Paleogene) biozonation after Martini (1971); CP (calcareous-Paleogene) biozonation after Okada and Burky (1980).

5. RESULTS

5.1. INTRODUCTION

Palynomorph recovery in Alo-1 well and ODP Hole 959D varies from poor to excellent and preservation is generally good. Pollen and spores are common in most samples but they are generally less abundant than dinocysts. Terrestrial components (pollen and spores) typically represent between 30 and 50% of the palynomorph count in Alo-1 and < 25% in Hole 959D, but they occur in percentages as high as 67% in some samples from Alo-1 and 41% in Hole 959D. A general decrease in the percentage of terrestrial palynomorphs is recorded from bottom to top in both sections (Fig. 5.1). Detailed analysis of pollen and spores was not attempted in this study.

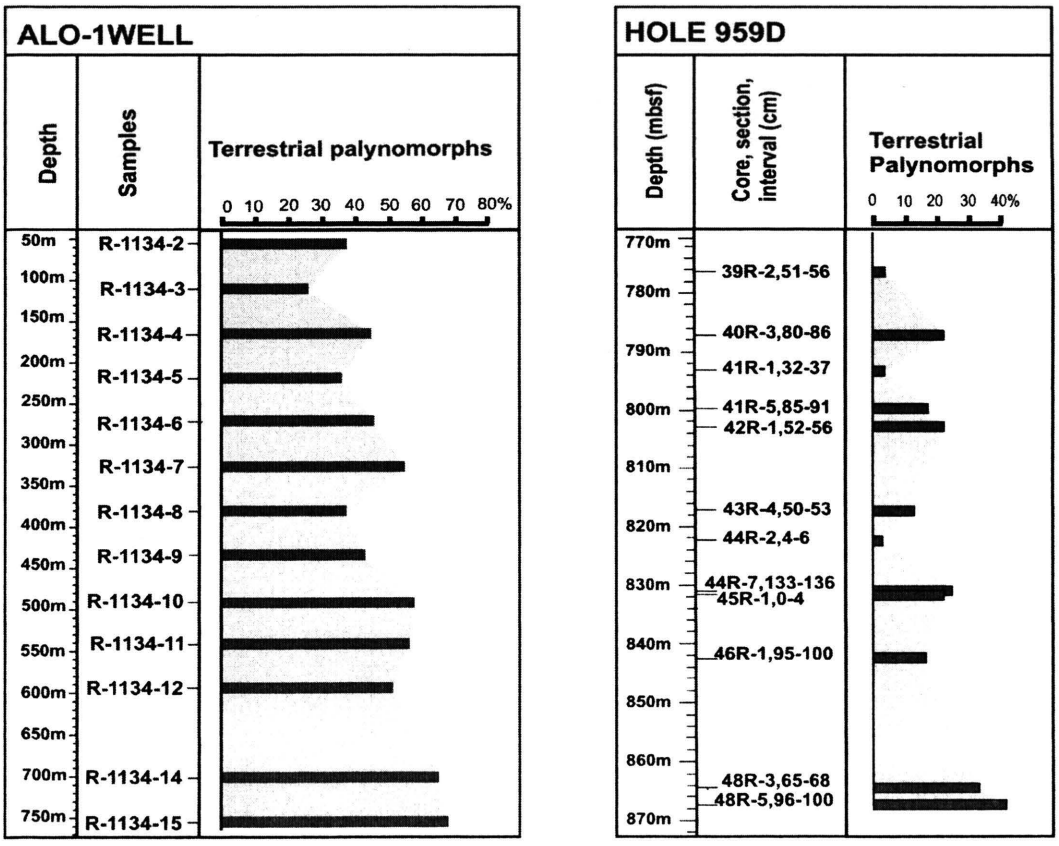

Figure 5.1. Plot of the percent terrestrial palynomorphs (pollen and spores) with depth in Alo-1 well and Hole 959D.

Sixty four dinocyst taxa were identified in Alo-1 and 54 in Hole 959D. The identified dinoflagellate cysts in both sections are listed alphabetically in section 5.2 and those of major relevance to this study are illustrated in Plates 1 to 6 (Appendix A). Appendices B and C list the total dinocyst counts for Hole 959D and Alo-1, respectively. Samples from Hole 959D generally yielded abundant and well preserved dinocyst assemblages (Appendix B). On the other hand, recovery and preservation was variable among the Alo-1 samples: Samples designated with the prefix R- (see Table 4.1) yielded abundant (generally >150) and well preserved dinocysts (Appendix C). In contrast, samples denoted with the prefix B- yielded few (<40) and poorly preserved dinocysts. Processing these sets of samples at different times most likely played a role in the preservation of dinocysts recorded in this study. Only samples from both boreholes with dinocyst counts >100 have been used for quantitative analysis and included in Figs. 5.1, 5.4, and 5.5.

5.2. SYSTEMATIC PALEONTOLOGY

All dinoflagellate cyst taxa found in Alo-1 well and Hole 959D are listed alphabetically according to their genera. Illustrated taxa are identified by plate and figure number. Systematics follow Fensome et al. (1993) to subclass level, whereas generic allocation of taxa and authorships follow Fensome and Williams (2004), unless otherwise stated. Some potentially new taxa have been identified and they are discussed below. These new taxa are designated with a letter (e.g., *Achomosphaera* sp. A), or given informal names indicated by quotation marks (e.g., *Ifecysta "heterospinosa"* or *Ifecysta "bipolaris"*). Quotation marks are used when several tentative new species of the same genus are described. Taxa designated with a number (e.g., *Canningia* sp. 1) are not perceived as new, but were not identified to species level due to time constraints or complex morphology. Informal names that have already been proposed in the literature (mainly from Fensome and Williams, 2005) and accepted in this work are indicated by an asterisk (*) and discussed in the text. Synonymies informally proposed in this study are also indicated. Refer to Appendix D for general illustrations and glossary of the terms used for the descriptions of the taxa below.

Division DINOFLAGELLATA (Bütschli 1885) Fensome et al. 1993
Subdivision DINOKARYOTA Fensome et al. 1993
Class DINOPHYCEAE Pascher 1914
Subclass PERIDINIPHYCIDAE Fensome et al. 1993

Achilleodinium bianii Hultberg 1985

Achilleodinium? sp.; Plate 1, Figure 1.
Remarks: This taxon is tentatively assigned to *Achilleodinium,* based on the morphology of the processes. These, are mesotabular to penitabular, hollow, distally closed and variable in size and shape depending on paraplate series; large boxlike processes occur in the pre- and postcingular and antapical series, and smaller cylindrical processes can be found on the apical zone. Paracingular and parasulcal areas lack processes. The cyst is proximochorate with a membranous periphragm. Archeopyle was not clearly observed but may be precingular (3").

Achomosphaera ramulifera (Deflandre 1937) Evitt 1963

Achomosphaera sp. A; Plate 1, Figure 2.
Description: Proximochorate cyst, spherical to subspherical body, slightly fibrous periphragm closely appressed to the endophragm except at the bases of processes. Processes are gonal, buccinate to infundibular, hollow, expanded distally with trifurcate or commonly quadrifurcate terminations. Some adjacent processes might be connected along their bases by thin lines of periphragm. Archeopyle is precingular, type $P_{3"}$, operculum free.
Size: 60-70 μm long, 50-60 μm wide (3 specimens measured).
Remarks: Differs from other species of *Achomosphaera* in having buccinate to infundibular, hollow, processes with trifurcate or quadrifurcate terminations.

Achomosphaera spp.

Adnatosphaeridium membraniphorum Jan du Chêne and Adediran 1985; Plate 1, Figure 3.

Adnatosphaeridium multispinosum Williams & Downie 1966; Plate 1, Figure 10.

Adnatosphaeridium sp.
Remarks: This includes poorly preserved specimens of *Adnatosphaeridium* that were not identifiable down to species level.

Andalusiella? sp.
Remarks: One poorly preserved specimen recovered from Alo-1 well, generally resembles the morphology of *A. rhomboides* with a rhomboidal central body, one apical horn, apparently only one antapical horn and a verrucose periphragm and verrucose endophragm. However, the state of preservation of this specimen makes it difficult to identify the orientation of the cyst, and therefore any taxonomic assignment very doubtful.

Apectodinium spp.; Plate 1, Figures 4 to 7.
Remarks: A variety of *Apectodinium* morphotypes within the *A. homomorphum-A. paniculatum* morphological complex are recognized. These taxa display wide variations in the development of apical, lateral and antapical horns and usually occur in abundant quantities in the samples, making species differentiation difficult. Species identified include *A. homomorphum, A. quinquelatum, A. parvum,* and *A. paniculatum.*

Apteodinium sp. A; Plate 1, Figures 8 and 9.
Description: Proximate gonyaulacoid cyst, acavate, subspherical to subpolygonal body, with one short apical horn and a microreticulate autophragm. Paracingulum delineated by a shallow transverse equatorial depression sometimes not clearly discernible. Archeopyle is precingular, type $P_{3''}$, operculum free.
Size: 43-55 μm long (without apical horn), 40-44 μm wide, apical horn 5-13 μm long (4 specimens measured).

Remarks: Differs from other species of *Apteodinium* in the character of the autophragm which is microreticulate.

Areoligera gippingensis Jolley 1992; Plate 1, Figure 11.

Areoligera spp.

Areosphaeridium sp. A; Plate 1, Figures 12 and 13.
Description: Chorate gonyaulacoid cyst, subspherical to ellipsoidal central body. Acavate. Processes mesotabular, solid, infundibular. Distal terminations of the processes may be clypeate, simulating the shapes of underlying individual paraplates but generally have irregular margins. Adjacent processes may connect distally. Process stems vary from finely perforate to fenestrate; areas between process bases finely and irregularly perforated. There is a single process at the antapex. Archeopyle apical, type (tA), operculum free.
Size: 55-60 μm long, 60-65 μm wide, processes 25-30 μm long (3 specimens measured).
Remarks: Differs from *A. diktyoplokus* in having processes with distal terminations with irregular margins that occasionally connect adjacent processes. In *A. diktyoplokus* processes are mainly clypeate and are not connected distally.

Canningia sp. 1; Plate 2, Figure 1.
Description: Areoligeracean proximate cyst, lenticular body, differentiated autophragm with fibrous structure in penicontabular arrangement. Pandasutural areas of undifferentiated autophragm slightly discernible. Paracingulum delineated by a shallow transverse equatorial depression. Archeopyle apical, type (tA), operculum free.
Size: 56 μm long, 68 μm wide (1 specimen measured).

Cerodinium boloniense (Riegel 1974) Lentin and Williams 1989; Plate 2, Figure 2.

**Cerodinium glabrum* Gocht 1969; Plate 2, Figure 3.
Remarks: *Cerodinium glabrum* is used here to designate cysts assignable to *Cerodinium* that do not show excessive elongation or distinctive ornamentation of any sort (as described in Fensome and Williams, 2005).

Cerodinium sp.
Remarks: This includes poorly preserved specimens of *Cerodinium* unidentifiable down to species level.

**Cordosphaeridium "delimurum"*; Plate 2, Figure 4.
Remarks: *Cordosphaeridium "delimurum"* as proposed by Fensome and Williams (2005), is used here to designate cysts of *Cordosphaeridium* that are similar to *C. Inodes* and *C. gracile* but have a thin central body and processes with thinner, lacier walls.

Cordosphaeridium fibrospinosum Davey and Williams 1966

Cordosphaeridium spp.

Coronifera oceanica Cookson and Eisenack 1958; Plate 2, Figure 10.

Damassadinium sp. cf. *D. impages* (Damassa 1979a) Fensome et al. 1993; Plate 2, Figure 5.
Remarks: Cysts assignable to *Damassadinium* cf. *D. impages* differ from specimens of *D. impages* originally described by Damassa (1979a), in having smooth rather than fibrous body wall.

Damassadinium heterospinosum (Matsuoka 1983) Fensome et al. 1993; Plate 2, Figure 7.

Damassadinium spp.

Dapsilidinium spp.

Deflandrea oebisfeldensis Alberti 1959; Plate 2, Figure 15.

Diphyes sp. A; Plate 2, Figures 8 and 9 (= *Diphyes* sp. 1 Jan du Chêne 1988)
Description: Proximochorate gonyaulacoid cyst, with spherical central body. Processes numerous, nontabular, buccinate, distally bifid and nearly uniform except for the antapical process which is broader, hollow, with both sides of the outline concave and denticulate distal margin. Antapical process has the same length as the rest of the processes. Archeopyle precingular type $P_{3''}$, or combination precingular-apical, type $(4A_{1-4'})P_{3''}$.
Size: 40 μm long, 40-42 μm wide, antapical process 10-13 μm long (2 specimens measured).
Remarks: Differs from other species of *Diphyes* in having bifid processes.

Diphyes sp. B; Plate 2, Figure 13.
Description: Proximochorate gonyaulacoid cyst, with spherical central body. Processes numerous (up to 3 per major paraplate area), nontabular, solid, tapering, distally open, with denticulate distal margins; processes are nearly uniform except for the antapical process which is larger and cylindrical in shape. Archeopyle combination precingular-apical, type $(4A_{1-4'})P_{3''}$.
Size: 35 μm long, 42 μm wide, processes 10-12 μm long, antapical process 15 μm long (1 specimen measured).
Remarks: Differs from *D. colligerum* in having tapering, distally open processes with denticulate distal margins rather than oblate processes.

Enneadocysta sp.
Remarks: Includes poorly preserved specimens of *Enneadocysta* unidentifiable down to species level.

Eocladopyxis peniculata Mongenroth 1966; Plate 2, Figures 11 and 12.

Eocladopyxis sp. 1; Plate 2, Figure 14.
Remarks: Cysts assignable to *Eocladopyxis* sp. 1 are similar to *E. peniculata* but have shorter processes (< 2 μm).

Fibrocysta axialis (Eisenack 1965) Stover and Evitt 1978

Fibrocysta spp.

Glaphyrocysta divaricata (Williams and Downie 1966) Stover and Evitt 1978; Plate 2, Figure 6.

Glaphyrocysta ordinata (Williams and Downie 1966) Stover and Evitt 1978; Plate 3, Figure 1.

Glaphyrocysta spp.

Hafniasphaera hyalospinosa Hansen 1977; Plate 3, Figure 8.

Homotryblium abbreviatum Eaton 1976

Homotryblium tenuispinosum Davey and Williams 1966; Plate 3, Figure 10.

Hystrichokolpoma rigaudiae Deflandre and Cookson 1955; Plate 3, Figure 3.

Hystrichokolpoma unispinum Williams and Downie 1966

Hystrichokolpoma sp.
Remarks: Includes poorly preserved specimens of *Hystrichokolpoma* unidentifiable down to species level.

Hystrichosphaeridium tubiferum (Ehrenberg 1838) Deflandre 1937; Plate 3, Figure 11.

Ifecysta Jan du Chêne and Adediran 1985

Remarks: *Ifecysta* is a monospecific genus characterized by: 1) An ellipsoidal to fusiform body; 2) A precingular archeopyle (type $P_{3''}$ only); 3) Fibrous endophragm and periphragm; 4) Distinct apical and antapical horn-like protrusions formed by closely appressed endophragm and periphragm; and 5) Large and solid fibrous penitabular processes. Specimens included here exhibit the first four characteristics listed for the genus, but differ in the morphology of the processes, which vary between nontabular processes, penitabular septa, and solid fibrous penitabular processes. Closely appressed endophragm and periphragm in the horn-like protrusions are features emphasized by Jan du Chêne and Adediran (1985) in the definition of *Ifecysta* and these are also consistent features in the specimens observed in this study. Therefore, *Ifecysta* is considered to be the closest fit. Since the definition of *Ifecysta* is based on the description of *Ifecysta pachyderma* alone, I recommend modifying the diagnosis of the genus to include forms with fibrous, nontabular processes and penitabular septa as well.

Ifecysta "bipolaris"; Plate 3, Figures 2, 4, 5, and 6.

Description: Cysts assignable to *Ifecysta "bipolaris"* are proximochorate with an ellipsoidal to fusiform body, fibrous endophragm and periphragm and distinct apical and antapical horn-like protusions. These protrusions can be as long as 30 μm. Endophragm and periphragm closely appressed together even apically and antapically. Fibrous expansions at the top of the horn-like protrusions are usually present. Processes nontabular (up to 3 per paraplate area), fibrous, tubiform to buccinate, of variable sizes among specimens. Paracingulum and parasulcus poorly defined. Archeopyle precingular, type $P_{3''}$, operculum free.

Size: 75-120 μm long (including apical and antapical horn-like protrusions), 45-65 μm wide, processes 10-20 μm long (7 specimens measured).

Remarks: *Ifecysta "bipolaris"* differs from *Ifecysta pachyderma* in having fibrous, nontabular tubiform to buccinate processes rather than large solid penitabular proceses.

Ifecysta "heterospinosa"; Plate 3, Figures 7 and 9.

Description: Cysts assignable to *Ifecysta "heterospinosa"* are proximochorate with an ellipsoidal to fusiform body, fibrous endophragm and periphragm and distinct apical and antapical horn-like protusions. Endophragm and periphragm closely appressed together even apically and antapically. Fibrous expansions at the top of the horn-like protrusions are usually present. Fibrous penitabular septa in simulate complexes delineate the major paraplate series. Paracingulum well defined by a series of linear complexes in transversal arrangement, each complex located in the center of the paracingular plate. Parasulcus not discernible. Paratabulation formula 4', 6'', 5s, 6''', 1'''', ?s. Archeopyle precingular, type $P_{3''}$, operculum free.

Size: 85-100 μm long (including apical and antapical horn-like protrusions), 60-70 μm wide, septa 15 μm high (4 specimens measured).

Remarks: Differs from *Ifecysta "bipolaris"* and *Ifecysta pachyderma* in having penitabular septa in simulate complexes rather than nontabular or large solid penitabular processes.

"Ifecysta" lappacea; Plate 4, Figures 1 and 2 (= *Fibrocysta lappacea* Drugg 1970)

Discussion: The generic description of *Fibrocysta* Stover and Evitt 1978 includes skolochorate cysts with small to long horn-like protussions and numerous solid or hollow, normally nontabular processes. However, the holotype of *Fibrocysta bipolaris* Cookson and Eisenack 1965, which is the type species of the genus does not exhibit projection of the endophragm outward below the horns, suggesting that the generic description of *Fibrocysta* requires some additional revision. Here I propose transferring *Fibrocysta lappacea* to *Ifecysta,* based on the presence of distinctive horn-like protrusions in the apex and the antapex, which I consider to be a determinant characteristic in the definition of the genus *Ifecysta.*

Remarks: Both *"Ifecysta" lappacea* and *Ifecysta "bipolaris"* have solid fibrous nontabular process, however, processes in *I. lappacea* are more densely distributed and thinner than in *I. "bipolaris"*.

Ifecysta pachyderma Jan du Chêne and Adediran 1985; Plate 4, Figures 6 and 12.

Ifecysta? "taeniata"; Plate 4, Figures 9 and 10.

Description: Cysts assignable to *Ifecysta? "taeniata"* are chorate, with a spherical to subspherical central body, fibrous endophragm and periphragm and a distinct antapical horn-like protrusion with outward projection of the periphragm. Fibrous expansions at the top of this protrusion usually present. Apical horn-like protrusion may be insinuated but is always poorly developed. Processes mesotabular, strongly fibrous, hollow, buccinate and nearly uniform in size. Paracingular processes strongly elongated transversely (taeniate). Paratabulation formula 4', 5-6'', 6c, 5''', 1'''', 3?s. Archeopyle precingular, type $P_{3''}$, operculum free.

Size: 45-65 μm long, 45-60 μm wide, processes 20-25 μm long (4 specimens measured).

Remarks: The morphology of *Ifecysta? "taeniata"* represents an intermediate stage between *Cordosphaeridium* and *Ifecysta*: *Cordosphaeridium* has a spherical to subespherical body without horn-like protusions, while *Ifecysta* has a fusiform body with distinct apical and antapical protrusions. Therefore, *Ifecysta? "taeniata"* does not exactly fit any of these generic descriptions. However, I consider *Ifecysta* to be the closest fit based on the presence on an antapical horn and the insinuation of an apical horn.

Comparison: *Ifecysta? "taeniata"* differs from other species of *Ifecysta* in lacking a distinct apical horn-like protrusion and having fibrous, buccinate, mesotabular processes.

Impagidinium celineae Jan du Chêne 1988; Plate 4, Figure 7.

Impagidinium crassimuratum Wilson 1988; Plate 4, Figure 8.

Impagidinium spp.

Impletosphaeridium spp.

Kallosphaeridium brevibarbatum De Coninck 1969

Kallosphaeridium orchiesense Jan du Chêne et al. 1985; Plate 4, Figures 3 and 4.
Remarks: Some individuals assignable to *Kallosphaeridium orchiesense* were observed to possess an epicystal archeopyle, type ($4A_{1-4}$,I_{1a})a6P_{1-6}'', not previously described for specimens of this genus.

Kallosphaeridium? sp. A; Plate 4, Figure 5.
Remarks: One specimen assignable to *Kallosphaeridium?* sp. A was recovered at Alo-1 well. It is characterized by having a proximate cyst, spherical to subspherical central body and smooth autophragm. Processes are nontabular, oblate, of nearly uniform size (~ 4 μm). Archeopyle epicystal, type ($4A_{1-4}$,I_{1a})a5-6P.
Size: Cyst diameter 40 μm.
Additional remarks: Assignment to *Kallosphaeridium* is tentative because of the configuration of the archeopyle which has not been described in species of this genus before.

Kallosphaeridium spp.

Lanternosphaeridium spp.; Plate 4, Figure 11; Plate 5, Figures 1 and 2.
Remarks: Taxa assignable to *Lanternosphaeridium* spp., are characterized by a radially disposed fibrous periphragm whose outer margin varies from deeply incised in parasutural areas to continuous throughout the cyst. These specimens were observed to represent several intermediate stages of a morphological series between *Ifecysta pachyderma* and *Lanternosphaeridium lanosum*. Taxa assigned to *Lanternosphaeridium* spp., however, do not have distinctive apical or antapical outward projections of the endophragm.

Lejeunecysta sp. 1; Plate 5, Figure 3.
Remarks: proximate peridinoid cyst, subpentagonal central body, acavate with poorly developed antapical horns. Autophragm smooth, brown-colored with numerous folds. Paracingulum indicated by parallel folds running transversally around the equatorial area. Archeopyle intercalary, type I_{2a}a.

Size: 100 μm long, 85 μm wide (2 specimens measured).

Magallanesium densispinatum (Stanley 1965) Quattrocchio and Sarjeant 2003; Plate 5, Figure 6.

Melitasphaeridium spp.

**"Minisphaeridium expansum"*; Plate 5, Figure 12.
Remarks: *Minisphaeridium* is an informal genus described by Fensome and Williams (2005) which is characterized by cysts that are small (~20 μm diameter, on average), proximochorate to chorate with apparently mesotabular processes and apical archeopyle. *M. expansum* is defined as a species of *Minisphaeridium* characterized by having taeniate processes.

Muratodinium spp.

**"Oligokolpoma"* sp. A; Plate 5, Figure 4.
Description: Chorate gonyaulacoid cyst, with ovoidal central body, acavate. Processes mesotabular of variable morphology including tubiform, flared and buccinate. Paracingular processes not clearly observed. Parasulcal processes distinctly thinner than pre- and postcingular processes. All processes except antapical are fenestrate, distally open and have denticulate distal margins or short tubules at their distal ends; antapical process is exceptionally large and bulbous in shape. Archeopyle apical, type (tA), operculum free.
Size: 55-60 μm long, 55-70 μm wide. Processes 15 μm long; antapical process 25-30 μm long (3 specimens measured).
Remarks: Specimens described here fit the informal generic description of *Oligokolpoma* Fensome and Williams 2005 which include taxa whose morphology generally resembles *Hystrichokolpoma* but lack paracingular processes.

Oligosphaeridium sp.
Remarks: This includes poorly preserved specimens of *Oligosphaeridium* unidentifiable down to species level.

Operculodinium tiara (Klumpp 1953) Stover and Evitt 1978; Plate 5, Figure 7.

Operculodinium spp.

Palaeocystodinium golzowenze Alberti 1961; Plate 5, Figure 14.

Palaeocystodinium sp. A; Plate 5, Figures 9 and 10.
Description: Proximate, cornucavate cyst, fusiform, with an ovoidal to subellipsoidal inner body, one short bluntly rounded apical horn and one short pointed antapical horn. Endophragm and periphragm are smooth. Archeopyle intercalary, type I_{2a}, hexa-style, isodeltaform.
Size: Endocyst 60-70 μm long, 45-55 μm wide. Length of horns: 12-23 μm (apical), 15-20 μm long (antapical) (5 specimens measured).
Remarks: This taxon can be distinguished from other species of *Palaeocystodinium* by its short bluntly rounded apical horn and short pointed antapical horn.

Phelodinium magnificum (Stanley 1965) Stover and Evitt 1978; Plate 5, Figure 8.

Polysphaeridium spp.; Plate 5, Figure 11.

Senoniasphaera sp.

Sentusidinium spp.
Remarks: Cysts assignable to *Sentusidinium* spp. are proximate and subspherical in shape, with numerous short, nontabular, uniformly distributed processes. Archeopyle apical, type (tA), operculum free.

Spinidinium sp.
Remarks: Includes poorly preserved assignable to *Spinidinium,* non recognizable down to species level.

Spiniferites microceras Cookson and Eisenack 1974

Spiniferites ramosus (Ehrenberg 1838) Mantell 1854

**Spiniferites "spongiosus"*
Remarks: *Spiniferites "spongiosus"* is an informal name used by Fensome and Williams (2005), to designate a species of *Spiniferites* with vesiculate, or spongy, autophragm in which the processes may contain occasional vesicles.

Spiniferites spp.

Tanyosphaeridium xanthiopyxides (Wetzel 1933) Stover and Evitt 1978

Tectatodinium rugulatum (Hansen 1977) McMinn 1988

Thalassiphora delicata Williams and Downie 1966; Plate 5, Figure 5.

Wilsodinium nigeriense Jan du Chêne and Adediran 1985; Plate 5, Figure 13.

Wilsodinium sp. A; Plate 7, Figures 3 to 6.
Description: Proximate peridinoid cyst, cornucavate, with one apical horn, two lateral horns and two antapical horns. All horns are prominent (as long as 30 μm) although size varies greatly from individual to individual. The endocyst is pentagonal with smooth walls. Periphragm smooth, bearing parasutural ridges supporting numerous short processes (< 4 μm), that may be acuminate or bifid. Continuity of parasutural ridges on the surface of the cyst is variable and in some individuals is only clearly discernible on

the ambitus and the surface of the horns. Archeopyle intercalary, type I/I_{2a} quadra-style, usually difficult to observe.

Size: 85-105 μm long (including apical and antapical horns), 80-110 μm wide (including lateral horns) (7 specimens measured).

Remarks: Differs from other species of *Wilsodinium* in the prominence of the apical, lateral and antapical horns.

5.3. STRATIGRAPHIC DISTRIBUTION OF DINOCYSTS

5.3.1. Alo-1. The stratigraphic distribution of selected taxa from Alo-1 is shown in Figure 5.2. The upper portion of Alo-1 (~ 50 to 218 m) is characterized by the presence of *Areosphaerdium* sp. A, *Ifecysta*? *"taeniata"*, *Glaphyrocysta ordinata, Glaphyrocysta divaricata, Polysphaeridium* spp., *Adnatosphaeridium* spp., *Spiniferites microceras* and *Muratodinium* spp. *Damassadinium* sp. cf. *D. impages* and *Impagidinium crassimuratum* are recorded only at 109.7 m. The last appearance datums (LADs) of *Apteodinum* sp. A, *Eocladopyxis* sp. 1, *Hafniasphaera hyalospinosa, Dyphies* sp. B, *Thalassiphora delicata*, *Wilsodinium* sp. A, and *"Oligokolpoma"* sp. A also occur at 109.7 m. *Phelodinium magnificum, "Ifecysta" lappacea, Damassadinium heterospinosum, Palaeocystodinium* sp. A, and *Cerodinium glabrum* all have their LADs toward the middle to upper middle part of the section at 164.6 m, 219.4 m, 329.2 m, 438.9 m and 475.5 m, respectively. *Impagidinium celineae* is only recorded at 493.7 m. The lower portion of the section, below 490 m, is characterized by the occurrence of *Magallanesium densispinatum, Areoligera gippingensis,* and *Diphyes* sp. A.

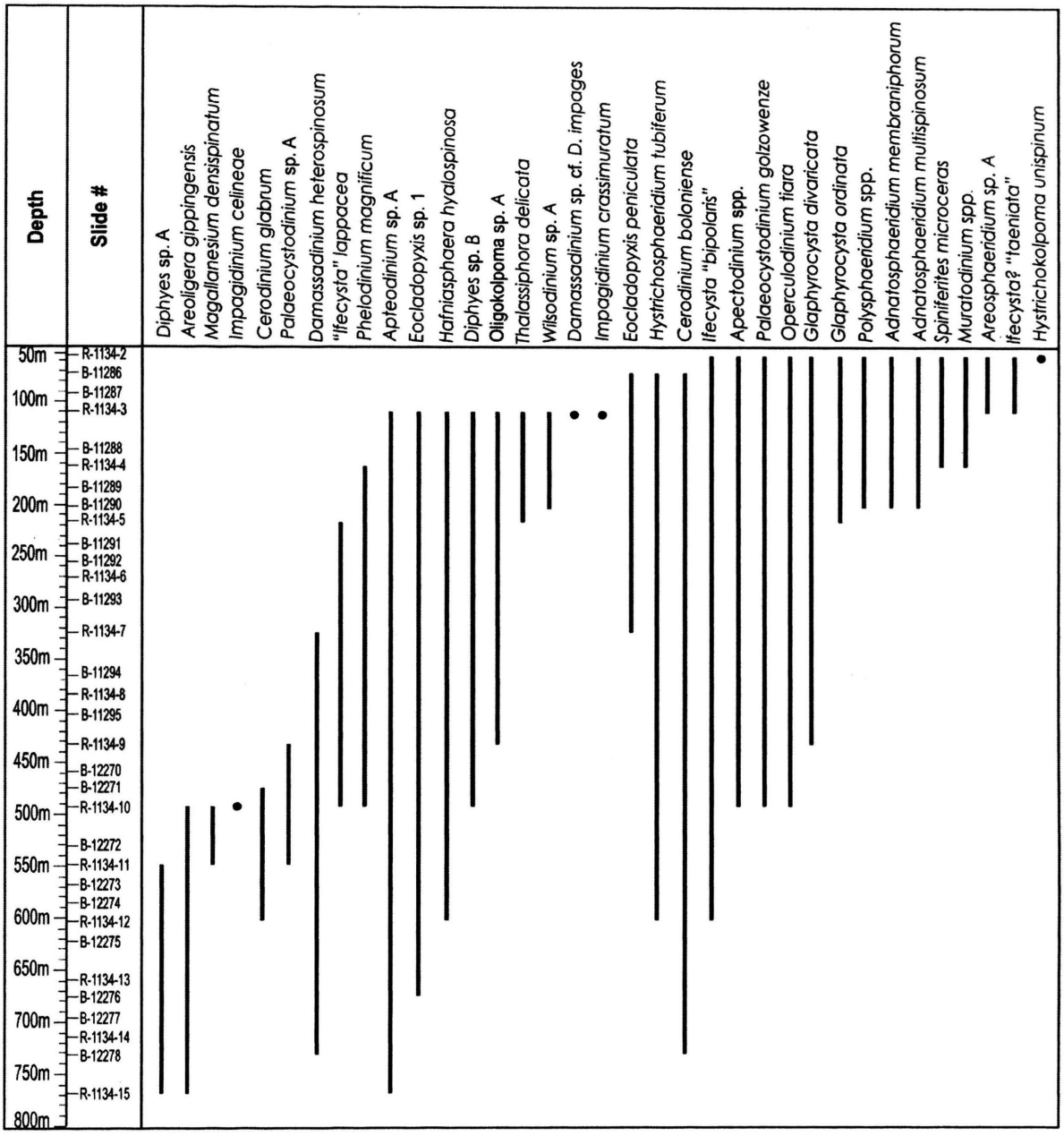

Figure 5.2. Stratigraphic distribution of selected dinocysts in Alo-1 well.

5.3.2. Hole 959D. The stratigraphic ranges of selected dinocysts in Hole 959D are shown in Figure 5.3, along with a summary of the Early Paleogene biostratigraphy based on calcareous nannofossils. The occurrence of *Muratodinium* spp., is restricted to nannoplankton subzone CP9a in the upper part of the section. *Polysphaeridium* spp., *Glaphyrocysta divaricata* and *Adnatosphaeridium multispinosum* have their LADs within

subzone CP9a in sample 159-959D-40R-3, 80-86 cm (787.35 mbsf). *Apectodinium* spp., and *Homotryblium* spp., are last recorded in the upper part of subzone CP8b in sample 159-959D-42R-1, 52-56 cm (803.12 mbsf). The LADs of *Thalassiphora delicata, Hafniasphaera hyalospinosa, Hystrichokolpoma unispinum* and the spot appearance of *Deflandrea oebesfildensis* occur in sample 159-959D-43R-4, 50-53 cm (817.3 mbsf) in nannofossil subzone CP8a. Several biostratigraphic events are recorded in samples 159-959D-44R-2, 4-6 cm (822.14 mbsf) and 159-959D-44R-7, 133-136 cm (830.93 mbsf): spot occurrences of *Spiniferites microceras, Wilsodinium nigeriense*, and *Enneadocysta* sp., and the LAD of *Hystrichosphaeridium tubiferum* occur in sample 159-959D-44R-2, 4-6 cm in zone CP7. Spot occurrences of *Glaphyrocysta ordinata*, *Palaeocystodinium* sp. A and *Areoligera gippingensis* are recorded in sample 159-959D-44R-7, 133-136 cm below zone CP7, and the first appearance datums (FADs) of *Hystrichosphaeridium tubiferum, Thalassiphora delicata*, *Hystrichokolpoma unispinum, Apectodinium* spp., *Glaphyrocysta divaricata* and *Adnatosphaeridium multispinosum* are also recorded in this sample. The presence of *Damassadinium* spp., *Impagidinium celineae, Cerodinium glabrum,* and *Fibrocysta axialis* characterize the lower portion of the section.

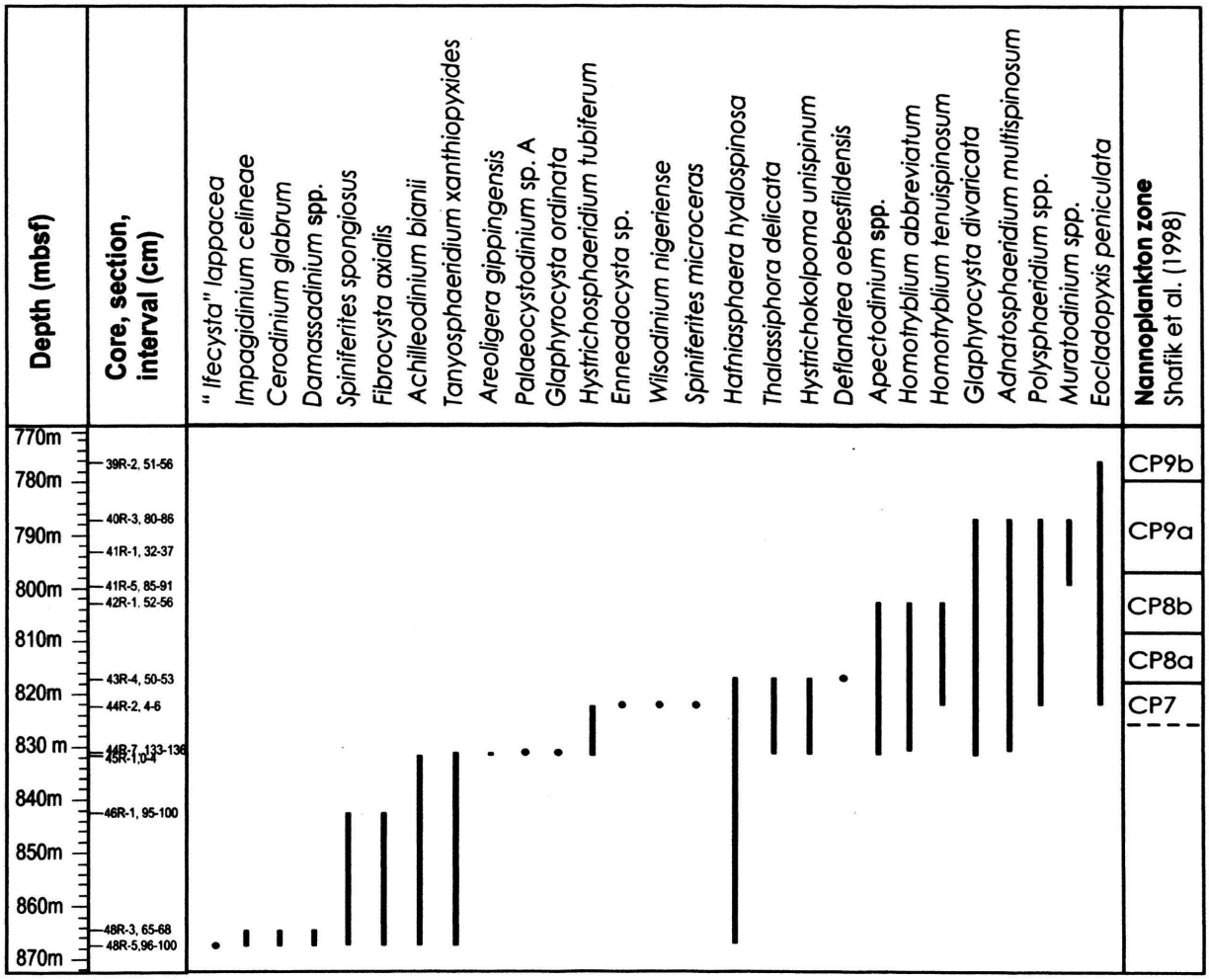

Figure 5.3. Stratigraphic distribution of selected dinocysts in Hole 959D.

5.4. QUANTITATIVE CHANGES IN THE DINOCYST DISTRIBUTION

The quantitative dinocyst distribution in Alo-1 and Hole 959D, as recorded from samples with dinocyst counts > 100 grains is shown in Figures 5.4 and 5.5. A few groups of morphologically related taxa typically represent 80-90% of the dinocyst association in all samples. These groups are: (1) *Adnatosphaeridium* spp., (2) *Cordosphaeridium* group (which includes *Cordosphaeridium* spp., *Ifecysta* spp., *Damassadinium* spp. and *Lanternosphaeridium* spp.), (3) *Polysphaeridium* group (combined *Polysphaeridium* spp., and *Eocladopyxis* spp), (4) species of *Spiniferites*, *Achomosphaera* and *Hafniasphaera*, (5) Apectodinium spp., (6) *Glaphyrocysta* group (*Glaphyrocysta* spp. and *Areoligera* spp.), and (7) *Operculodinium* spp.

5.4.1. Alo-1. Representatives of the *Polysphaeridium* group are abundant to superabundant in the upper part of the borehole between 54.9 and 73 m. Successive abundances of *Adnatosphaeridium-Cordosphaeridium* spp. (109.7 m), *Spiniferites* spp. (164.6 m), *Apectodinium* spp. (219.4 m), *Cordosphaeridium* spp. (384 m) and again *Spiniferites* spp. (493.7 m) are then recorded downsection. In the lower part of the succession (below 548.6 m), the *Cordosphaeridium* group dominates the assemblage and constitutes more than 60% of the association. Representatives of this group, mainly *Ifecysta* spp, were observed to exhibit wide variations in the development of apical and antapical protrusions, and the morphology of the processes especially in this part of the section.

5.4.2. Hole 959D. The dinocyst association in Hole 959D is dominated by *Spiniferites* spp. (mainly subspecies of *S. ramosus*), which represent 30 to 98% of the assemblage in all samples (Fig. 5.5). The *Operculodinium* group is present in all samples in percentages higher than 10%, typically between 10-20%. Intervals of frequent to abundant *Adnatosphaerdium-Glaphyrocysta* spp. (sample 159-959D-40R-3, 80-86 cm, 787.5 mbsf), *Polysphaeridium-Cordosphaeridium* spp. (sample 159-959D-41R-5, 85-91, 799.8 mbsf), *Apectodinium* spp. (sample 159-959D-44R-2, 4-6 cm, 822.14 mbsf), *Adnatosphaerdium-Glaphyrocysta* spp. (sample 159-959D-44R-7, 133-136 cm, 830.92 mbsf), and *Cordosphaerdium* group (mainly *Ifecysta* spp) (sample 159-959D-48R-5, 96-100, 867.6 mbsf) are also recorded at Hole 959D.

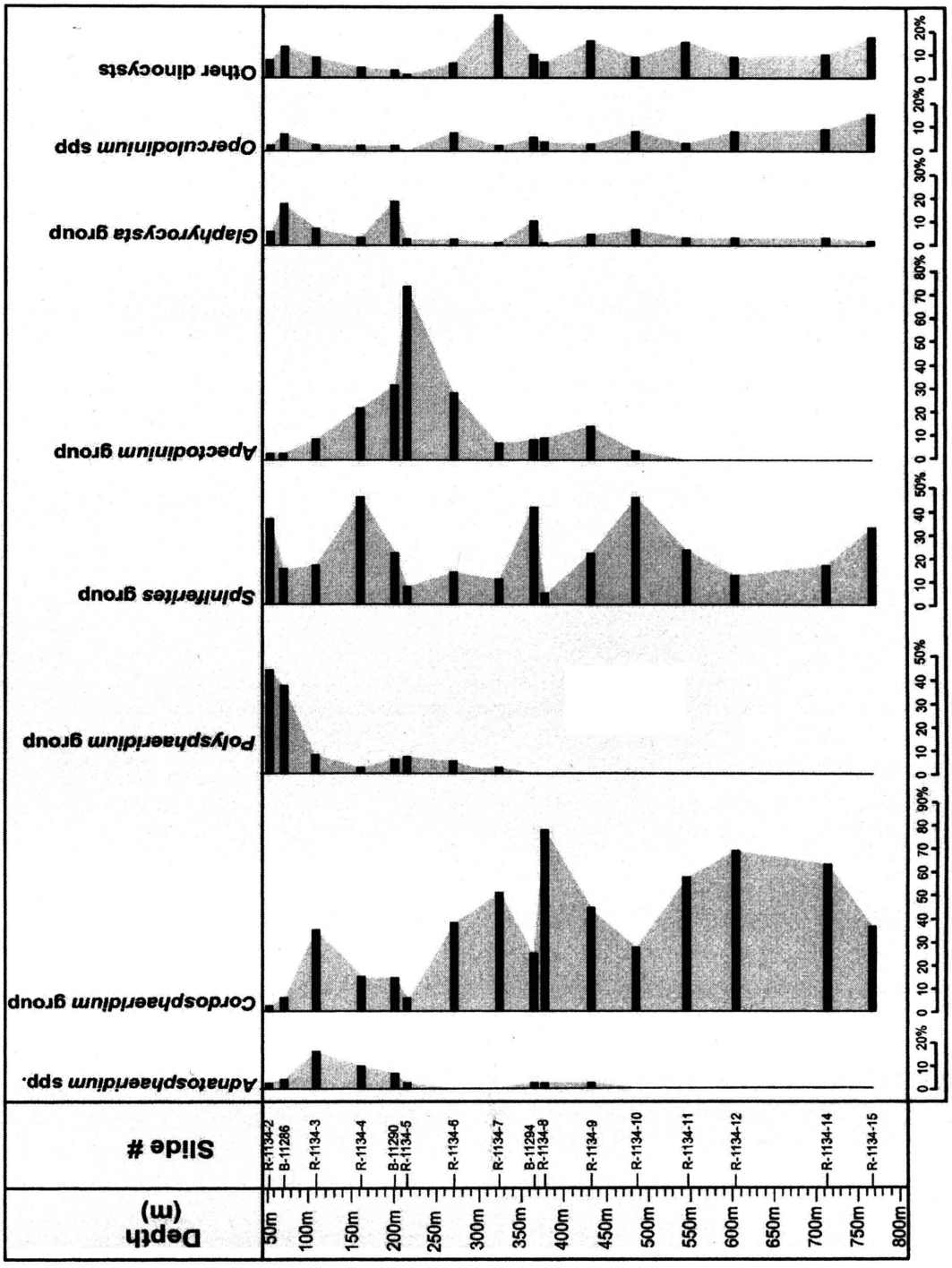

Figure 5.4. Quantitative distribution of dinocyst morphogroups in the Paleocene-Early Eocene interval of Alo-1 well. Only samples with >100 recovered specimens are shown.

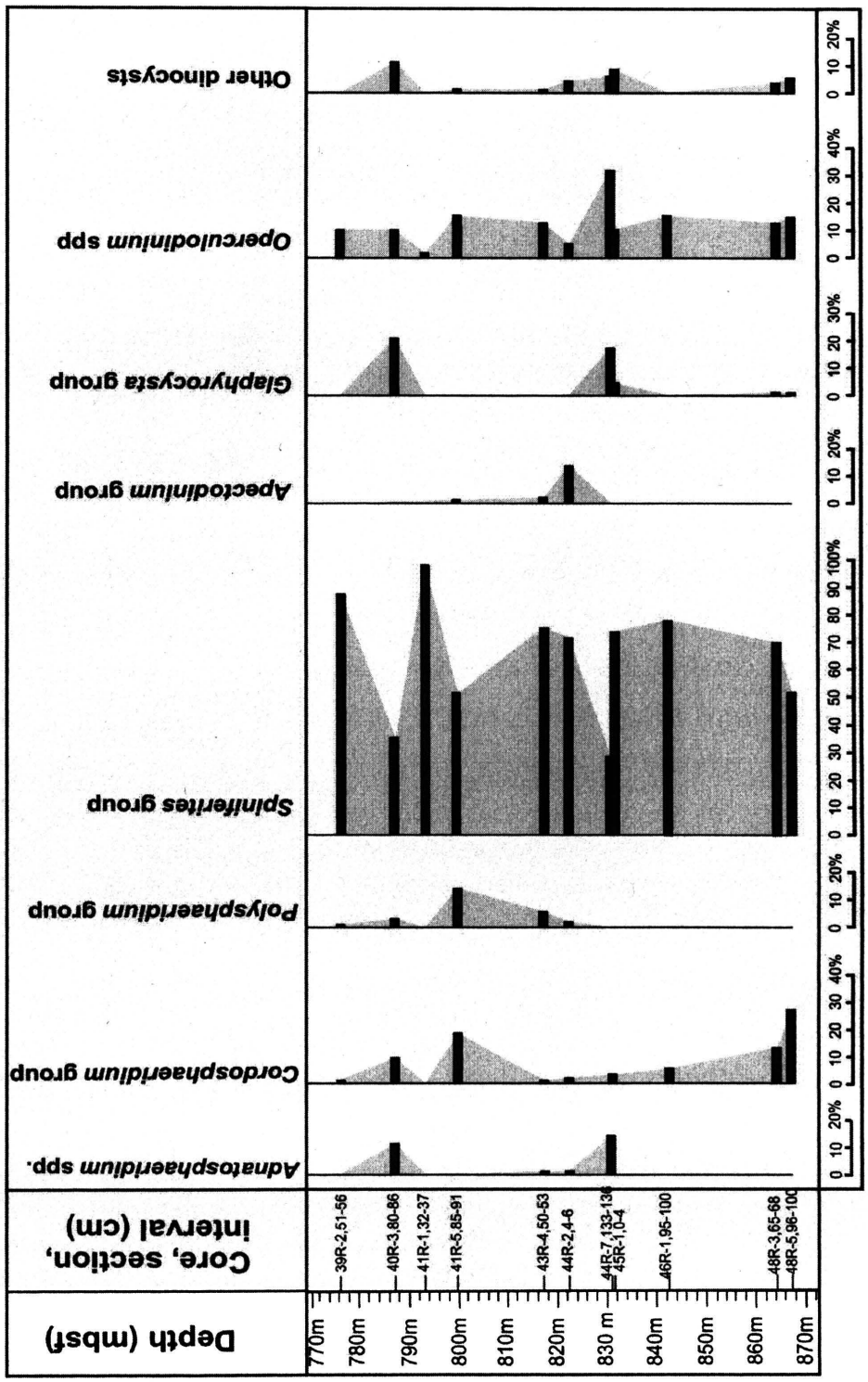

Figure 5.5. Quantitative distribution of dinocyst morphogroups in the Paleocene-Early Eocene interval of Hole 959D. Only samples with >100 recovered specimens are shown.

6. DISCUSSION

6.1. INFERRED LITHOSTRATIGRAPHY OF ALO-1 WELL

Lithologic and palynologic data have been used to reconstruct the lithostratigraphy of Alo-1 well. The upper ~580 m of the interval examined are considered to correspond to the lower part of the Imo Formation, while the lower 180 m belong to the upper Nsukka Formation. The contact between the Imo and Nsukka formations is tentatively interpreted as the transition from muddy sandstone to mudstone, as deduced from the abrupt change in the sand percentage profile at ~580 m (Shell Petroleum, 1976; Fig. 6.1). This pattern is somewhat similar to the data presented by Oboh-Ikuenobe et al. (2005; fig. 15). The percentage of terrestrial palynomorphs is also observed to change from <50% to >50% below ~ 500 m (Fig. 5.1), reflecting the more proximal character of deposition of the Nsukka Formation (Reyment, 1965; Murat, 1972). Of note are the unconformities observed in other studies (Oboh-Ikuenobe et al., 2005), which cannot be observed here because of the absence of a continuous core.

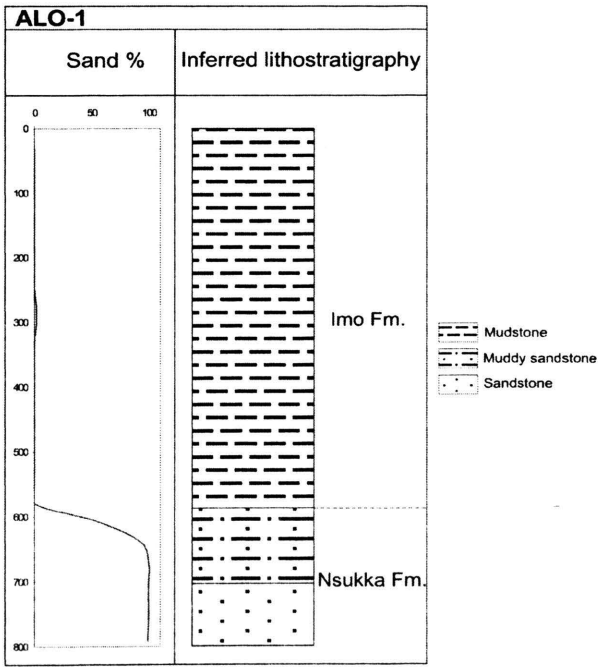

Figure 6.1. Inferred lithostratigraphy for the interval studied in Alo-1. Sand percentage from Shell Petroleum (1976).

6.2. COMPARISON OF THE ALO-1 AND HOLE 959D DINOCYST ASSEMBLAGES

The overall composition of the dinocyst assemblages in Alo-1 and Hole 959D is consistent with different depositional settings for the two sections. Typically, inner neritic shallow marine genera such as *Damassadinium*, *Ifecysta*, *Polysphaeridium*, *Adnatosphaeridium,* and *Apectodinium* (e.g., Crouch, 2001; Sluijs et al., 2005), dominate the Alo-1 assemblage. In contrast, more offshore groups such as *Spiniferites* and *Operculodinium* dominate the assemblage in Hole 959D. The quantitative distribution of terrestrial vs. marine palynomorphs (Fig. 5.1) is also consistent with a more proximal depositional setting for Alo-1, which is characterized by higher percentages of terrestrial palynomorphs. Similar quantitative changes in the dinocyst distribution are recognized in both sections; however, these changes are more difficult to observe in Hole 959D because of the offshore nature of the assemblages where *Spiniferites* dominates. The occurrence of some taxa in only one of the sections (Table 6.1) could be related to different depositional settings but may also be explained by a number of factors including incomplete sequences, sampling gaps and/or processing techniques.

Table 6.1. List of dinocyst species recorded in only one section.

Dinocyst taxa recorded at Alo-1 only	**Dinocyst taxa recorded at Hole 959D only**
Adnatosphaeridium membraniphorum, *Areosphaeridium* sp. A, *Cerodinium boloniense*, *Ifecysta*? *"taeniata"*, *Coronifera oceanica*, *Damassadinium* sp. cf. *D. impages*, *Diphyes* sp. A, *Eocladopyxis* sp. 1, *Oligokolpoma* sp. A, *Impagidinium crassimuratum*, *Kallosphaeridium orchiesense*, *Lejeunecysta* sp. 1, *Wilsodinium* sp. A	*Achilleodinium bianii*, *Achomosphaera ramulifera*, *Canningia* sp. 1, *Deflandrea oebesfildensis*, *Enneadocysta* sp., *Homotryblium abbreviatum*, *Homotryblium tenusipinosum*, *Melitasphaeridium* spp., *Minisphaeridium expansum*, *Spiniferites "spongiosus"*, *Tanyospheridium xanthiopyxides*, *Tectatodinium rugulatum*, *Wilsodinium nigeriense*

Despite these differences, several dinocyst bioevents occur in the same stratigraphic order in both Alo-1 and Hole 959D, and have been used for correlation. The youngest sediments studied occur in Hole 959D where the last occurrence of species of *Apectodinium* was recorded above the LADs of *Thalassiphora delicata* and

Hafniasphaera hyalospinosa (Fig. 5.3). This bioevent is not recorded at Alo-1 where the LADs of *T. delicata* and *H. hyalospinosa* occur near the top of the section (Fig. 5.2). Intervals of abundant *Polysphaeridium* spp., also occur above the LADs of these two species at both successions. These events are then followed downsection by peaks in *Apectodinium* spp., and the LADs of *Palaeocystodinium* sp. A, *Cerodinium glabrum* and *Impagidinium celineae* (Figs. 5.2 to 5.5).

6.3. BIOSTRATIGRAPHY

Five informal biostratigraphic zones (A to E) are recognized, based on the analysis of qualitative and quantitative dinocyst bioevents from Alo-1 and Hole 959D. The dinocyst zones are defined by last occurrence or last abundance events of one or more taxa of dinocysts. When possible, the zones are calibrated with the Early Paleogene calcareous nannoplankton biostratigraphy of Hole 959D (Shafik et al., 1998). Otherwise, age determinations are based on dinocyst bioevents previously reported in different Paleocene to Early Eocene sections around the world, or in global range charts (e.g., Williams and Bujak, 1985; Stover et al., 1996; Williams et al., 2004). Biostratigraphic summaries for Alo-1 and Hole 959D are presented in Figures 6.2 and 6.3 respectively. Going downsection, the five zones are described below.

Dinocyst Zone A

Definition: The top of the zone is not defined in this study. The base of the zone is defined by the LAD of species of *Apectodinium*.

Characteristics: This zone is identified only in Hole 959D and is characterized by *Polysphaeridium* spp., *Adnatosphaeridium multispinosum, Muratodinium* spp., and *Eocladopyxis peniculata*.

Age: Earliest Eocene (Sparnacian-earliest Ypresian). The lower boundary correlates with the middle part of calcareous nannoplankton subzone CP8b.

Comments: The co-occurrence of *Eocladopyxis peniculata, Adnatosphaeridium multispinosum, Polysphaeridium* spp., and *Muratodinium* spp., is restricted to the Early and Middle Eocene as indicated in global dinocyst range charts (e.g., Williams and Bujak, 1985; Stover et al., 1996).

Dinocyst Zone B

Definition: The top of the zone is defined by the LAD of *Apectodinium* spp. The base of the zone is defined by the he LADs of *Thalassiphora delicata* and *Hafniasphaera hyalospinosa.*

Characteristics: Typical dinocysts of this zone are *Polysphaeridium* spp, *Adnatosphaeridium multispinosum, Eocladopyxis peniculata and Apectodinium* spp. *Ifecysta*? "taeniata" is restricted to the upper part of this zone in Alo-1.

Age: Latest Paleocene (Late Thanetian)-Earliest Eocene (Sparnacian).The upper boundary correlates with the middle part of calcareous nannoplankton subzone CP8b. The lower boundary is tentatively correlated to the base of subzone CP8a.

Comments: Harland (1979) indicated that most species of *Apectodinium* in northwest Europe were restricted to nannofossil zones CP8-CP9. This study suggests that the LAD of the genus was probably older in low-latitudes. The top of the zone is not recognized in Alo-1; therefore, the presence of Lower Eocene sediments in this well, as suggested by Shell Petroleum (1976) data (see section 3.3.1), is questioned.

Dinocyst Zone C

Definition: The top of the zone is defined by the LADs of *Thalassiphora delicata* and *Hafniasphaera hyalospinosa.* The base of the zone is defined by the peak of *Apectodinium.*

Characteristics: Typical of this zone are common to frequent species of *Apectodinium* and *Wilsodinium* co-occurring with *T. delicata* and *H. hyalospinosa.*

Age: Late Paleocene (mid Thanetian). This zone correlates with calcareous nannoplankton zone CP7.

Comments: The LAD of *T. delicata* recorded here is significatively older than that in Northwest Europe (Middle Eocene, 39 Ma) and the Southern hemisphere (Early Eocene, 52 Ma) (Williams et al., 2004).

Dinocyst Zone D

Definition: The top of the zone is defined by the peak of *Apectodinium.* The base of the zone is defined by the LAD of *Impagidinium celineae.*

Characteristics: The occurrence of abundant *Apectodinium* toward the upper part of the zone is followed by common to abundant *Cordosphaeridium* group. In Hole 959D, a peak in the abundance of *Adnatosphaeridium* spp., immediately follows the *Apectodinium* peak.

Age: Late Paleocene (Selandian-mid Thanetian). The top of the zone is tentatively correlated with the middle part of calcareous nannoplankton zone CP7.

Comments: An interval of abundant *Adnatosphaeridium* occurring below assemblages dominated by *Apectodinium* was reported by Jan du Chêne and Adediran (1985) in Late Paleocene sediments of southwestern Nigeria. Wide morphological variations in the *Cordosphaerdium* group, similar to those observed in this study (see section 6.4.2), were also noted by Crouch et al. (2003) in the Thanetian strata of Tunisia. High percentages (>30%) of *the Cordosphaeridium* group were observed by Guasti et al. (2005) below nannoplankton zone CP6 at the El Kef section, which is also in Tunisia. Abundant spot appearances, LADs and FADs of different dinocyst species in the upper part of the zone in Hole 959D (Fig. 5.3) may indicate condensation horizons or hiatuses in this part of the section. The presence of such intervals was previously suggested by Shafik et al. (1998). They identified several hiatuses in Paleocene sediments from the nearby Site 960 but could not identify them in Hole 959D, because of the absence of calcareous nannoplankton in the sediments.

Dinocyst Zone E

Definition: The top of the zone is defined by the LAD of *Impagidinium celineae.* The base of the zone is not defined in this study.

Characteristics: Typical dinocysts include *Cerodinium glabrum* and *Impagidinium celineae* occurring with high numbers of species of the *Cordosphaeridium* group. *Magallanesium densispinatum* and *Diphyes* sp. A are restricted to this zone in Alo-1.

Age: Early Paleocene (Danian-basal Selandian).

Comments: *Impagidinium celineae* and *Diphyes* sp. A have previously been described from the Danian of Senegal (Jan du Chêne, 1988). *Magallanesium densispinatum* was recorded in a narrow interval spanning the Danian-Selandian boundary by Thomsen and Heilmann-Clausen (1984), and in the basal part of the Selandian at several localities in

the northern hemisphere (De Coninck, 1975; Hansen 1980). The inferred contact between the Nsukka and Imo formations (see section 6.1) is considered to be late Danian in age (Fig. 6.2).

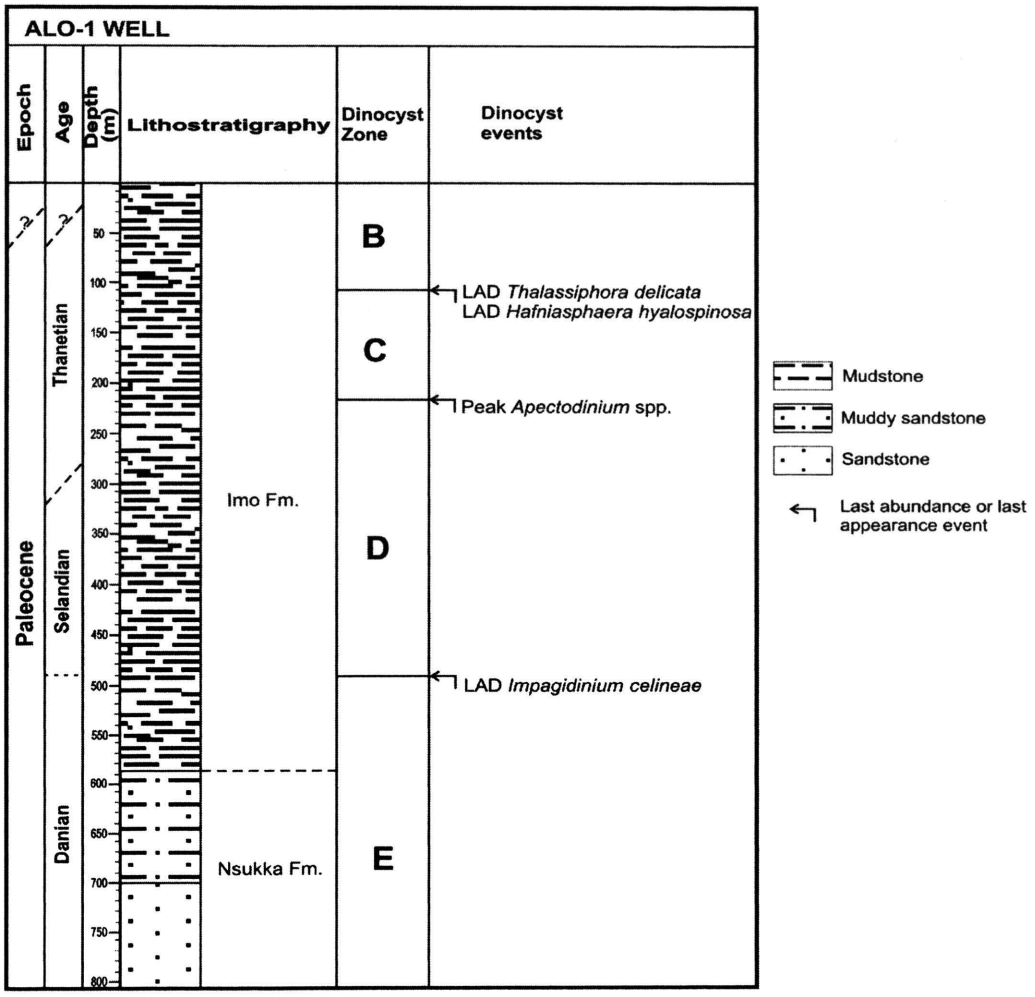

Figure 6.2. Biostratigraphic summary for the Early Paleogene interval of Alo-1 well. The top of dinocyst zone B is not recognized in this section.

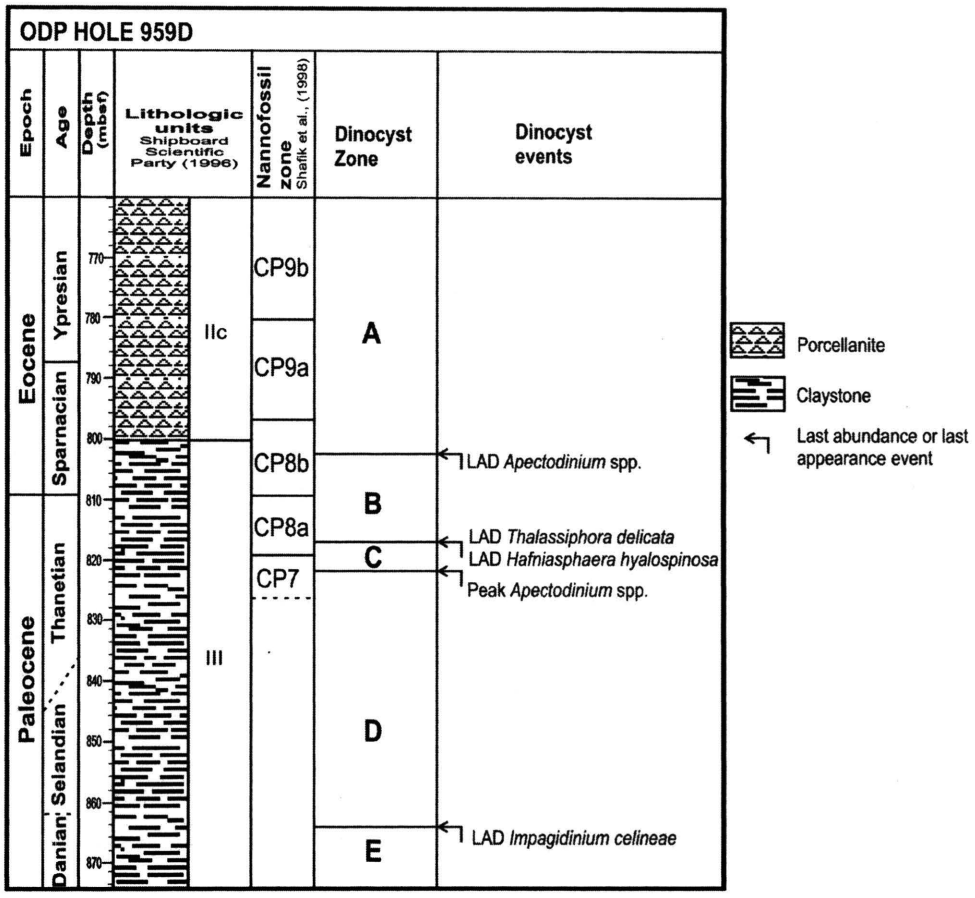

Figure 6.3. Biostratigraphic summary for the Early Paleogene interval of ODP Hole 959D.

6.4. COMPARISON WITH PREVIOUS DINOCYST STUDIES

6.4.1. Mid- to high-latitudes. The Paleocene to Early Eocene dinocyst assemblages recorded in Alo-1 and Hole 959D have been compared to those described in mid- to high latitudes of the northern and southern hemispheres. Specifically, they were compared to those assemblages in such localities of the northern hemisphere like Northwest Europe (Bujak and Mudge, 1994; Mudge and Bujak, 1996), Western Siberia (Iakovleva and Kulkova, 2003), and Greenland (Nøhr-Hansen, 2003). Data used for comparison in the southern hemisphere were from the following localities: New Zealand (Crouch, 2001), Southern Chile (Quattrocchio and Sarjeant, 2003) and offshore Tasmania (Brinkhuis et al., 2003).

The Alo-1 and Hole 959D assemblages differ considerably from those in the aforementioned localities. Notable absences include Paleocene taxa of biostratigraphic importance such as *Alisocysta margarita*, *Alisocysta reticulata*, *Palaeoperidinium pyrophorum*, *Apectodinium augustum* and species of *Isabelidinium*. Representatives of the Wetzellielloidea subfamily (e.g., *Wetzeliella astra*, *W. meckelfeldensis*, *Dracodinium simile*, *Rhombodinium subtile*) and *Deflandrea phosphoritica* are absent in the Early Eocene interval. Representatives of *Wetzeliella* and *Dracodinium* are particularly important in the Early Eocene (Ypresian) dinocyst biostratigraphy of the North Sea Basin, where the Wetzellielloidea subfamily underwent significant evolution and diversification during this interval of time (Bujak and Brinkhuis, 1998).

Dinocysts recognized in this study that are common components of mid- to high latitude assemblages of both hemispheres include *Palaeocystodinium golzowense*, *Deflandrea oebesfildensis*, *Phelodinium magnificum*, *Thalassiphora delicata*, *Hystrichosphaeridium tubiferum*, *Magallanesium densispinatum*, *Glaphyrocysta ordinata*, *Glaphyrocysta divaricata*, *Areoligera gippingensis*, *Apectodinium parvum*, *Apectodinium homomorphum,* and *Spiniferites* spp.

Noteworthy is the presence of a peak in the abundance of *Apectodinium* during the Late Paleocene in Alo-1 and Hole 959D. The timing of the highest abundance of *Apectodinium* in both boreholes within nannoplankton zone CP6/7 appears to be approximately coeval with other Late Paleocene occurrences of *Apectodinium* recorded in several locations in the Northern Hemisphere (Bujak and Brinkhuis, 1998; Iakovleva et al., 2001; Crouch et al., 2003). The abundance of *Apectodinium* in these areas is associated with a combination of factors including elevated sea-surface temperatures and high nutrient levels. *Apectodinium* is considered to be a thermophilic genus which originated in tropical latitudes during the mid Paleocene and migrated into higher latitudes during short-lived intervals in the Late Paleocene and the Paleocene-Eocene boundary (Crouch et al., 2001; Sluijs et al., 2005). The coincidence in the timing of *Apectodinium* abundance events in lower latitudes and mid-to high latitudes is probably associated with short-lived intervals of climatic warming or "hyperthermals" (Crouch et al., 2003). At present, the occurrence of short-lived migrations of *Apectodinium* into the Southern Hemisphere during the Late Paleocene is not well established (Crouch, 2001).

6.4.2. Mid latitudes. Assemblages identified in this study are more comparable to Paleocene-Early Eocene dinocyst assemblages in mid latitude areas such as the Mediterranean region (e.g., Crouch et al., 2003; Guasti et al., 2005) and the U.S. Gulf Coast (Gregory and Hart, 1995; Harrington and Kemp, 2001). Dinocysts recognized in this study that are typically recorded in these zones include *Adnatosphaeridium multispinosum*, *Polysphaeridium* spp., *Hystrichokolpoma* spp., *Eocladopyxis* spp., *Kallosphaeridium* spp., and the *Cordosphaeridium* group. Furthermore, there is a remarkable similarity in the general pattern of the quantitative distribution of dinocysts observed in Alo-1 and that observed in other Paleocene-Early Eocene successions in mid to low latitudes. As previously mentioned, such quantitative changes are also recognized in Hole 959D but the offshore nature of the dinocyst assemblages, which are dominated by *Spiniferites,* makes their interpretation more difficult. Hence, more focus is placed on the dinocyst changes in Alo-1. The main features are discussed below.

(1) The *Cordosphaeridium* group, mainly *Ifecysta,* dominates the Danian-early Thanetian dinocyst assemblages in Alo-1. Representatives of this group exhibit wide morphological variations in the development of apical and antapical protrusions and substantial variation in the development of the periphragm which can take the shape of processes, spines or penitabular septa. Specimens recording similar morphological features and referred to as the *Kenleyia* complex (Crouch et al., 2003) occur in high percentages during the Early Paleogene in mid latitude localities such as Egypt (Brinkhuis et al., 1994), Tunisia (Crouch et al., 2003; Guasti et al., 2005), and Uzbekistan (Crouch et al., 2003). The occurrence of high percentages of this group in Alo-1 further confirms the preference for warm water conditions attributed to these taxa in earlier studies (e.g., Brinkhuis and Zachariasse, 1988; Brinkhuis et al., 1994), and indicates that the observed morphological variations might be restricted to the Danian-early Thanetian interval.

(2) High percentages of *Apectodinium* characterize the Thanetian in Alo-1. The timing of the *Apectodinium* peak appears to be coeval to other Late Paleocene occurrences of *Apectodinium* in higher latitudes that mark episodes of intense climatic warming (as discussed in section 6.4.1). Appearances of *Apectodinium* at higher latitudes, however are sporadic and short-lived. In contrast, as observed in this study, *Apectodinium*

can be frequent to abundant in low- to mid latitude settings during most of the Late Paleocene. This observation confirms previous findings in Egypt (Brinkhuis et al., 1994) and Tunisia (Crouch et al., 2003).

(3) The presence of species of *Wilsodinium* (*Wilsodinium nigeriense* and *Wilsodinium* sp. A), during the Late Paleocene in Alo-1 and Hole 959D is also noteworthy. *Wilsodinium* is a member of the Wetzelielloideae subfamily which also includes taxa like *Rhombodinium* and *Wetzeliella.* Representatives of this subfamily are considered to characterize the Early Eocene in higher latitudes (Bujak and Brinkhuis, 1998). Recent studies in Kazakhstan (Iakovleva et al., 2001) and Uzbekistan (Crouch et al., 2003), reported the occurrence of species of *Wilsodinium* and *Rhombodinium* during the Late Paleocene. This study, therefore, provides further evidence for the appearance of this group prior to the Early Eocene.

6.4.3. Significance for Early Paleogene paleoclimatic reconstruction. Results from this study indicate a high level of provincialism in the dinocyst associations during the Early Paleogene, with favorably comparable tropical to subtropical assemblages but marked differences with assemblages somewhere else. Since sea surface temperature is the main controlling parameter in the global distribution of dinocysts (e.g., Sluijs et al., 2005), the observed pattern suggests the existence of a relatively high sea-surface temperature latitudinal gradient during the studied interval. This latitudinal gradient would be significantly reduced during hyperthermal events, resulting in a more equable global climate and reduced provincialism in the dinocyst associations, as indicated by the global dominance of *Apectodinium*.

7. CONCLUSIONS

Twelve potentially new dinocyst species were identified in Alo-1 well and Hole 959D; These are: *Achomosphaera* sp. A, *Apteodinium* sp. A, *Areosphaeridium* sp. A, *Diphyes* sp. A, *Diphyes* sp. B, *Ifecysta "bipolaris"*, *Ifecysta "heterospinosa"*, *Ifecysta*? *"taeniata"*, *Kallosphaeridium* sp. A, *"Oligokolpoma"* sp. A, *Palaeocystodinium* sp. A, and *Wilsodinium* sp. A. A revision of the generic diagnosis of *Ifecysta* was proposed.

Five informal biostratigraphic zones (A to E) defined by last occurrence or last abundance dinocyst bioevents, were recognized in the Paleocene to Early Eocene interval of Hole 959D; only four zones, excluding zone A, occur in Alo-1 well. Calibration with calcareous nannofossil data from the Early Paleogene interval of Hole 959D indicates a earliest Ypresian-Sparnacian age for zone A, a Sparnacian-Late Thanetian age for zone B, a mid Thanetian age for zone C, and a mid Thanetian-Selandian age for zone D. On the other hand, the occurrence of stratigraphically significant dinocyst species indicates a basal Selandian-Danian age for zone E.

Biostratigraphic results for Alo-1 differ from previous assessments by Shell Petroleum biostratigraphers, who placed the top of the Paleocene at 274 m, below an interval reported as barren of palynomorphs. This "barren" interval was found to be productive in this study, and was assigned a Late Paleocene (Thanetian) age.

The lithostratigraphy of Alo-1 was reconstructed using lithologic and palynologic data. The upper 580 m of this well are considered to correspond to the lower part of the Imo Formation, while the lower 180 m of the interval studied belong to the upper Nsukka Formation. The contact between the Imo and Nsukka formations is tentatively interpreted as the transition from muddy sandstone to mudstone, and is assigned a late Danian age.

It appears that condensed horizons or hiatuses occur at the top of dinocyst zone D in Hole 959D, based on several biostratigraphic events (spot appearances, LADs, and FADs of dinocyst species) concentrated in this part of the section. This observation is in accordance with previous findings in Paleocene sediments from nearby ODP sites in the Côte d'Ivore Ghana Transform Margin (Shafik et al., 1998).

Dinocyst assemblages recorded in Alo-1 and Hole 959D differ considerably from those in mid- to high latitudes of the northern and southern hemisphere. On the other

hand, they are more comparable to Paleocene-Early Eocene dinocyst assemblages in mid- to low latitude areas such as the Mediterranean region and the US Gulf Coast. The main observations are as follow:

(1) The Danian-early Thanetian is characterized by the presence of abundant thermophilic taxa such as the *Cordosphaeridium* group (e.g., *Ifecysta, Fibrocysta, Damassadinium*). This group displays wide morphological variations during this interval of time.

(2) The mid to late Thanetian interval records abundant to extremely abundant numbers of *Apectodinium* spp. This pattern is probably related to the globally recognized events that spanned the Late Paleocene to Earliest Eocene interval, such as high sea-surface temperatures and productivity increases in marginal marine settings (Crouch, 2001).

(3) Representatives of *Wilsodinium* are already present by the Late Paleocene. *Wilsodinium* belongs to the Wetzellieloideae subfamily, a group of taxa that is particularly important in the Early Eocene northern hemisphere biostratigraphy and was previously thought to be restricted to this interval of time.

The high provincialism observed in the dinocyst assemblages, suggests the existence of a relatively high sea-surface temperature latitudinal gradient during the Early Paleogene interval. Hyperthermal events are characterized by reduced provincialism in the dinocyst associations and therefore, a reduced sea surface temperature latitudinal gradient.

APPENDIX A.

ILLUSTRATIONS OF SELECTED DINOCYSTS IDENTIFIED IN ALO-1 AND HOLE 959D.

[Each specimen is identified by sample number (refer to Tables 4.1 and 4.2), and coordinates in the Leica #5 microscope in the Paleontology Lab at UMR.]

PLATE 1

Figure 1. *Achilleodinium*? sp., uncertain view, high focus, slide R-1134-4, 30.1 x 145.3.

Figure 2. *Achomosphaera* sp. A, lateral view, high focus, slide R-1134-3, 32.8 x 118.7.

Figure 3. *Adnatosphaeridium membraniphorum,* antapical view, low focus, slide R-1134-3, 18.7 x 141.1.

Figure 4. *Apectodinium* spp., dorsoventral view, high focus, slide R-1134-3, 23.5 x 118.5.

Figure 5. *Apectodinium* spp., uncertain view, high focus, slide R-1134-4, 23.5 x 112.2.

Figure 6. *Apectodinium* spp., dorsoventral view, high focus, slide R-1134-3, 32.3 x 121.2.

Figure 7. *Apectodinium* spp., dorsoventral view, high focus, slide R-1134-8, 38.1 x 146.6.

Figure 8. *Apteodinium* sp. A, dorsal view, high focus, slide R-1134-3, 23.6 x 123.6.

Figure 9. *Apteodinium* sp. A, oblique lateral view, high focus, slide R-1134-10, 25.8 x 112.6.

Figure 10. *Adnatosphaeridium multispinosum*, uncertain view, high focus, slide R-1134-2, 34.1 x 132.7.

Figure 11. *Areoligera gippingensis,* ventral view, high focus, slide R-1134-10, 24.3 x 138.2.

Figure 12. *Areosphaeridium* sp. A, uncertain view, high focus, slide R-1134-2, 32.5 x 140.1.

Figure 13. *Areosphaeridium* sp. A, uncertain view, high focus, slide R-1134-2, 24.9 x 137.1.

PLATE 1

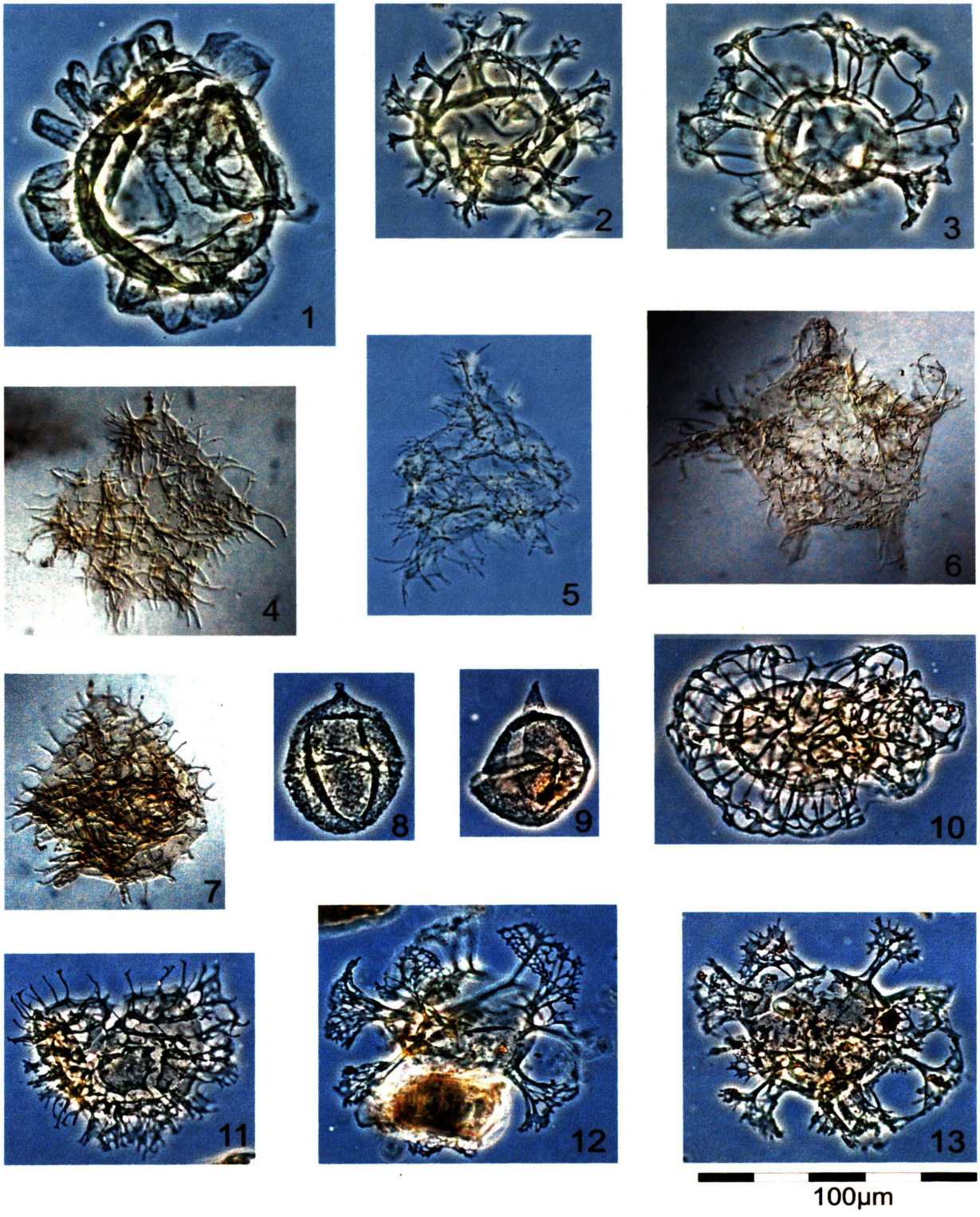

PLATE 2

Figure 1. *Cannigia* sp. 1, ventral view, high focus, slide 159-959D-44R-2, 4-6 cm, 33 x 135.7.

Figure 2. *Cerodinium boloniense*, ventral view, low focus, slide B-11286, 23.2 x 130. 3.

Figure 3. *Cerodinium glabrum,* dorsal view, high focus, slide R-1134-12, 30 x 115.9.

Figure 4. *Cordosphaeridium delimurum,* right lateral view, slide R-1134-3, 22 x 135.2.

Figure 5. *Damassadinium* sp. cf. *D. impages*, oblique dorsal view, high focus, slide R-1134-3, 23 x 122.7.

Figure 6. *Glaphyrocysta divaricata,* dorsal view, high focus, slide R-1134-3, 34.9 x 141.5.

Figure 7. *Damassadinium heterospinosum,* antapical view, mid focus, slide R-1134-7, 33.3 x 142.8.

Figure 8. *Diphyes* sp. A, uncertain view, mid focus, slide R-1134-12, 22.2 x 135.1.

Figure 9. Diphyes sp. A, oblique dorsal view, high focus, slide R-1134-15, 36 x 137.8.

Figure 10. *Coronifera oceanica*, uncertain view, mid focus, slide R-1134-3, 21.3 x 135.7.

Figure 11. *Eocladopyxis peniculata,* uncertain view, mid focus, slide R-1134-5, 32.3 x 133.9.

Figure 12. *Eocladopyxis peniculata,* uncertain view, mid focus, slide 159-959D-44R-2, 4-6 cm, 30.4 x 112.8.

Figure 13. *Diphyes* sp. B, dorsal view, mid focus, slide R-1134-4, 26.2 x 139.7.

Figure 14. *Eocladopyxis* sp. 1., lateral view, mid focus, slide R-1134-9, 28.8 X 115.

Figure 15. *Deflandrea oebisfeldensis,* ventral view, low focus, 159-959D-43R-4, 50-53 cm, 36.8 x 141.

PLATE 2

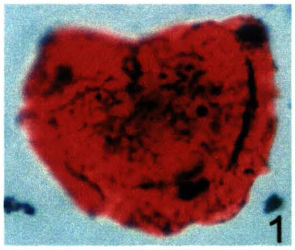

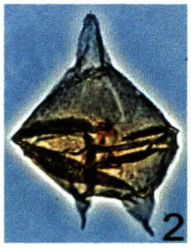

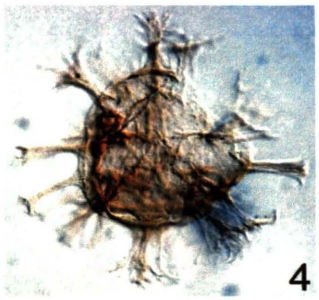

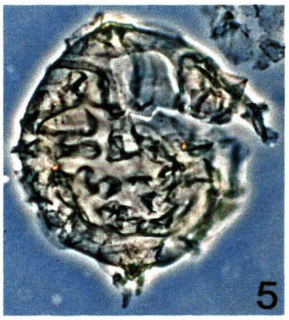

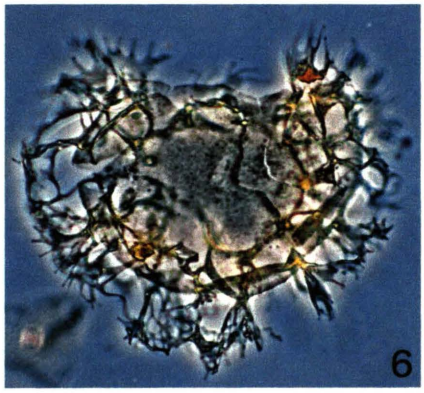

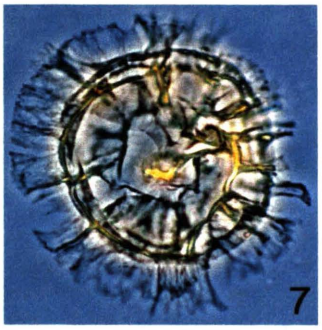

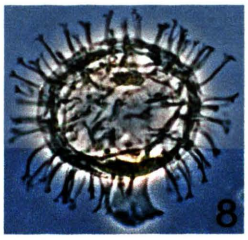

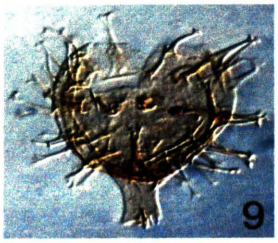

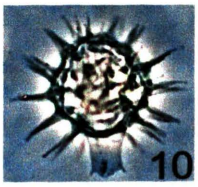

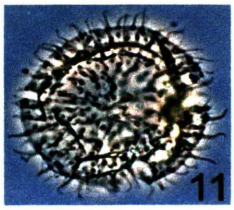

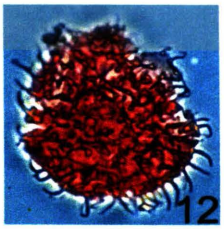

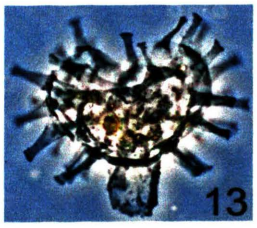

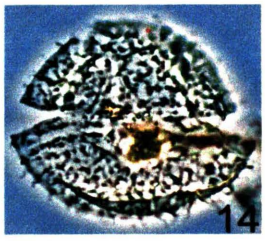

100µm

PLATE 3

Figure 1. *Glaphyrocysta ordinata,* ventral view, high focus, slide R-1134-2, 37.4 x 140.7.

Figure 2. *Ifecysta "bipolaris"*, oblique dorsal view, high focus, slide R-1134-8, 32.4 x 140.1.

Figure 3. *Hystrichokolpoma rigaudiae,* uncertain view, mid focus, slide 159-959D-45R-1, 0-4 cm, 19.2 x 141.9.

Figure 4. *Ifecysta "bipolaris"*, right lateral view, mid focus, slide R-1134-3, 18.8 x 114.3.

Figure 5. Ifecysta "bipolaris", oblique dorsal view, high focus, slide R-1134-10, 31.7 x 122.

Figure 6. *Ifecysta "bipolaris"*, oblique dorsoventral view, high focus, slide R-1134-4, 35.5 x 142.1.

Figure 7. *"Ifecysta" heterospinosa,* oblique dorsal view, high focus, slide R-1134-12, 30.1 x 123.4.

Figure 8. *Hafniasphaera hyalospinosa,* right lateral view, mid focus, slide R-1134-3, 21.4 X 142.9.

Figure 9. *"Ifecysta" heterospinosa,* right lateral view, high focus, slide R-1134-7, 35.1 x 127.1.

Figure 10. *Homotryblium tenuispinosum*, dorsoventral view, high focus, slide 159-959D-44R-2, 4-6 cm, 34.5 x 141.9.

Figure 11. *Hystrichosphaeridium tubiferum,* apical view, low focus, slide 159-959D-44R-2, 4-6 cm, 18.5 x 139.9.

PLATE 3

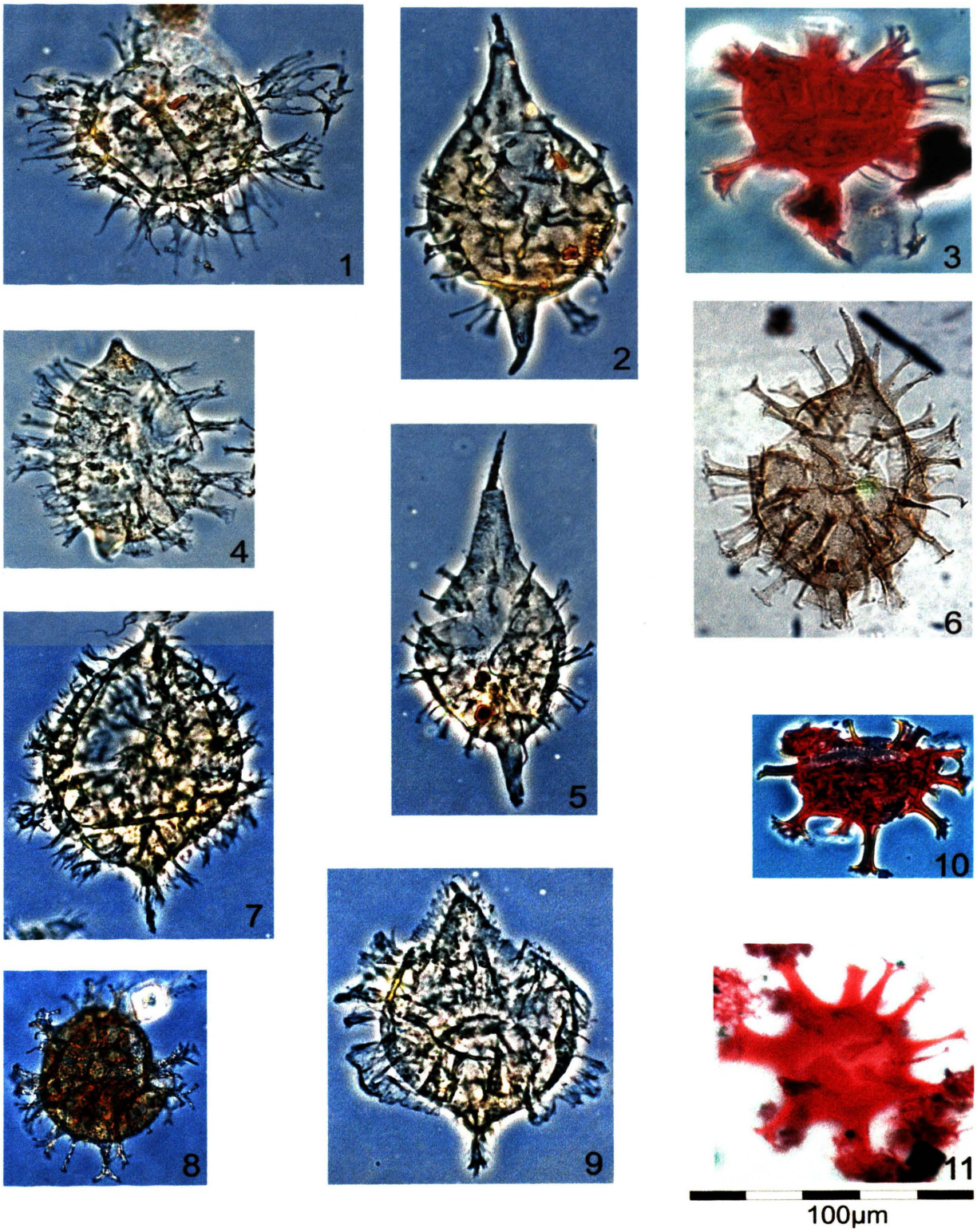

PLATE 4

Figure 1. "*Ifecysta*" *lappacea,* left lateral view, high focus, slide R-1134-12, 35.8 x 126.1.

Figure 2. "*Ifecysta*" *lappacea,* oblique dorsal view, high focus, slide R-1134-8, 32.9 x 132.

Figure 3. *Kallosphaeridium orchiesense,* oblique dorsal view, high focus, slide R-1134-3, 17.6 x 127.6.

Figure 4. Kallosphaeridium orchiesense, oblique ventral view, slide R-1134-4, 24.8 x 117.8.

Figure 5. *Kallosphaeridium*? sp. A, oblique dorsal view, mid focus, slide R-1134-2, 25.8 x 146.1.

Figure 6. *Ifecysta pachyderma,* oblique dorsal view, high focus, slide R-1134-3, 20 x 142.

Figure 7. *Impagidinium celineae,* oblique dorsal view, high focus, slide R-1134-10, 27.4 x 130.5.

Figure 8. *Impagidiunium crassimuratum*, right lateral view, mid focus, slide R-1134-3, 27.7 x 121.1.

Figure 9. *Ifecysta*? *"taeniata",* dorsal view, mid focus, slide R-1134-3, 17.8 x 143.2.

Figure 10. *Ifecysta*? *"taeniata",* ventral view, mid focus, slide R-1134-3, 25.4 x 136.1.

Figure 11. *Lanternosphaeridium* spp., uncertain view, high focus, slide R-1134-5, 31.5 x 141.8.

Figure 12. *Ifecysta pachyderma*, uncertain view, high focus, slide R-1134-14, 33.2 x 124.

PLATE 4

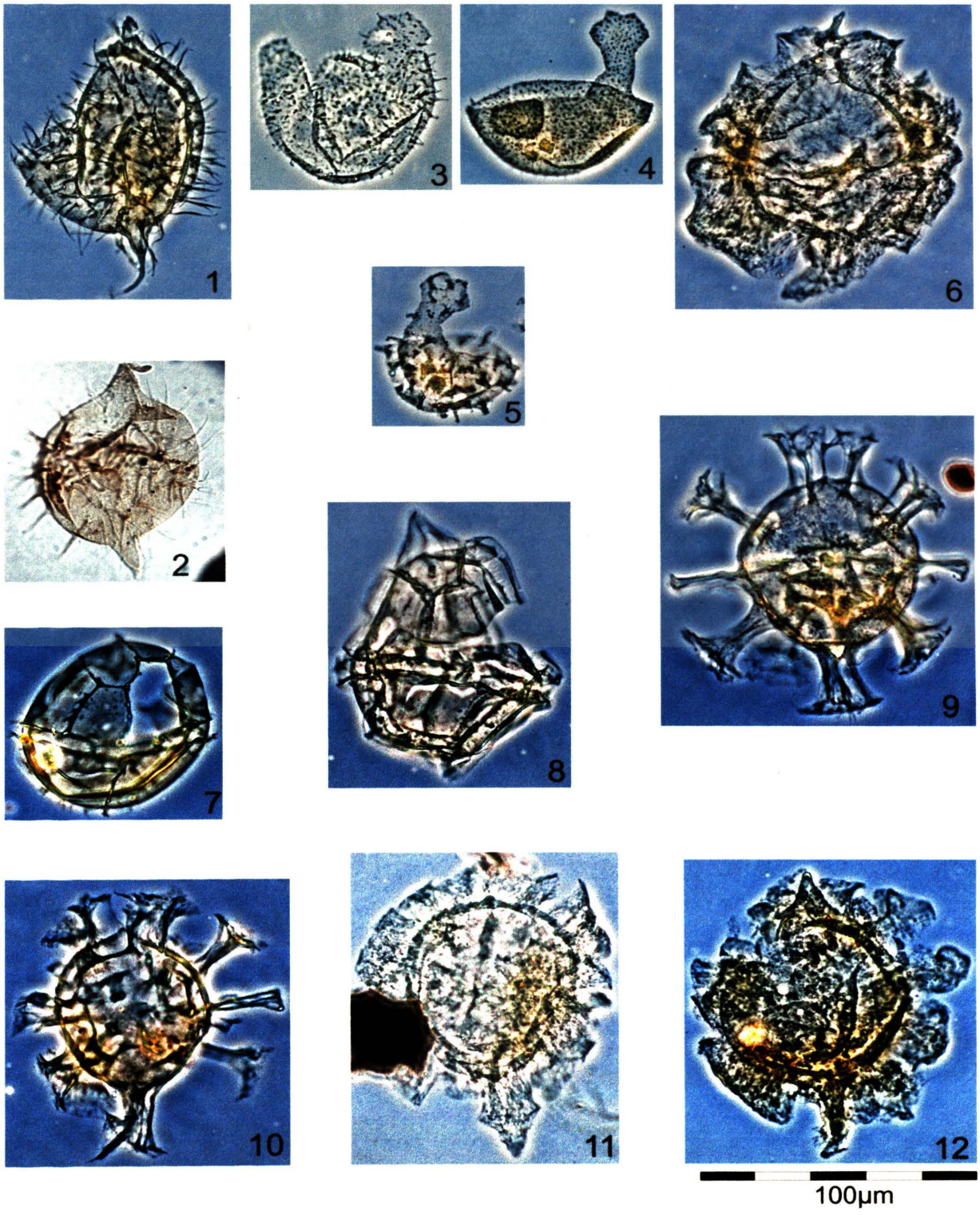

PLATE 5

Figure 1. *Lanternosphaeridium* spp., right lateral view, mid focus, slide R-1134-5, 34.9 x 113.2.

Figure 2. *Lanternosphaeridium* spp., oblique lateral view, mid focus, slide R-1134-7, 22.2 x 122.8.

Figure 3. *Lejeunecysta* sp. 1, dorsal view, high focus, slide B-11286, 33.9 x 120.3.

Figure 4. *Oligokolpoma*? sp. A, lateral view, mid focus, slide R-1134-8, 25.3 x 139.4.

Figure 5. *Thalassiphora delicata*, uncertain view, high focus, slide 159-959D-45R-1, 0-4 cm, 37.5 x 118.

Figure 6. *Magallanesium densispinatum,* dorsal view, high focus, slide R-1134-10, 29.7 x 145.4.

Figure 7. *Operculodinium tiara,* oblique lateral view, mid focus, slide R-1134-9, 32.1 x 144.4.

Figure 8. *Phelodinium magnificum,* ventral view, high focus, slide R-1134-10, 31.6 x 123.6.

Figure 9. *Palaeocystodinium* sp. A, oblique lateral view, high focus, slide R-1134-9, 30.1 x 129.5.

Figure 10. *Palaeocystodinium* sp. A, right lateral view, high focus, slideR-1134-9, 23.9 x 143.2.

Figure 11. *Polysphaeridium* spp., uncertain view, mid focus, slide R-1134-2, 29.2 x 142.

Figure 12. *Minisphaeridium expansum,* uncertain view, mid focus, 159-959D-44R-7, 133-136 cm, 37.2 x 123.3.

Figure 13. *Wilsodinium nigeriense,* ventral view, low focus, ODP Hole 959D 822.14 m 21.2 x 143.1.

Figure 14. *Palaeocystodinium golzowenze,* dorsal view, high focus, slide R-1134-2, 26.5 x 139.2.

PLATE 5

PLATE 6

Figure 1. *Wilsodinium* sp. A, dorsal view, high focus, slide B-11290, 36.3 x 116.

Figure 2. *Wilsodinium* sp. A, dorsal view, high focus, slide R-1134-3, 24.5 x 144.4.

Figure 3. *Wilsodinium* sp. A, dorsal view, high focus, slide R-1134-3 30.3 x 143.

Figure 4. *Wilsodinium* sp. A, dorsal view, high focus, slide R-1134-3, 19.7 x 127.3.

PLATE 6

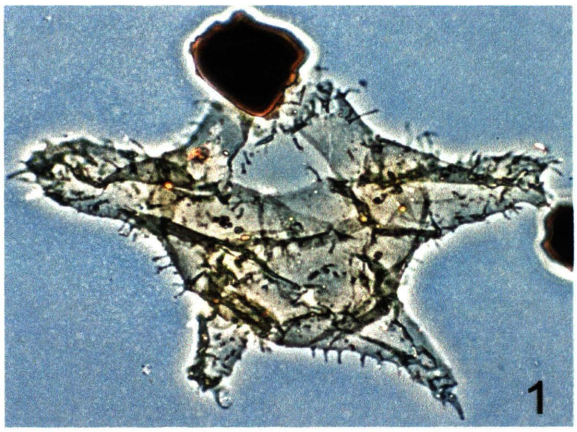

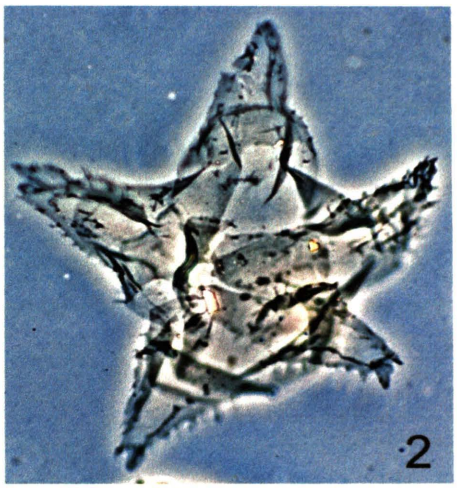

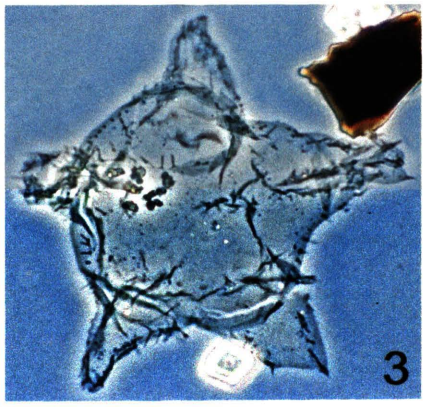

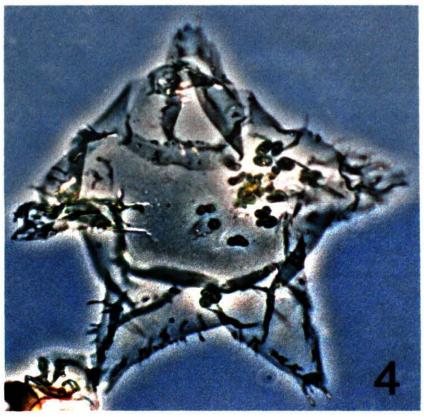

100µm

APPENDIX B.

QUANTITATIVE DINOCYST DATA FOR HOLE 959D.

Depth (mbsf)	776.32	787.35	793.35	799.88	803.12	817.3	822.14	830.93	831.64	842.25	864.25	867.6
159-959D-Core-Section, Interval (cm)	39R-2, 51-56	40R-3, 80-86	41R-1, 32-37	41R-5, 85-91	42R-1, 52-56	43R-4, 50-53	44R-2, 4-6	44R-7, 133-136	45R-1, 0-4	46R-1, 95-100	48R-3, 65-68	48R-5, 96-100
Achilleodinium bianii	0	0	0	0	0	0	0	0	3	0	1	1
Achomosphaera ramulifera	0	0	0	0	0	0	5	0	1	0	0	0
Achomosphaera sp. A	0	8	0	0	0	5	5	1	2	0	0	0
Achomosphaera spp.	0	0	0	1	0	1	0	0	2	6	3	0
Adnatosphaeridium multispinosum	0	15	0	0	0	3	4	40	0	0	0	0
Apectodinium spp.	0	0	0	0	3	7	39	0	*	0	0	0
Apteodinium sp. A	0	0	0	0	0	0	0	2	*	0	0	0
Areoligera gippingensis	0	0	0	0	0	0	0	19	*	0	0	0
Areoligera spp.	0	0	0	0	0	0	0	10	6	1	2	3
Canningia sp. 1	0	0	0	0	0	0	3	0	0	0	0	0
Cerodinium glabrum	0	0	0	0	0	0	0	0	0	0	1	1
Cordosphaeridium delimurum	2	0	0	0	0	0	1	0	0	0	0	0
Cordosphaeridium spp.	0	5	*	11	0	3	6	4	3	13	23	61
Damassadinium spp.	0	0	0	0	0	0	0	0	0	0	1	4
Dapsillidinium spp.	0	0	0	0	0	0	0	0	2	0	0	0
Deflandrea oebisfeldensis	0	0	0	0	0	*	0	0	0	0	0	0
Diphyes sp. B	0	1	0	0	0	1	0	1	4	0	0	4
Enneadocysta sp.	0	0	0	0	0	0	*	0	0	0	0	0
Eocladopyxis peniculata	2	1	*	0	2	*	7	0	0	0	0	0
Fibrocysta axialis	0	0	0	0	0	0	0	0	0	3	1	0
Fibrocysta spp.	0	0	0	0	0	0	0	0	0	0	0	3
Glaphyrocysta divaricata	0	0	0	0	0	0	0	5	4	0	0	0
Glaphyrocysta ordinata	0	0	0	0	0	0	0	2	0	0	0	0
Glaphyrocysta spp.	1	29	0	0	0	0	0	11	5	0	0	0
Hafniasphaera hyalospinosa	0	0	0	0	0	9	0	3	5	4	10	36
Homotryblium abbreviatum	0	0	0	0	1	0	6	1	0	0	0	0
Homotryblium tenuispinosum	0	10	0	0	4	0	4	0	0	0	0	0
Hystrichokolpoma rigaudiae	0	0	0	0	0	0	0	0	0	0	0	1
Hystrichokolpoma unispinum	0	0	0	0	0	*	0	0	*	0	0	0
Hystrichosphaeridium tubiferum	0	0	0	0	0	0	*	0	2	0	0	0
Ifecysta "bipolaris"	0	0	0	0	0	0	0	0	0	0	0	4
"Ifecysta" lappacea	0	0	0	0	0	0	0	0	0	0	6	15
Impagidinium celineae	0	0	0	0	0	0	0	0	0	0	1	1
Impagidinium spp.	1	0	0	0	0	0	0	0	4	0	0	4
Kallosphaeridium brevibarbatum	0	0	0	1	0	*	0	0	2	0	0	0
Melitasphaeridium spp.	0	0	0	0	0	0	0	3	2	0	0	0

Minisphaeridium expansum	0	0	0	0	0	0	0	3	3	0	0	0
Muratodinium spp.	0	9	0	4	0	0	0	0	0	0	0	0
Oligosphaeridium sp.	0	2	0	0	0	0	0	0	0	0	0	0
Operculodinium spp.	29	14	5	12	0	40	7	40	16	32	25	34
Operculodinium tiara	0	0	0	0	3	5	10	49	15	9	6	12
Palaeocystodinium golzowenze	0	0	0	0	0	*	1	1	1	0	0	3
Palaeocystodinium sp. A	0	0	0	0	0	0	0	2	0	0	0	0
Phelodinium magnificum	0	0	0	0	0	0	0	0	1	0	0	0
Polysphaeridium spp.	0	3	1	11	2	19	*	0	0	0	0	0
Sentusidinium spp.	0	0	0	0	0	0	0	2	4	1	3	1
Spinidinium sp.	0	2	0	0	0	0	0	0	0	0	0	0
Spiniferites "spongiosus"	0	0	0	0	0	0	0	0	0	3	1	4
Spiniferites microceras	0	0	0	0	0	0	73	0	0	0	0	0
Spiniferites ramosus	0	8	190	15	0	13	40	15	30	24	12	0
Spiniferites spp.	262	34	103	24	0	215	99	60	193	179	150	131
Tanyosphaeridium xanthiopyxides	0	0	0	0	0	0	0	1	4	0	1	4
Tectatodinium rugulatum	0	0	0	0	0	1	0	2	0	0	1	0
Thalassiphora delicata	0	0	0	0	0	*	0	1	2	0	0	0
Unidentified cysts	0	0	0	0	0	0	0	1	0	0	4	2
Wilsodinium nigeriense	0	0	0	0	0		*	0	0	0	0	0
Total	297	141	299	79	15	322	310	279	316	275	252	329

* Taxa not included in the dinocyst count.

APPENDIX C.

QUANTITATIVE DINOCYST DATA FOR ALO-1 WELL.

Depth (m)	54.9	73	91.4	109.7	146.3	164.6	182.9	201	219.4	237.7	256	274.3	292.6	329.2	365.8	384
Slide #	R-1134-2	B-11286	B-11287	R-1134-3	B-11288	R-1134-4	B-11289	B-11290	R-1134-5	B-11291	B-11292	R-1134-6	B-11293	R-1134-7	B-11294	R-1134-8
Achilleodinium? sp.	0	0	0	0	0	2	0	0	0	0	0	0	0	0	0	0
Achomosphaera sp. A	0	1	0	14	0	22	0	1	1	0	0	1	0	0	0	0
Achomosphaera spp.	0	0	0	0	0	8	0	0	0	0	0	1	0	0	0	0
Adnatosphaeridium membraniphorum	2	3	0	28	2	21	1	4	*	0	0	0	0	0	0	1
Adnatosphaeridium multispinosum	2	3	4	23	0	1	0	0	1	0	0	0	0	0	0	1
Adnatosphaeridium sp.	0	0	0	0	1	7	1	1	2	0	0	0	0	0	1	0
Andallusiela? sp.	0	0	0	0	0	0	0	0	0	0	0	0	0	0	0	0
Apectodinium spp.	2	2	1	20	0	68	6	32	232	35	3	48	15	10	6	30
Apteodinium sp. A	0	0	0	*	0	1	0	0	0	0	0	0	0	0	0	0
Areoligera gippingensis	0	0	0	0	0	0	0	0	0	0	0	0	0	0	0	0
Areoligera spp.	0	7	0	0	0	0	0	0	4	0	0	1	0	0	0	0
Areosphaeridium sp. A	7	0	2	2	0	0	0	0	0	0	0	0	0	0	0	0
Cerodinium boloniense	0	2	0	0	0	0	0	0	0	0	0	0	0	0	0	0
Cerodinium glabrum	0	0	0	0	0	0	0	0	0	0	0	0	0	0	0	0
Cerodinium sp.	0	1	0	0	0	0	0	0	0	0	0	0	0	0	0	0
Cordosphaeridium delimurum	0	0	0	8	0	0	0	0	0	0	0	0	0	0	0	0
Cordosphaeridium fibrospinosum	0	0	0	5	0	0	0	0	0	0	0	0	0	0	0	0
Cordosphaeridium spp.	0	0	0	9	0	0	0	0	1	0	0	0	0	0	0	0
Coronifera oceanica	3	2	0	2	0	0	0	1	2	1	0	4	6	4	3	0
Damassadinium sp. cf. D. impages	0	0	0	1	0	0	0	0	0	0	0	0	0	0	0	0
Damassadinium heterospinosum	0	0	0	0	0	0	0	0	0	0	0	0	0	8	0	*
Dapsilidinium spp.	0	0	0	0	0	0	0	0	0	0	0	0	0	0	0	0
Diphyes sp. A	0	0	0	0	0	0	0	0	0	0	0	0	0	0	0	0
Diphyes sp. B	0	0	0	1	0	2	0	0	0	0	0	0	0	0	0	0
Eocladopyxis peniculata	0	3	3	11	0	6	1	4	22	1	1	8	1	3	0	0
Eocladopyxis sp. 1	0	0	0	7	0	0	0	0	0	0	0	0	0	0	0	0
Fibrocysta spp.	0	0	0	0	0	0	0	0	0	0	0	0	0	0	0	0
Glaphyrocysta divaricata	6	5	7	7	1	5	1	11	*	0	0	2	0	0	0	0
Glaphyrocysta ordinata	4	0	0	0	0	0	0	0	1	0	0	0	0	0	0	0
Glaphyrocysta spp.	4	15	6	16	0	3	1	9	2	0	0	0	1	1	8	2
Hafniaphaera hyalospinosa	0	0	0	5	3	1	2	0	0	0	0	0	0	2	1	1
Hystrichokolpoma sp.	0	0	0	0	0	0	0	1	0	0	0	0	0	0	0	0
Oligokolpoma sp. A	0	0	0	2	0	0	0	0	0	0	0	0	0	1	0	3
Hystrichokolpoma unispinum	1	0	0	0	0	0	0	0	0	0	0	0	0	0	0	0
Hystrichosphaeridium tubiferum	0	1	0	0	0	0	0	0	0	0	0	0	0	0	0	0
Ifecysta "bipolaris"	1	0	0	38	1	10	0	0	0	0	0	2	0	1	1	5
"Ifecysta" lappacea	0	0	0	0	0	0	0	0	*	0	0	5	0	5	1	70
Ifecysta? *"taeniata"*	1	0	0	5	0	0	0	0	0	0	0	0	0	0	0	0
Ifecysta pachyderma	0	0	0	3	1	4	4	9	15	0	5	11	1	43	2	154
Ifecysta "heterospinosa"	0	1	1	42	0	19	4	1	1	3	2	44	0	6	16	9
Impagidinium celineae	0	0	0	0	0	0	0	0	0	0	0	0	0	0	0	0
Impagidinium crassimuratum	0	0	0	*	0	0	0	0	0	0	0	0	0	0	0	0

Impagidinium spp.	0	0	0	*	0	1	0	0	*	2	0	1	0	0	0	1
Impletosphaeridium spp.	0	7	0	1	0	6	1	0	1	0	0	3	4	41	5	13
Kallosphaeridium orchiesense	0	2	0	1	0	3	1	0	0	0	0	0	0	0	0	0
Kallosphaeridium? sp. A	1	0	0	0	0	0	0	0	0	0	0	0	0	0	0	0
Kallosphaeridium spp.	0	0	0	0	0	0	0	0	0	0	0	1	0	0	0	1
Lanternosphaeridium spp.	0	0	1	0	0	7	0	4	0	0	0	0	0	21	0	5
Lejeunecysta sp. 1	0	1	0	0	0	0	1	0	0	0	0	0	0	0	0	0
Kallosphaeridium? sp. A	1	0	0	0	0	0	0	0	0	0	0	0	0	0	0	0
Magallanesium densispinatum	0	0	0	0	0	0	0	0	0	0	0	0	0	0	0	0
Muratodinium spp.	1	1	0	0	0	1	0	0	0	0	0	0	0	0	0	0
Operculodinium spp.	2	4	1	5	0	7	0	1	1	1	0	5	0	1	2	14
Operculodinium tiara	4	5	1	0	0	2	0	1	0	0	0	7	1	3	2	0
Palaeocystodinium golzowenze	8	2	0	*	0	1	0	0	*	0	0	1	0	0	0	*
Palaeocystodinium sp. A	0	0	0	0	0	0	0	0	0	0	0	0	0	0	0	0
Phelodinium magnificum	0	0	0	0	0	*	0	1	0	0	0	0	0	0	0	0
Polysphaeridium spp.	137	57	3	11	0	2	0	3	0	0	0	0	0	0	0	0
Senoniasphaera sp.	0	0	0	0	0	0	1	0	0	0	0	0	0	0	0	0
Sentusidinium spp.	3	2	0	0	0	0	0	0	0	0	0	0	0	1	0	0
Spiniferites microceras	68	0	0	0	0	1	0	0	0	0	0	0	0	0	0	0
Spiniferites ramosus	12	0	4	8	0	12	1	0	5	0	0	3	0	6	0	1
Spiniferites spp.	39	23	13	25	5	111	6	23	19	4	4	17	9	10	31	10
Thalassiphora delicata	0	0	0	*	0	0	0	0	1	0	0	0	0	0	0	0
Wilsodinium sp. A	0	0	0	9	0	2	0	1	0	0	0	0	0	0	0	0
Unidentified cysts	0	1	0	3	0	1	0	0	0	1	0	0	0	0	0	0
Total counted	309	151	47	312	14	337	32	108	311	48	15	165	38	167	79	321

* Taxa not included in the dinocyst count.

Depth (m)	402.3	438.9	457.2	475.5	493.7	530.3	548.6	566.9	585.2	603.5	621.8	658.4	676.6	695	713.2	731.5	768.1
Slide #	B-11295	R-1134-9	B-12270	B-12271	R-1134-10	B-12272	R-1134-11	B-12273	B-12274	R-1134-12	B-12275	R-1134-13	B-12276	B-12277	R-1134-14	B-12278	R-1134-15
Achilleodinium? sp.	0	0	0	0	0	0	0	0	0	0	0	0	0	0	0	0	0
Achomosphaera sp. A	0	2	0	0	0	0	2	0	0	0	0	0	0	0	0	0	0
Achomosphaera spp.	0	0	0	0	0	0	0	0	0	0	0	0	0	0	0	0	0
Adnatosphaeridium membraniphorum	0	2	0	0	0	0	0	0	0	0	0	0	0	0	0	0	0
Adnatosphaeridium multispinosum	0	1	0	0	0	0	0	0	0	0	0	0	0	0	0	0	0
Adnatosphaeridium sp.	0	0	0	0	0	0	0	0	0	0	0	0	0	0	0	0	0
Andallusiela? sp.	0	0	0	0	0	0	0	0	0	0	0	0	0	0	1	0	0
Apectodinium spp.	0	41	0	0	8	0	0	0	0	0	0	0	0	0	0	0	0
Apteodinium sp. A	0	0	0	0	2	0	0	0	0	0	0	0	0	0	0	0	3
Areoligera gippingensis	0	0	0	0	20	0	3	2	0	4	0	0	0	0	2	0	1
Areoligera spp.	0	5	0	0	0	0	0	0	0	0	0	0	0	0	0	0	0
Areosphaeridium sp. A	0	0	0	0	0	0	0	0	0	0	0	0	0	0	0	0	0
Cerodinium boloniense	0	0	0	0	0	0	0	0	0	0	0	0	0	0	0	1	0
Cerodinium glabrum	0	0	0	1	0	0	0	0	0	1	0	0	0	0	0	0	0
Cerodinium sp.	0	0	0	0	0	0	0	0	0	0	0	1	1	0	2	0	0
Cordosphaeridium delimurum	0	3	0	0	3	0	0	0	0	0	0	0	0	0	0	0	0
Cordosphaeridium fibrospinosum	0	0	0	0	0	0	0	0	0	0	0	0	0	0	0	0	0
Cordosphaeridium spp.	0	0	0	0	0	0	0	0	0	0	0	0	0	0	0	0	0
Coronifera oceanica	0	3	2	0	3	0	1	0	0	4	1	1	0	0	6	0	4
Damassadinium sp. cf. *D. impages*	0	0	0	0	0	0	0	0	0	0	0	0	0	0	0	0	0
Damassadinium heterospinosum	0	3	2	0	0	0	2	0	0	6	1	0	0	0	0	1	0
Dapsilidinium spp.	0	0	0	0	1	0	0	0	0	2	0	0	0	0	0	0	0
Diphyes sp. A	0	0	0	0	0	0	2	1	0	5	0	0	0	0	0	0	3
Diphyes sp. B	0	0	0	0	2	0	0	0	0	0	0	0	0	0	0	0	0
Eocladopyxis peniculata	0	0	0	0	0	0	0	0	0	0	0	0	0	0	0	0	0
Eocladopyxis sp. 1	0	0	0	0	0	0	0	0	0	0	0	0	1	0	0	0	0
Fibrocysta spp.	0	0	2	0	0	0	0	0	0	0	0	0	0	0	0	0	0
Glaphyrocysta divaricata	0	1	0	0	0	0	0	0	0	0	0	0	0	0	0	0	0
Glaphyrocysta ordinata	0	0	0	0	0	0	0	0	0	0	0	0	0	0	0	0	0
Glaphyrocysta spp.	0	6	2	0	3	0	0	0	0	0	0	0	0	0	1	0	0
Hafniaphaera hyalospinosa	0	*	0	0	5	0	0	0	0	1	0	0	0	0	0	0	0
Hystrichokolpoma sp.	0	0	0	0	0	0	0	0	0	0	0	0	0	0	0	0	0
Oligokolpoma sp. A	0	1	0	0	0	0	0	0	0	0	0	0	0	0	0	0	0
Hystrichokolpoma unispinum	0	0	0	0	0	0	0	0	0	0	0	0	0	0	0	0	0
Hystrichosphaeridium tubiferum	0	0	0	0	0	0	0	0	0	1	0	0	0	0	0	0	0
Ifecysta "bipolaris"	0	1	0	0	1	0	2	0	0	1	0	0	0	0	0	0	0
"Ifecysta" lappacea	1	52	4	0	42	2	53	8	2	89	4	2	1	1	78	19	0
Ifecysta? *"taeniata"*	0	0	0	0	0	0	0	0	0	0	0	0	0	0	0	0	0
Ifecysta pachyderma	0	67	0	1	32	8	41	0	3	34	0	4	1	0	40	0	8
Ifecysta "heterospinosa"	0	12	0	0	4	0	0	0	0	0	0	0	0	0	0	0	32
Impagidinium celineae	0	0	0	0	6	0	0	0	0	0	0	0	0	0	0	0	0
Impagidinium crassimuratum	0	0	0	0	0	0	0	0	0	0	0	0	0	0	0	0	0
Impagidinium spp.	0	1	0	0	5	0	1	0	1	0	0	0	0	0	1	0	0
Impletosphaeridium spp.	10	37	0	1	0	0	16	0	0	3	4	1	0	1	8	0	6

Kallosphaeridium orchiesense	0	0	0	0	0	0	0	0	0	0	0	0	0	0	0	0	0
Kallosphaeridium? sp. A	0	0	0	0	0	0	0	0	0	0	0	0	0	0	0	0	0
Kallosphaeridium spp.	0	0	0	0	0	0	0	0	0	1	0	0	0	0	1	0	0
Lanternosphaeridium spp.	0	1	0	0	9	0	0	0	0	0	0	0	0	0	0	0	0
Lejeunecysta sp. 1	0	0	0	0	0	0	0	0	0	0	0	0	0	0	0	0	0
Kallosphaeridium? sp. A	0	0	0	0	0	0	0	0	0	0	0	0	0	0	0	0	0
Magallanesium densispinatum	0	0	0	0	5	0	1	0	0	0	0	0	0	0	0	0	0
Muratodinium spp.	0	0	0	0	0	0	0	0	0	0	0	0	0	0	0	0	0
Operculodinium spp.	0	4	0	1	18	0	5	4	1	15	0	1	0	0	16	3	17
Operculodinium tiara	0	6	0	0	8	0	0	0	0	0	0	0	0	0	0	0	0
Palaeocystodinium golzowenze	1	6	0	0	1	0	0	0	0	0	0	0	0	0	0	0	1
Palaeocystodinium sp. A	0	4	0	0	0	0	1	0	0	0	0	0	0	0	0	0	0
Phelodinium magnificum	0	1	0	0	2	0	0	0	0	0	0	0	0	0	0	0	0
Polysphaeridium spp.	0	0	0	0	0	0	0	0	0	0	0	0	0	0	0	0	0
Senoniasphaera sp.	0	0	0	0	0	0	0	0	0	0	0	0	0	0	0	0	0
Sentusidinium spp.	0	0	2	0	0	0	3	0	0	0	0	1	0	0	0	0	0
Spiniferites microceras	0	0	0	0	0	0	0	0	0	0	0	0	0	0	0	0	0
Spiniferites ramosus	0	8	0	0	9	0	0	0	0	0	0	0	0	0	0	0	5
Spiniferites spp.	6	57	7	10	134	5	38	6	4	22	6	3	1	1	30	5	29
Thalassiphora delicata	0	0	0	0	0	0	0	0	0	0	0	0	0	0	0	0	0
Wilsodinium sp. A	0	0	0	0	0	0	0	0	0	0	0	0	0	0	0	0	0
Unidentified cysts	0	1	12	0	1	1	0	0	0	0	0	0	0	0	1	0	2
Total counted	18	326	33	14	324	16	171	21	11	189	16	14	5	3	187	29	111

* Taxa not included in the dinocyst count.

APPENDIX D.

GLOSSARY OF THE TERMINOLOGY APPLIED TO DINOCYSTS.

(For further definitions, please see glossary in Williams et al., 2000, and Fensome and Williams, 2005. Illustrations were taken from the manual of organic walled dinocysts from Lab. Palaeobotany and Palynology, University of Utrecht.)

Acavate: Term for a cyst having no cavities between the wall layers.

Accessory archeopyle suture: A partially developed suture between paraplates around the archeopyle or operculum margin.

Aculeate: Term for a process with an ending that is drawn out into pointed spinelets, usually of equal length (Fig. 5-25).

Acuminate: Term for a process that has a pointed ending (Fig. 5-11).

Annulate: Term for processes or other features that are arranged in a circle (Fig. 6-1).

Apiculocavate: Term for a cyst wall with cavities at the base of or throughout the length of the processes.

Archeopyle: The excystment opening in a dinocyst (see Fig. 2 for illustrations of different archeopyle types).

Arcuate: Term for processes or other features that are arranged in an arc (Fig. 6-3).

Atabular: A situation in which there are no features reflecting tabulation, other than possibly the cingulum, on the cyst wall.

Attached operculum: An operculum that remains partially attached to the main body after excystment (Fig. 2).

Autophragm: The single-layered wall of acavate dinocysts, or the inner wall of holocavate dinocysts.

Bifid: Term for a closed or solid process that is angularly divided into two short, equal parts.

Bifurcate: Term for a process that is divided distally into two branches (Fig. 5-34).

Bulbous: Term for a solid or closed process that is distally swollen and has the appearance of a club (Fig. 5-13).

Cavate: Term for a cyst with a cavity or cavities between wall layers.

Central body: The body from which arise the processes or septa in a chorate or proximochorate cyst (Fig. 4).

Chorate: Term for a cyst with processes or septa that in height are more than 30% of the shortest diameter of the central body (see Figs. 3 and 4).

Cingulum: In motile dinokont dinoflagellates, the furrow (or equivalent feature on cysts) that divides the episome and hyposome and in which, in the motile stage, lies the transverse flagellum (Fig. 1).

Circumcavate: Term for a cyst with two wall layers that are continuously separated around the ambitus.

Clypeate: Term for a process bearing a distal perforate, quadrate to polygonal platform.

Combination archeopyle: An archeopyle formed by the loss of paraplates from more than one paraplate series.

Contabular: Term for a situation in which ornamental features or process clusters are clearly grouped within paraplate areas (Fig. 6-11). See also penicontabular.

Cornucavate: Term for a cyst with two wall layers that are separated in the vicinity of the horns only.

Cyst: A coccoid cell with a cell wall and a reproductive or dormancy function; in the context of this study, the term cyst is equivalent to dinoflagellate cyst, or dinocyst.

Digitate: Term for an open process in which the distal margin is drawn out to form finger-like extensions (Fig. 5-19).

Distal: Towards the outside, for example the free ends of processes.

Dorso-ventral: Term referring to the view when either the dorsal or the ventral surface is uppermost.

Ectophragm: The wall layer external to the periphragm or autophragm and supported by processes, membranes or other structures.

Endophragm: The innermost wall layer of a dinocyst with two or more walls that are not connected by supporting structures.

Epicyst: The area of a dinocyst anterior to the cingulum. Equivalent to the epitheca in the motile stage (Fig. 1); the term episome can refer to epitheca or epicyst.

Fusiform: Term describing a spindle-shaped cyst, in which single horns are developed at apical and antapical poles.

Gonal: Term descibing the position of processes or other features that are situated at a junction between three paraplates.

Holocavate: Term referring to a situation in which there are supporting structures between the two wall layers (usually ectophragm and autophragm) of a cavate dinocyst.

Horn: An extension of the cell or cyst wall into a blunt or pointed structure which protrudes from the ambitus.

Hypocyst: The area of a dinocyst posterior to the cingulum. Equivalent to the hypotheca in the motile stage. The term hyposome can refer to both theca and cyst.

Intratabular: Features that are within the parasutures of individual paraplates.

Linear: Term referring to processes or other features arranged in a straight line.

Linear complex: A series of processes or septa arranged in a straight line, linked or unlinked proximally, along their length or distally (Fig. 6-4).

Marginate: Term referring to lateral location when the cyst is orientated dorso-ventrally (Fig. 3).

Marginate ornamentation: Ornamentation that is located on the lateral margin when the cyst is orientated dorso-ventrally.

Mesotabular: Term for a single process that is centrally located on a paraplate (Fig. 6-9).

Nontabular: Term referring to a situation in which the processes or other ornamentation of a dinocyst do not show any relationship to paratabulation (Fig. 6-15).

Pandasutural area: The area between parasutures and linear penitabular features, where these are present. The penitabular boundary may sometimes be in the form of an imaginary line that bounds pandasutural ornament.

Pandasutural band: A zone of ornamentation that occurs across and on both sides of a plate boundary. Commonly, the band is transversely striate.

Paraplate: That area on the cyst eqivalent to a plate on the theca.

Parasutural crest: A crest the arises from a parasuture.

Parasutural process: A process originating from a parasuture.

Paratabular: Refers to a situation in which a cyst shows paratabulation.

Paratabulation: The cyst equivalent of thecal tabulation; reflected tabulation on the cyst.

Penitabular: Term referring to features that are aligned parallel to and just with the plate boundaries.

Penicontabular: Term refrerring to a special form of the contabular condition in which ornament is contained within penitabular limits or by penitabular features.

Peridinioid: Having the outline of Peridinium; that is, dorso-ventrally compressed and with a single apical horn and generally two antapical horns. The left antapical horns may be reduced or absent.

Periphragm: The outer layer in dinoflagellate cysts with two wall layers that are unconnected by supporting structures, or the outermost layer where the middle layer is termed the mesophragm, again with no supporting structures.

Process: A structure which arises generally from an external surface and is columnar or spine-like. Processes may be simple or intricately branched and interconnected.

Process complex: The association of three or more adjacent contabular processes to form a distinctly arranged and aligned group; they are often united, proximally, along their length and/or distally.

Proximal: Term for a feature that is at or close to the point of origin of a process, crest or similar structure.

Proximochorate: Term for a cyst with processes or septa that are of lower height than those of a chorate cyst (Fig.4B).

Septum: A delicate linear projection on the wall of a dinoflagellate cyst. A partial synonym of crest (Fig. 6-8).

Simulate complex: A synonym of penitabular complex (Fig. 6-5).

Spongeous: A wall that contains a usually dense arrangement of cavities and is usually not easily resolvable into layers.

Sulcal: Pertaining to the sulcus.

Tabulation: The arrangement of the plates on the theca. In situations where both the tabulation and paratabulation are implied, the term tabulation is used in the general sense to include both.

Taeniate process: A process in the form of a continuous or discontinuous ribbon or membrane, formed from a linear outgrowth of the periphragm.

Trabeculum (plural trabecula): A flattened or tubular connection between processes.

Trabeculate: Having trabecula (Fig. 3).

Trifurcate: Term for a process that divides, usually distally, into three branches.

Trifurcate process: A process that distally divides into three branches (Fig. 5-22).

Wetzelielloidean: A peridiniacean in which the middorsal anterior intercalary plate is quadra (i.e. four-sided).

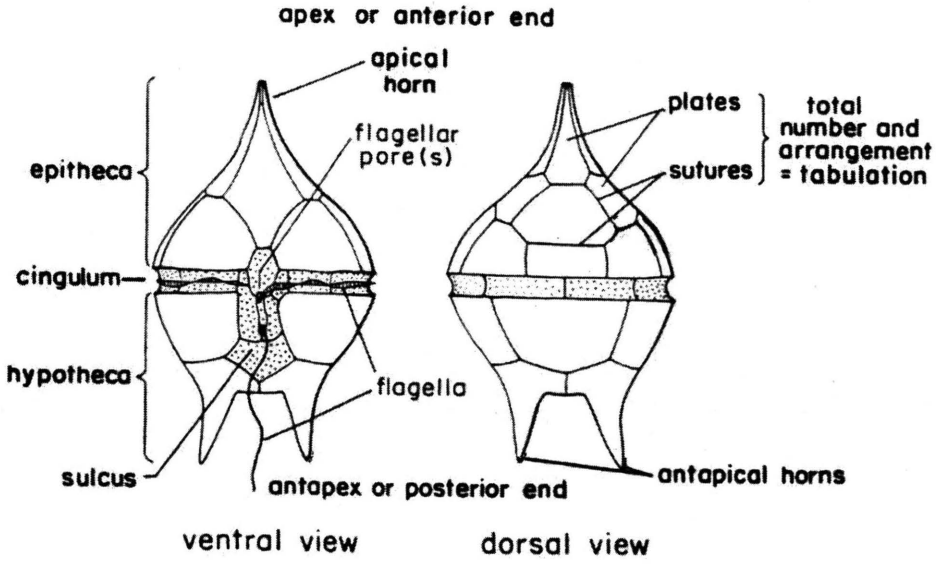

Figure 1. Principal features of the theca in a dinoflagellate.

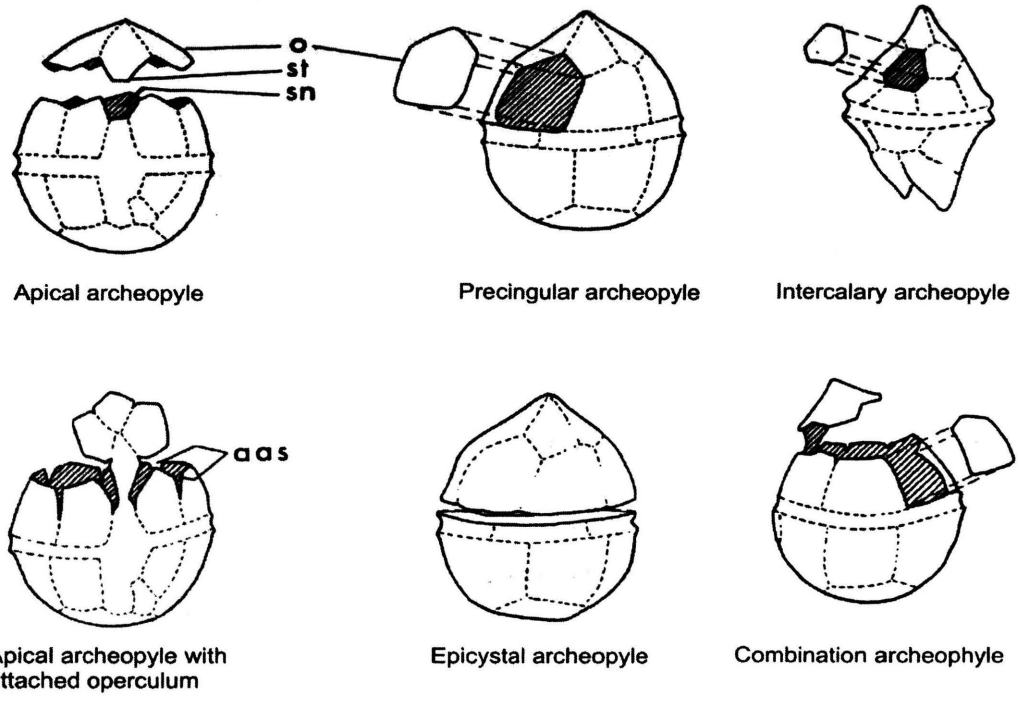

Figure 2. Schematic diagrams illustrating formation of various archeopyle types (Archeopyle shaded); o = operculum, st = parasulcal tongue, sn = parasulcal notch, aas = accessory archeopyle parasuture, pas = principal archeopyle suture.

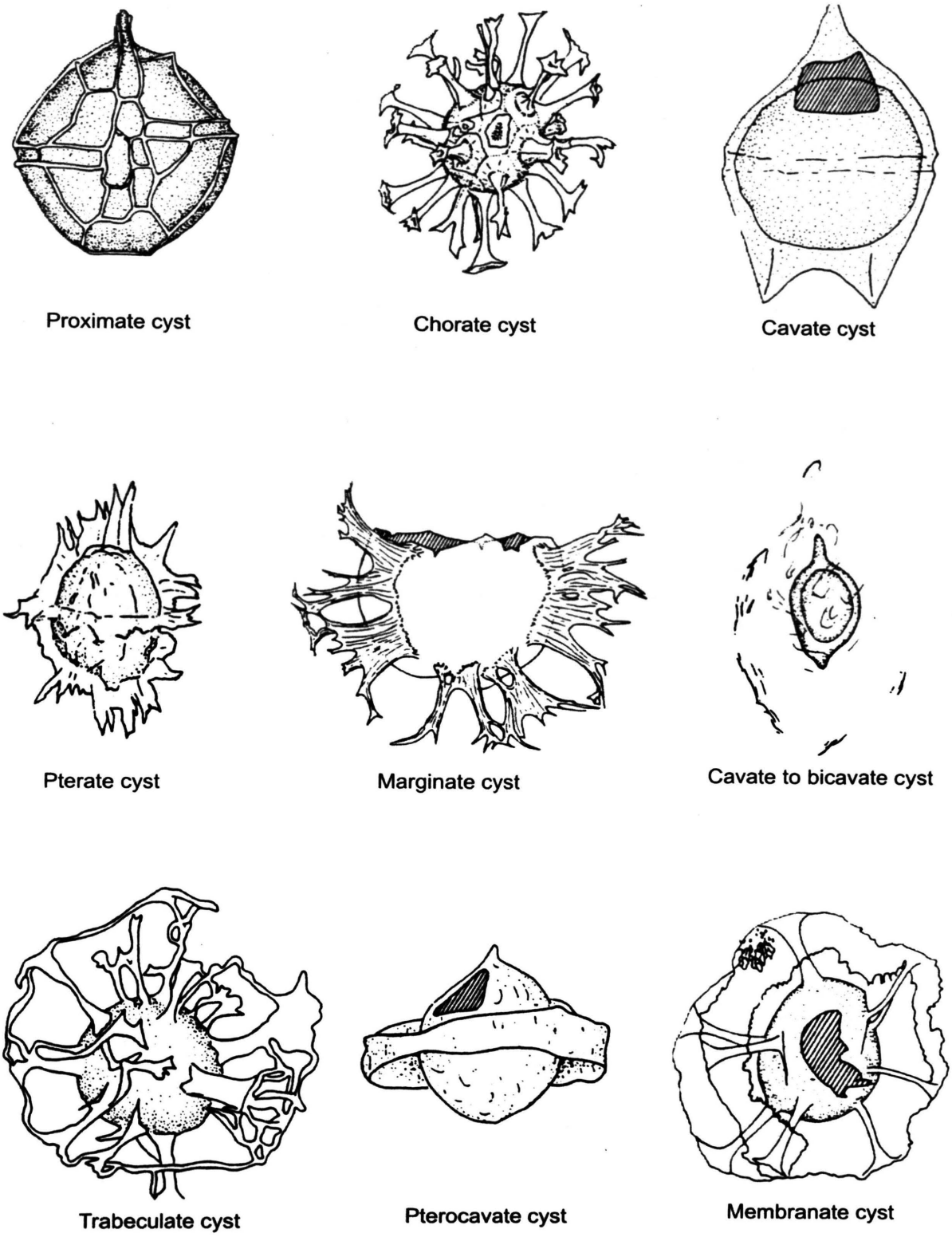

Figure 3. Illustrations of fossil cyst types.

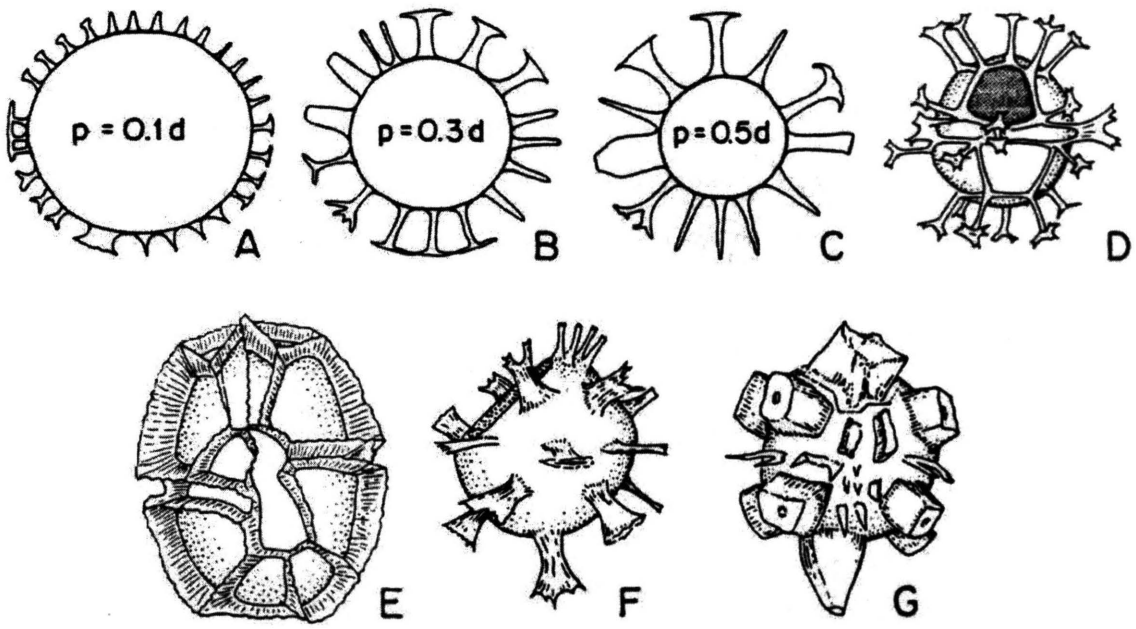

Figure 4. Some examples of surface relief.

A-C – Diagrams to show surface relief of different height relative to the diameter of the main body. A – Maximum height of relief (less than 10% of main body) present on proximate cysts. B – Maximum height of relief (about 30% of main body) on proximochorate cyst. C – Chorate cyst with relief height equal to 50% of main body.

D- Skolochorate cyst with parasutural ridges giving rise at their intersections to trifurcate processes.

E- Murochorate cyst having paratabulation indicated by parasutural septa.

F-G - Skolochorate cysts without clear parasutural markings but with processes situated in the central portions of paraplates (intratabular).

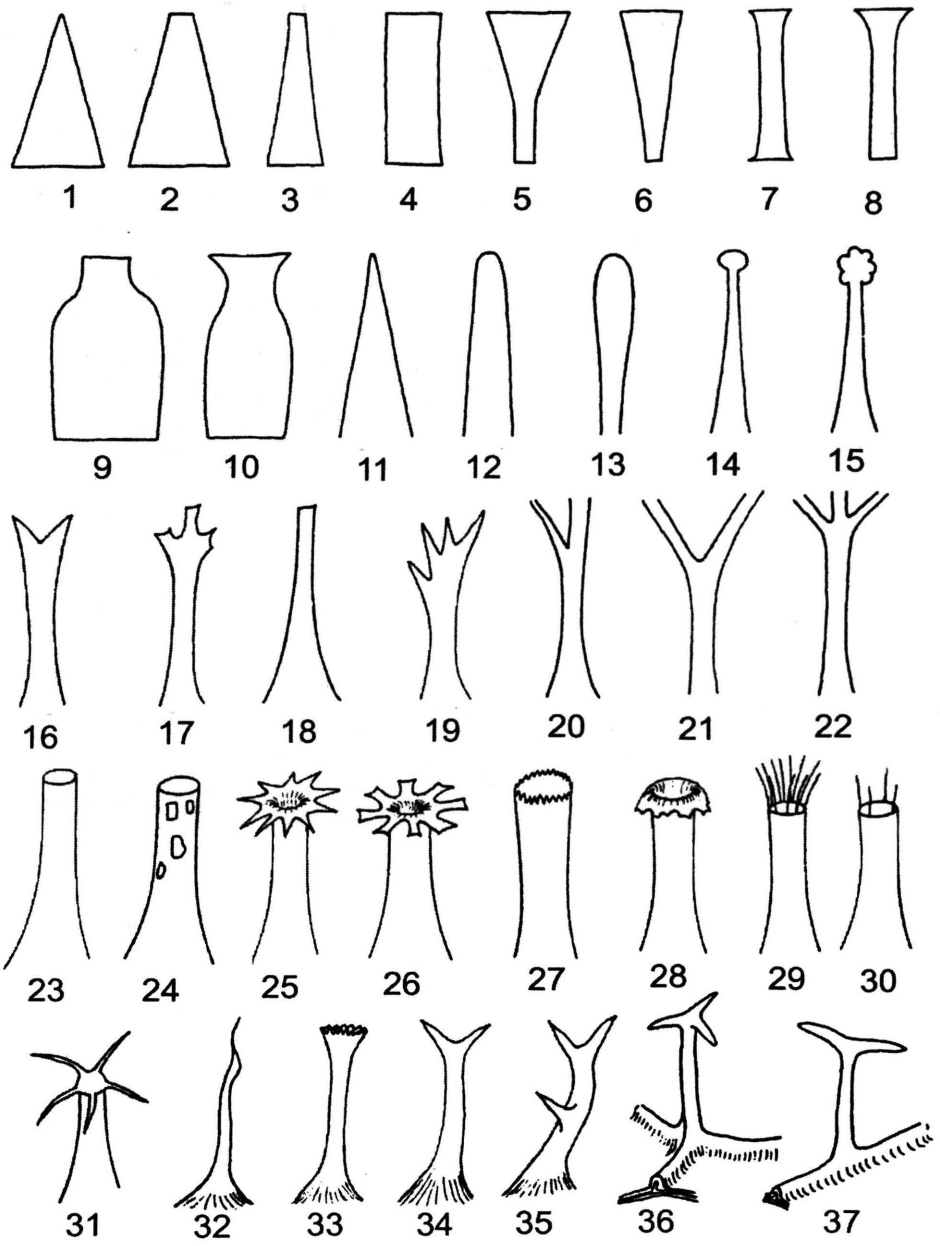

Figure 5. Schematic illustrations of process shapes and process tip terminology. (1) conical, (2) subconical, (3) tapering, (4) cylindrical, (5) infundibular, (6) flared, (7) tubiform, (8) buccinate, (9) lagenate, (10) bulbose, (11) acuminate, (12) evexate, (13) bulbous, (14) capitate, (15) cauliflorate, (16) bifid, (17) foliate, (18) oblate, (19) digitate, (20) branched, (21) bifurcate, (22) trifurcate, (23) entire, (24) fenestrate, (25) aculeate, (26) secate, (27) denticulate, (28) recurved, (29) patulate, (30) dirigate, (31) orthogonal, (32) acicular, (33) tubiform, (34) bifid, (35) branched-bifid, (36) trifurcate gonal, (37) bifurcate intergonal.

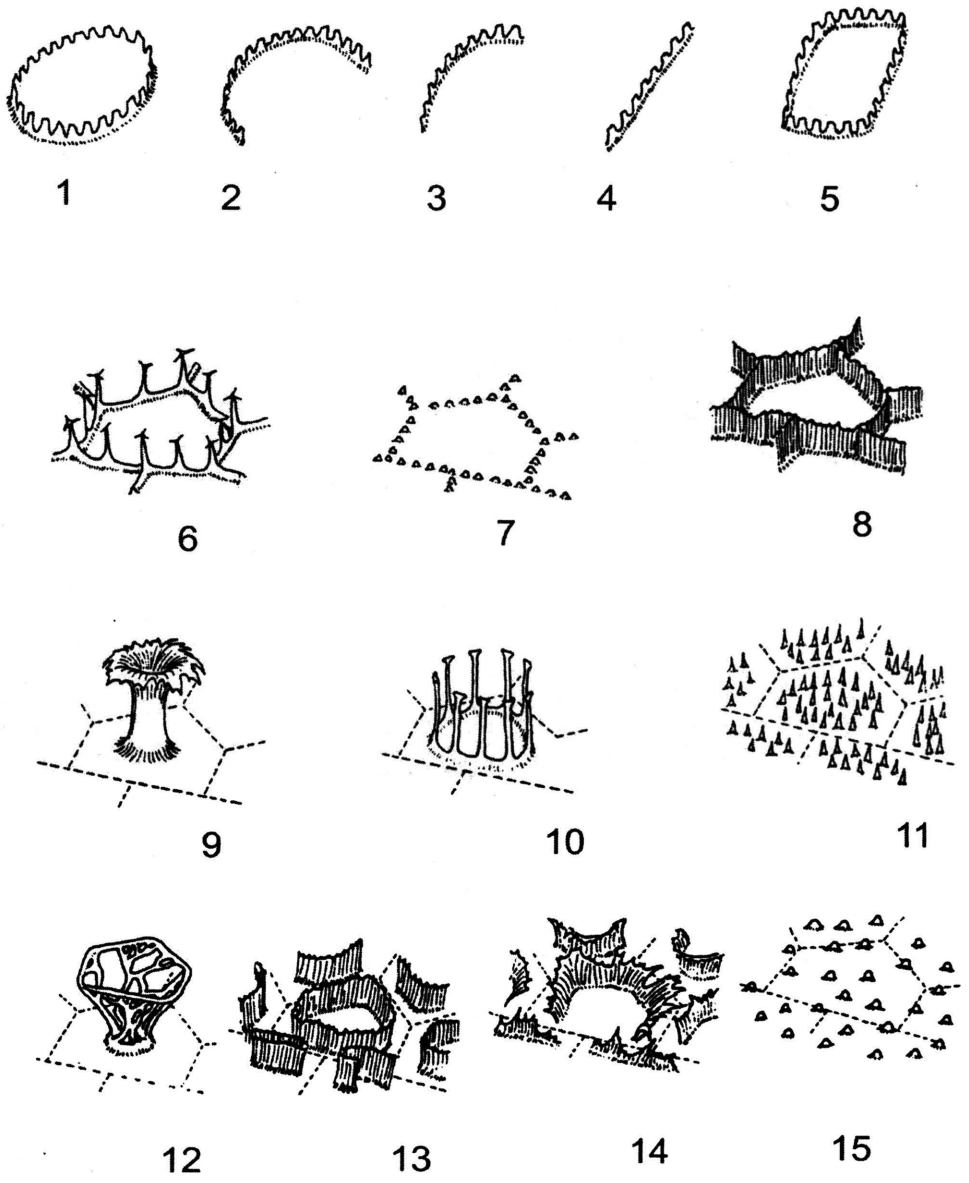

Figure 6. Surface features of fossil dinoflagellates. (1) annulate complex, (2) soleate complex, (3) arcuate complex, (4) linear complex, (5) simulate complex, (6) paratabulation reflected by gonal trifurcate and intergonal bifurcate processes, (7) paratabulation reflected by large granules, (8) paratabulation reflected by thin septa, (9) mesotabular hollow tubiform process, (10) annulate complex, (11) paratabulation reflected by intratabular (contabular) arrangement of spines, (12) large processes with constricted proximal end and a polygonal distal end, (13) penitabular paratabulation reflected by thin septa, (14) paratabulation reflected by dissected and incomplete thin septa, (15) coarse granules distributed in a nontabular arrangement.

BIBLIOGRAPHY

Adegoke, O.S., 1969. Eocene stratigraphy of southern Nigeria. Colloque sur l' Eocene, III. Bureau de Recherches Geologiques et Minieres, vol. 69, pp. 22-48.

Adegoke, O. S., Jan du Chene, R. E., Agumanu, A. E., and Ajayi, P. O., 1978. Palynology and age of the Kerri-Kerri Formation, Nigeria. Revista Espanola de Micropaleontologia. vol. 10, pp. 267-283.

Adegoke, O.S., Arua, I., Oyegoke, O., 1980. Two new nautiloids from the Imo Shale, (Paleocene) and Ameki Formation (Middle Eocene), Anambra State, Nigeria. Journal of Mining and Geology, vol. 17, pp. 85–89.

Arua, I., 1980. Palaeocene Macrofossils from the Imo Shale in Anambra State, Nigeria. Journal of Mining and Geology, vol. 17, pp. 81-84.

Aubry, M.P., Berggren, W., Van Couvering, J.A., Ali, J., Brinkhuis, H., Cramer, B., Kent, D.V., Swicher, C.C., Dupuis, C., Gingerich, P.D., Heilmann-Clausen, C., King, C., Ward, D., Knox, R.W., Ouda, K., Stott, L.D., and Thiry, M., 2003. Chronostratigraphic terminology at the Paleocene/Eocene boundary. In: Wing, S.L., Gingerich, P.D., Schmitz, B., Thomas, E. (Editors). Causes and consequences of globally warm climates in the early Paleogene. Geological Society of America Special Paper 369, pp. 551-566.

Avbovbo, A.A., 1978. Tertiary lithostratigraphy of Niger Delta. American Association of Petroleum Geologists Bulletin, vol. 62, pp. 295-300.

Benkhelil, J., Mascle, J., and Huguen, C., 1998. Deformation patterns and tectonic regimes of the Cote d'Ivoire-Ghana Transform Margin as deduced from Leg 159 results. In: Mascle, J., Lohman, G.P., and Moullade, M. (Editors). Proceedings of the Ocean Drilling Program, Scientific Results, vol. 159, pp. 13-23.

Berggren W.A., 1960. Paleocene biostratigraphy and planktonic foraminifera of Nigeria (West Africa). International Geological Congress, Copenhahen, Report 21, pp. 41-55.

Berggren, W. A., Kent, D. V., Swisher II, C.C. and Aubry, M-P., 1995. A revised Cenozoic Geochronology and Chronostratigraphy. In: Berggren, W. A., Kent, D. V., Aubry, M., and Hardenbol, J. (Editors). Geochronology Time Scales and Global Stratigraphic Correlation. SEPM Special Publication, vol. 54, pp. 129-212.

Berggren, W.A., Lucas, S., and Aubry, M.P., 1998. Late Paleocene-Early Eocene climatic and biotic evolution: an overview. In: Aubry, M.P., Lucas, S. and Berggren, W. (Editors). Late Paleocene-Early Eocene climatic and biotic events in the marine and terrestrial records. Columbia University Press, pp. 1-17.

Bignot, G., 1998. Middle Eocene benthic foraminifers from Holes 960A and 960C, central Atlantic Ocean. In: Mascle, J., Lohmann, G.P. and Moullade. (Editors). Proceedings of the Ocean Drilling Program, Scientific Results, vol. 159, pp. 433-444.

Brinkhuis, H., and Zachariasse, W.J., 1988. Dinoflagellate cysts, sea level changes and planktonic foraminifera across the Cretaceous-Tertiary boundary at El Haria, northwest Tunisia. Marine Micropaleontology, vol. 13, pp. 153-191.

Brinkhuis, H., Romein, A.J.T., Smit, J., and Zachariasse, W.J., 1994. Danian-Selandian dinoflagellate cysts from lower latitudes with special reference to the El Kef section, NW Tunisia. GFF. vol. 116, pp. 46-48.

Brinkhuis, H., Sengers, S., Sluijs, A.,Warnaar, J., and Williams, G.L., 2003. Latest Cretaceous–earliest Oligocene and Quaternary dinoflagellate cysts, ODP Site 1172, East Tasman Plateau. In Exon, N.F., Kennett, J.P., and Malone, M.J. (Editors). Proceedings of the Ocean Drilling Program, Scientific Results, vol. 189, pp. 1–48 [Online]. Available from World Wide Web: <http://www-odp.tamu.edu/publications/189_SR/VOLUME/CHAPTERS/106.PDF>.

Bujak, J., and Brinkhuis, H., 1998. Global warming and dinocyst changes across the Paleocene/Eocene Epoch boundary. In: Aubry, M.P., Lucas, S., and Berggren, W. (Editors). Late Paleocene-Early Eocene climatic and biotic events in the marine and terrestrial records. Columbia University Press, pp. 277-295.

Bujak, J.P., and Mudge, D.C., 1994. A high resolution North Sea Eocene dinocyst zonation. Journal of the Geological Society of London, vol. 151, pp. 449-462.

Burke, K.C., 1996. The African Plate. South African Journal of Geology, vol. 99, pp. 339-409.

Burke, K.C., Dessauvagie, T.F.J., and Whiteman, A.J., 1971. The opening of the Gulf of Guinea and the geological history of the Benue depression and Niger Delta. Nature Physical Science, vol. 233, pp. 51-55.

Caro, Y., 1973. Contribution a la connaissance des dinoflagelles du Paleocene-Eocene inferieur des Pyrenees espagnoles. Revista Española de Micropaleontologia, vol. 5, pp. 329-372.

Châteauneuf, J.J., and Gruas-Cavagnetto, C., 1978. Les zones de Wetzeliellaceae (Dinophyceae) du bassin de Paris. Comparaison et correlations avec les zones du Paleogene des bassins bassins du Nord-Ouest de l'Europe. Bulletin du Bureau de Recherches Geologiques et Minieres (2me Sér.), Section IV, pp. 59-93.

Cookson, I.C., and Eisenack, A., 1965. Microplankton from the Paleocene Pebble Point Formation, south western Victoria. Proceedings of the Royal Society of Victoria, vol. 79, pp. 139-146.

Cookson, I.C., and Eisenack, A., 1967. Some microplankton from the Paleocene Rivernook Bed, Victoria. Proceedings of the Royal Society of Victoria, vol. 80, pp. 247- 257.

Costa, L.I., and Downie, C., 1976. The distribution of the dinoflagellate Wetzeliella in the Palaeogene of north-western Europe. Palaeontology, vol. 19, pp. 591-614.

Crouch, E.M., 2001. Environmental change at the time of the Paleocene-Eocene biotic turnover. LPP Contributions Series, 14. Utrecht University, 216 pp.

Crouch, E.M., Heilmann-Clausen, C., Brinkhuis, H., Morgans, H., Rogers, K.M., Egger, H. and Schmitz, B., 2001. Global dinoflagellate event associated with the Late Paleocene thermal maximum. Geology, vol. 29(4), pp. 315-318.

Crouch, E.M., Brinkhuis, H., Visscher, H., Adatte, T. and Bolle, M-P., 2003. Late Paleocene-early Eocene dinoflagellate cyst records from the Tethys; further observations on the global distribution of Apectodinium. In: Wing, SL., Gingerich, P., Schmitz, B., Thomas, E. (Editors). Causes and consequences of globally warm climates in the early Paleogene. Geological Society of America Special Paper 369, pp. 113-131.

Damassa, S.P., 1979a. Eocene dinoflagellates from the Coastal Belt of the Franciscan Complex, northern California. Journal of Paleontology, vol. 53, pp. 815-840.

Damassa, S.P., 1979b. Danian dinoflagellates from the Franciscan Complex, Mendocino County, California. Palynology, vol. 3, pp. 191-207.

Damassa, S.P., Goodman, D.K., Kidson, E.J., and Williams G.L., 1990. Correlation of Paleogene dinoflagellate assemblages to standard nannofossil zonation in North Atlantic DSDP sites. Review of Paleobotany and Palynology, vol. 65, p. 331-339.

De Coninck, J., 1975. Organic-walled microfossils from the Upper Danian and Middle Paleocene of Southern Sweden. Geologiska Foereningen i Stockholm Foerhandlingar, vol. 97, pp. 326-337.

Deflandre, G., and Cookson, I.C., 1955. Fossil microplankton from Australian Late Mesozoic and Tertiary sediments. Australian Journal of Marine and Freshwater Research, vol. 6, pp. 242-313.

De La Rue, S.R., 2000. Late Paleocene-Early Oligocene palynomorphs from the Cote d'Ivoire-Ghana Transform Margin, eastern equatorial Atlantic: Biostratigraphic

and paleoenvironmental significance. MS Thesis, University of Missouri-Rolla, 211 pp.

De La Rue, S.R., and Oboh-Ikuenobe, F.E., 2003. Temporal dynamics of Paleogene paleovegetational response to climatic changes and regional upwelling, West Africa (ODP Site 959). Transactions - Gulf Coast Association of Geological Societies, vol. 53, pp. 160-169.

Doust, H., and Omatsola, E., 1990. Niger Delta. In: Edwards, J.D., Santogrossi, P.A. (Editors). Divergent/Passive Margin Basins. American Association of Petroleum Geologists Memoir, vol. 48, pp. 201–238.

El Beialy, S. Y., 1998. Stratigraphic and palaeoenvironmental significance of Eocene palynomorphs from the Rusayl Shale Formation, Al Khawd, northern Oman. Review of Palaeobotany and Palynology, vol. 102, pp. 249-258.

Emery, K.O., Uchupi, E., Phillips, J., Bowin, C., and Mascle, J., 1975. Continental margin off western Africa: Angola to Sierra Leone. American Association of Petroleum Geologists Bulletin, vol. 59, pp. 2209-2265.

Evamy, B.D., Haremboure, J., Kamerling, P., Knaap, W.A., Molloy, F.A., and Rowlands, P.H., 1978. Hydrocarbon habitat of the Tertiary Niger Delta. American Association of Petroleum Geologists Bulletin, vol. 62, pp.1-39.

Fayose, E.A., and Ola, P.S., 1990. Radiolarian occurrences in the Ameki type section, eastern Nigeria. Journal of Mining and Geology, vol. 26, pp. 75-80.

Fensome, R.A., and Williams, G.L., 2004. The Lentin and Williams index of fossil dinoflagellates 2004 Edition. American Association of Stratigraphic Palynologists Contributions Series No. 42, 892 pp.

Fensome, R.A., and Williams, G.L., 2005. Scotian Margin Palyatlas Version 1. Geological Survey of Canada, Open File 4677, 180 pp.

Fensome, R.A., Taylor, F.J.R., Norris, G., Sarjeant, W.A.S., Wharton, D.I. and Williams, G.L., 1993. A classification of fossil and living dinoflagellates. Micropaleontology Press Special Paper, No. 7, 351 pp.

Firth, J.V., 1987. Dinoflagellate biostratigraphy of the Maastrichtian to Danian interval in the U.S. Geological Survey Albany Core, Georgia, U.S.A. Palynology, vol. 11, pp. 199-216.

Frederiksen, N.O., 1994. Middle and late Paleocene angiosperm pollen from Pakistan. Palynology, vol. 18, pp. 91-137.

Germeraad, J. H., Hopping, C. A., and Muller, J. 1968. Palynology of Tertiary sediments from tropical areas. Review of Palaeobotany and Palynology, vol. 6, pp. 189-348.

Gingerich, P.D., 2003. Mammalian responses to climate change at the Paleocene-Eocene boundary: Polecat Bench record in the northern Bighorn Basin, Wyoming. In: Wing, S.L., Gingerich, P.D., Schmitz, B., and Thomas, E. (Editors). Causes and Consequences of Globally Warm Climates in the Early Paleogene. Geological Society of America Special Paper 369, pp. 463–478.

Gradstein, F.M., Ogg, J.G., and Smith, A.G., 2004. A Geologic Time Scale 2004. Cambridge University Press, 500 pp.

Gregory, W.A., and Hart, G.F., 1995. Distribution of dinoflagellates in a subsurface marine Wilcox (Paleocene-Eocene) section in southwest Louisiana. Palynology, vol. 19, pp. 45-75.

Guasti, E., Kounwenhoven, T., Brinkhuis, H. and Speijer, 2005. Paleocene sea-level and productivity changes at the southern Tethyan margin (El Kef, Tunisia). Marine Micropaleontology, vol. 55, pp. 1-17.

Hansen, J.M., 1980. Stratigraphy and structure of the Paleocene in central West Greenland and Denmark. PhD thesis, Copenhagen University, 155 pp.

Harrington, G.J., and Kemp, S.J., 2001. US Gulf coast vegetation dynamics during the latest Paleocene. Palaeogeography, Palaeoclimatology, Palaeoecology, vol. 167, pp. 1-21.

Harland, R., 1979. The Wetzeliella (Apectodinium) homomorphum plexus from the Paleocene/Earliest Eocene of northwest Europe. Proceedings of the International Palynological Conference, Lucknow, vol. 2, pp. 59-70.

Heilmann-Clausen, C., 1985. Dinoflagellate stratigraphy of the uppermost Danian to Ypresian in the Viborg 1 borehole, central Jylland, Denmark. Danmarks Geologiske Undersogelse, ser. A, 7, pp. 1-69.

Iakovleva, A.I., Brinkhuis, H., and Cavagnetto, C., 2001. Late Paleocene-early Eocene dinoflagellate cysts from the Turgay Strait, Kazakhstan; correlations across ancient seaways. Palaeogeography, Palaeoclimatology, Palaeoecology, vol. 172, pp. 243-268.

Iakovleva, A.I., and Kulkova, I.A., 2003. Paleocene-Eocene dinoflagellate zonation in Western Siberia. Review of Palaeobotany and Palynology, vol. 123, pp. 185-197.

Jan du Chêne, R. E., 1988. Etude systematique des Kystes de dinoflagelles de la Formation des Madeleines (danien du Senegal). Cahiers de micropaleontologie, Centre nationale de la recherche scientifique, vol. 2, pp. 147-174.

Jan du Chêne, R.E., and Adediran, S.A., 1985. Late Paleocene to early Eocene dinoflagellates from Nigeria. Cahiers de micropaléontologie, Centre nationale de la recherche scientifique, vol. 3, pp. 3-38.

Jan du Chene, R., and Salami, M. B., 1978. Palynology and micropaleontology of the Upper Eocene of the well Nsukwa 1 (Niger Delta, Nigeria). Archives des Sciences Physiques et Naturelles, vol. 13, pp. 5-9.

Jan du Chene, R. E., Onyike, M. S., and Sowunmi, M. A., 1978. Some new Eocene pollen of the Ogwashi-Asaba Formation, south-eastern Nigeria. Revista Espanola de Micropaleontologia, vol. 10, pp. 285-322.

Jaramillo, C.A., 2002. Response of tropical vegetation to Paleogene warming. Paleobiology, vol. 28, pp. 222-243.

Jaramillo, C.A., and Dilcher, D. L., 2001. Middle Paleogene palynology of Central Colombia, South America: A study of pollen and spores from tropical latitudes. Palaeontotographica Abt. B, 258, pp. 87-213.

Kar, R.K., 1985. The fossil floras of Kachchh-IV. Tertiary palynostratigraphy. Palaeobotany, vol. 34. pp. 1-279.

Keiser, G., and Jan du Chêne, R., 1979. Periretisyncolpites n. gen. & Terscissus Tschudy 1970, grands pollen syncolpes du Maastrichtien du Sénegal et du Nigéria. Revista espanola de Micropaleontologia, vol. 11, pp. 321-334.

Kogbe, C.A., 1976. Paleogeographic history of Nigeria from Albian times. In: Kogbe, C.A. (Editors). Geology of Nigeria. Elizabethan Publishers, Lagos, pp. 237-252.

Köthe, A., Khan, A.M., and Ashraf, M., 1988. Biostratigraphy of the Surghar Range, Salt Range, Sulaiman Range and the Kohat area, Pakistan, according to Jurassic through Paleogene calcareus nannofossils and Paleogene dinoflagellates. Geologisches Jahrbuch, B71, pp. 3-87.

Kuhnt, W., Moullade, M., and Kaminski, M.A., 1998. Upper Cretaceous, K/T Boundary, and Paleocene agglutinated foraminifers from Hole 959D (Cote d'Ivoire-Ghana Transform Margin. In: Mascle, J., Lohmann, G.P. and Moullade. (Editors). Proceedings of the Ocean Drilling Program, Scientific Results, vol. 159, pp. 389-411.

Laboratory of Paleobotany and Palynology, undated. Organic walled dinoflagellate cysts: manual and exercises. Faculty of Biology and Botanical Palaeoecology, Universiteit Utrecht, 69 pp.

Legoux, O., 1978. Quelques espèces de pollen caractéristiques du Néogène du Nigéria. Bulletin des Centres de Recherches Exploration-Production Elf-Aquitaine, vol. 2, pp. 265-317.

Legoux, O., Belsky, C. Y., and Jardinè, S., 1971. Pollens nouveaux de l'Eocene d'Afrique occidentale. Vleme Coll. Afr. Micropalèontol., Abidjan 1970, pp. 226-236.

Mandal, J., Chandra, A., and Kar, R.K., 1994. Palynofossils from the Kadamtala coal, Middle Andaman, India. Geophytology, vol. 23, pp. 209-214.

Martini, E., 1971. Standard Tertiary and Quaternary calcareous nannoplankton zonation. Proceedings - Planktonic Conference, Roma, vol. 2, pp. 739-777.

Mascle, J., Lohmann, G.P., Clift, P.D., and Shipboard Scientific Party, 1996. Introduction. In: Mascle, J., Lohmann, G.P., Clift, P.D., et al. (Editors). Proceedings of the Ocean Drilling Program, Initial Reports, vol. 159, pp. 5-16.

Masure, E., Rauscher, R., Dejax, J., Schuler, M., and Ferre, B., 1998. Cretaceous-Paleocene palynology from the Côte d'Ivoire-Ghana Transform Margin, Sites 959, 960, 961, and 962. Proceedings of the Ocean Drilling Program, Scientific Results, vol. 159, pp. 253-276.

Mehrotra, N.C. and Singh, K., 2003. Atlas of dinoflagellate cysts from Mesozoic-Tertiary sediments of Krishnagodavari Basin: Tertiary dinoflagellate cysts. KDMIPE, ONGC, Dehra Dun Highlights Publications, vol. II, 134 pp.

Mudge, D.C., and Bujak, J.P., 1996. Paleocene biostratigraphy and sequence stratigraphy of the UK central North Sea. Marine and Petroleum Geology, vol. 13, pp. 295-312.

Muller, J., Di Giacomo, E., and Van Erve, A., 1987. A palynologic zonation for the Cretaceous, Tertiary and Quaternary of northern South America. American Association of Stratigraphic Palynologists Contribution Series No. 19, pp. 7-76.

Murat, R.C., 1972. Stratigraphy and paleogeography of the Cretaceous and lower Tertiary in southern Nigeria. In: Dessauvagie, T.F.J., and Whiteman, A.J. (Editors). African Geology. Ibadan University Press, Ibadan, pp. 635-646.

Nøhr-Hansen, H., 2003. Dinoflagellate cyst stratigraphy of Palaeogene strata from Hellefisk-1, Ikermiut-1, Kangamiut-1, Nukik-1, Nukik-2 and Qulleq-1 wells, offshore West Greenland. Marine and Petroleum Geology, vol. 20, pp. 987-1016.

Norris, R.D., 1998. Planktonic foraminifer biostratigraphy: Eastern Equatorial Atlantic. In: Mascle, J., Lohmann, G.P. and Moullade. (Editors). Proceedings of the Ocean Drilling Program, Scientific Results, vol 159, pp. 445-479.

Nwajide, C.S., 1979. A lithostratigraphic analysis of the Nanka Sands, southeastern Nigeria. Journal of Mining and Geology, vol. 16, pp. 103-109.

Obi, C.G., Okogbue, C.O., and Nwajide, C.S., 2001. Evolution of the Enugu Cuesta: A tectonically driven erosional process. Global Journal of Pure and Applied Science, vol. 7, pp. 321-330.

Oboh-Ikuenobe, F.E., Hoffmeister, A.P., and Chrisfield, R.A., 1999. Cyclical distribution of dispersed organic matter and dinocysts, ODP Site 959 (early Oligocene-early Miocene, Cote d'Ivoire-Ghana transform margin). Palynology, vol. 23, pp. 87-96.

Oboh-Ikuenobe, F.E., Obi, C.G., and Jaramillo, C.A, 2005. Lithofacies, palynofacies, and sequence stratigraphy of Palaeogene strata in Southeastern Nigeria. Journal of African Earth Sciences, vol. 41, pp. 79-102.

Oboh-Ikuenobe, F. E., Yepes, O., and ODP Leg 159 Scientific Party, 1997. Palynofacies analysis of sediments from the Côte d'Ivoire-Ghana Transform Margin: preliminary correlation with some regional events in the eastern Equatorial Atlantic. Palaeogeography, Palaeoclimatology, Palaeoecology, vol. 129, pp. 291-314.

Oboh-Ikuenobe, F. E., Yepes, O., and Gregg, J. M., 1998. Palynostratigraphy, palynofacies and thermal maturation of Cretaceous-Paleocene sediments from the Côte d'Ivoire-Ghana Transform Margin. Proceedings of the Ocean Drilling Program, Scientific Results, vol. 159, pp. 277-318.

Okada, H., and Bukry, D., 1980. Supplementary modification and introduction of code numbers to the low-latitude coccolith biostratigraphic zonation (Bukry, 1973; 1975). Marine Micropaleontolology, vol. 5, pp. 321-325.

Pardo-Trujillo, A., Jaramillo, C., and Oboh-Ikuenobe, F.E., 2003. Paleogene palynostratigraphy of the Eastern Middle Magdalena Valley, Colombia. Palynology, vol. 27, pp. 155-178.

Patridge, A.D., 1976. The geological expression of eustacy in the early Tertiary of the Gippsland Basin. The APEA Journal, vol. 16, pp. 73-79.

Powell, A.J., Brinkhuis, H., and Bujak, J.P., 1996. Upper Paleocene-lower Eocene dinoflagellate cyst sequence biostratigraphy of southeast England. In: Knox, R.W.O'B., Corfield, R.M., and Dunay, R.E. (Editors). Correlation of the early Paleogene in Northwest Europe. Geological Society Special Publication No. 101, pp. 145-183.

Quattrocchio, M.E., and Sarjeant W.A., 2003. Dinoflagellates from the Chorillo Chico Formation (Paleocene) of Southern Chile. Ameghiniana. Asociación Paleontológica Argentina, vol. 40, pp. 129-153.

Rao, V. R., and Kumaran. K. P. N., 1988. A short survey of paleobotanical studies (Cretaceous and Tertiary) in Nigeria. Review of Palaeobotany and Palynology, vol. 54, pp. 151-158.

Regali, M., Uesugui, N., and Santos, A., 1974. Palinologia dos Sedimentos Meso-Cenozoicos do Brasil. Boletim tecnico da Petrobras, vol. 17, pp. 177-191.

Reijers, T.J.A., Petters, S.W., and Nwajide, C.S., 1997. The Niger Delta Basin. In: Selley, R.C. (Editor). African Basins. Sedimentary Basins of the World 3: Amsterdam, Elsevier Science, pp. 151-172.

Reyment, R.A., 1965. Aspects of the Geology of Nigeria. Ibadan University Press, Ibadan, 145 pp.

Royer, D.L., Wing, S.L., Beerling, D.J., Jolley, D.W., Koch, P.L., Kickey, L.J., and Berner, R.A., 2001. Palaeobotanical evidence for near present day levels of atmospheric CO2 during part of the Tertiary. Science, vol. 292, pp. 2310-2313.

Rull, V., 1999. Palaeofloristic and palaeovegetational changes across the Paleocene/Eocene boundary in northern South America. Review of Palaeobotany and Palynology, vol. 107, pp. 83-95.

Salami, M. B., 1984. Three new sporomorph form genera from the Late Cretaceous and Paleogene of southwestern Nigeria. Grana, vol. 23, pp. 163-166.

Salard-Cheboldaeff, M., 1978. Sur la palynoflore Maestrichtienne et Tertiaire du bassin sedimentaire littoral du Cameroun. Pollen Spores, vol. 20, pp. 215-260.

Salard-Cheboldaeff, M., 1979. Palynologie Maestrichtienne et Tertiaire du Cameroun, Etude Qualitative et Repartition Verticale des Principales Especes. Review of Palaeobotany and Palynology, vol. 28, pp. 365-388.

Salard-Cheboldaeff, M., 1990. Intertropical African palynostratigraphy from Cretaceous to Late Quaternary times. Journal of African Earth Sciences, vol. 11, pp. 1-24.

Salard-Cheboldaeff, M., and Dejax, J., 1991. Evidence of Cretaceous to Recent West African intertropical vegetation from continental sediment spore-pollen analysis. Journal of African Earth Sciences, vol. 12, pp. 232-361.

Shafik, S., Watkins, D.K., and Shin, I.C., 1998. Calcareous nannofossil Paleogene biostratigraphy, Cote D'Ivore-Ghana Marginal Ridge, Eastern Equatorial Atlantic. In: Mascle, J., Lohmann, G.P. and Moullade (Editors). Proceedings of the Ocean Drilling Program, Scientific Results, vol. 159, pp. 413-430.

Shell Petroleum, 1976. Preliminary lithostratigraphy and biostratigraphy of the Alo-1 well, Southeastern Nigeria. Shell Petroleum Development Company of Nigeria (unpublished report), 5 pp.

Shipboard Scientific Party, 1996. Site 959. In: Mascle, J., Lohmann, G.P., Clift, P.D., et al. (Editors). Proceedings of the Ocean Drilling Program, Initial Reports, vol. 159, pp. 65-150.

Sluijs, A., Pross, J., and Brinkhuis, H., 2005. From greenhouse to icehouse; organic-walled dinoflagellate cysts as paleoenvironmental indicators in the Paleogene. Earth Science Reviews, vol. 68, pp. 281-315.

Stott, L.D., and Kennett, J.P., 1990. Antarctic Paleogene planktonic foraminiferal biostratigraphy: ODP Leg 113, Sites 689 and 590. Proceedings of the Ocean Drilling Program, Scientific Results, vol. 113, pp. 549-570.

Stover, L.E., Brinkhuis, H., Damassa, S.P., de Verteuil, L., Helby, R.J., Monteil, E., Patridge, A.D., Powell, A.J., Riding, J.B., Smelror, M., and Williams, G.L., 1996. Mesozoic-Tertiary dinoflagellates, acritarchs and prasinophytes. In: Jansonius, J., and McGregor, D.C. (Editors). Palynology: principles and applications. American Association of Stratigraphic Palynologists Foundation 2, pp. 641-750.

Strand, K., 1998. Sedimentary facies and sediment composition changes in response to tectonics of the Cote d'Ivore-Ghana Transform Margin. In: Mascle, J., Lohman, G.P., and Moullade, M. (Editors). Proceedings of the Ocean Drilling Program, Scientific Results, vol. 159, pp. 113-123.

Thomsen, E., and Heilmann-Clausen, H., 1984. The Danian-Selandian boundary at Svejstrup with remarks on the biostratigraphy of the boundary in western Denmark. Bulletin of the Geological Society of Denmark, vol. 33, pp. 341-361.

Traverse, A., 1988. Paleopalynology. Academic Press, New York, 600 pp.

Van der Hammen, T., and Wijmstra, T.A., 1964. A palynological study of the Tertiary and Upper Cretaceous of British Guiana. Leidse Geologische Mededelingen, vol. 30, pp. 183-241.

Van Hoeken-Klinkenberg, P.M.J., 1966. Maastrichtian, Paleocene and Eocene pollen and spores from Nigeria. Leidse Geologische Mededelingen, vol. 38, pp. 37-48.

Varma, C.P. and Dangwal, A.K., 1964. Tertiary hystrichosphaerids from India. Micropaleontology, vol. 10, pp.53-71.

White, E.I., 1926. Eocene fishes from Nigeria. Bulletin of the Geological Survey of Nigeria, vol. 10, pp. 1-78.

Williams, G.L. and Bujak, J.P., 1985. Mesozoic and Cenozoic dinoflagellates. In: Bolli, H.M., Saunders, J.B. and Perch-Nielsen, K. (Editors). Plankton stratigraphy. Cambridge University Press, Cambridge, pp. 847-964.

Williams, G.L., Brinkhuis, H., Pearce, M.A., Fensome, R.A., and Weejink, J.W., 2004. Southern ocean and global dinoflagellate cyst events compared: Index events for the Late Cretaceous-Neogene. In: Exon, N.F., Kennett, J.P., and Malone, M.J. (Editors). Proceedings of the Ocean Drilling Program, Scientific Results, vol. 189, pp. 1-98 [Online]. Available from World Wide Web: <http:// www-odp.tamu.edu/publications/ 189_SR/VOLUME/CHAPTERS/ 107.PDF> .

Williams, G.L., Fensome, R.A., Miller, M.A.,and Sarjeant, W.A.S., 2000. A glossary of the terminology applied to dinoflagellates, acritarchs and prasinophytes, with emphasis on fossils, third edition. Association of Stratigraphic Palynologists Contributions Series No. 37, 370 pp.

Willumsen, P.S., Antolinez, H., Jaramillo, C., and Oboh-Ikuenobe, F., 2004. Maastrichtian to Early Eocene dinoflagellate cysts of Nigeria, West Africa. Abstracts XI International Palynological Congress, Polen, vol. 14, p. 414.

Wilson, G.J., 1984. New Zealand Late Jurassic to Eocene dinoflagellate biostratigraphy-a summary. Newsletters on stratigraphy, vol. 13, pp. 104-117.

Wilson, G.J., 1988. Paleocene and Eocene dinoflagellate cysts from Waipawa, Hawkes Bay, New Zealand. New Zealand Geological Survey Paleontological Bulletin, vol. 57, 96 pp.

Wing, S.L., and Greenwood, D.R., 1993. Fossils and fossil climate: the case for equable continental interiors in the Eocene. Philosophical Transactions of the Royal Society of London, B341, pp. 243-252.

Wrenn, J., and Hart, G.F., 1984. Dinocyst biostratigraphy of Tertiary deposits of Seymour Island, Antarctica. Memorias Congreso Latinoamericano de Paleontologia, vol. 3, pp. 546-554.

Zachos, J., Pagani, M., Sloan, L., Thomas, E., and Billups, K., 2001. Trends, rhythms, and aberrations in global climate 65 Ma to present. Science, vol. 292, pp. 686-693.

Zachos, J.C., Stott, L.D., and Lohmann, K.C., 1994. Evolution of early Cenozoic marine temperatures. Paleoceanography, vol. 9, pp. 353-387.

VITA

Hernan Antolinez-Delgado was born on November 8, 1979 in Bucaramanga, Colombia. He received a Bachelor of Science degree in Geology from the Universidad Industrial de Santander in June, 2004. Following graduation, he was accepted for graduate studies at the University of Missouri-Rolla and moved to Rolla in August 2004 where he has held a graduate teaching assistantship for the period August 2004 to May 2006.